

**Production, modification, and comparative of medium chain-length
polyhydroxyalkanoates biosynthesized from long chain fatty acids**

by

Christopher N. B. Dartiailh

A Thesis submitted to the Faculty of Graduate Studies of

The University of Manitoba

in partial fulfillment of the requirements of the degree of

DOCTOR OF PHILOSOPHY

Department of Biosystems Engineering

University of Manitoba

Winnipeg

Copyright © 2020 by Christopher N. B. Dartiailh

Supervisory Committee

Dr. David B. Levin (Supervisor) - Department of Biosystems Engineering, University of
Manitoba

Dr. Nazim Cicek (Supervisor) - Department of Biosystems Engineering, University of
Manitoba

Dr. Song Liu - Department of Biosystems Engineering, University of Manitoba

Dr. John L. Sorensen - Department of Chemistry, University of Manitoba

Thesis Abstract

Medium chain length (mcl) polyhydroxyalkanoate (PHA) polymers were produced by *Pseudomonas putida* LS46 from the hydrolysed long-chain fatty acids (LCFAs) of vegetable oils. LCFAs are sustainable and economical substrates for mcl-PHA production which get converted into mcl-PHAs from the microbial fatty acid degradation pathway. As such, good polymer yields have been obtained from fatty acids and their functional groups can be retained in the polymer. The length and degree of unsaturation in the substrate is correlated to the polymer composition. A high cell density cultivation using LCFAs for improved volumetric productivity which used a dissolved oxygen limitation for PHA induction obtained $0.65 \text{ g L}^{-1} \text{ h}^{-1}$. Productivity could have been further improved by driving up biomass with higher flow rates of oxygen. The challenge with using dissolved oxygen limitation was the loss of real-time feedback. Using the data obtained, models to predict the decays in substrate consumption were produced.

Chapter 5 compares the mcl-PHA synthesis using octanoic acid or LCFAs of *P. putida* LS46. The response of *P. putida* LS46 to microaerophilic conditions differs based on substrate. Grown on octanoic acid, cell division ceased under microaerophilic conditions with carbon flux towards mcl-PHA accumulation. In contrast, growth continued on LCFAs at a linear rate consistent with the growth rate at onset of limitation ($0.36 \text{ g L}^{-1} \text{ h}^{-1}$), but mcl-PHA accumulation also began to increase. Mcl-PHA titers from LCFAs were doubled that from octanoic acid due to the increased cell titer from continued cell division. Co-feeding the two substrates promoted continued cell growth after onset of oxygen limitation, but higher intracellular PHA content of unproportionally higher C8 content was obtained. The result was higher volumetric productivity than could be achieved from single

substrate cultivation. This work demonstrated the differential biochemical response in microaerophilic conditions of *P. putida* LS46 and indicated that feeding strategies could be designed to improve productivity, tailor polymer properties and reduce production costs.

The polymer properties of mcl-PHAs produced using varied carbon substrates were analysed to determine the effect of substrate biochemistry on monomer composition and crystallinity. Significant variations in monomer composition and molecular weights were observed based on substrate, and whether *de novo* fatty acid synthesis or fatty acid degradation pathways were necessary for metabolism. The highest molecular weights were obtained from medium chain-length fatty acids, which are highly related to the preferred mcl-PHA monomer composition. Thermal degradation appeared to be solely related to the ester group and therefore similar for all PHAs. The glass transition temperatures varied from -39.4 °C to -52.7 °C. The melting points of semi-crystalline mcl-PHAs ranged from 43.2 °C to 51.2 °C, but many of the substrates produced mcl-PHAs lacking crystallinity. The highest crystallinity was obtained from PHAs with the highest contents of C8-C10 monomers, and unsaturated monomers were detrimental to crystallinity (Chapter 6).

Due to the absent crystallinity of mcl-PHAs from unsaturated substrates, alternative applications involving the functionalization from these moieties are required for mcl-PHAs from many LCFAs. We hypothesized that oxidative cleavage of the unsaturated mcl-PHA side chains would reintroduce crystallinity. Unsaturated mcl-PHAs were produced from hydrolysed canola or flax oil. Ozonolysis and osmium-tetroxide catalysed olefin cleavage were investigated in Chapter 7. The resulting polymers has limited residual unsaturation and higher purity is achieved as contaminant fatty acids are further removed. Unsaturated mcl-PHAs appeared to cross-link because of secondary oxidation during ozonolysis but the

concerted osmium-tetroxide catalysed cleavage yielded desired results. The product formed a semi-crystalline film immediately after solvent evaporation: a crystallization rate reserved for scl-PHAs. The oxidative cleavage product of highly unsaturated mcl-PHAs from flax fatty acids became soluble in methanol, a common anti-solvent for mcl-PHA purification.

Contents

Supervisory Committee	ii
Thesis Abstract.....	iii
Author's Declaration.....	x
List of Abbreviations	xi
List of Tables	xv
List of Figures	xvi
List of Copyrighted Material with Permission.....	xviii
Acknowledgements.....	xix
Chapter 1: Thesis Overview.....	20
1.1. Thesis Objectives	20
1.2. Thesis Structure.....	22
Chapter 2: Literature Review.....	23
2.1. Preface.....	23
2.2. Introduction to Polyhydroxyalkanoates	23
2.3. Biosynthesis of PHAs	24
2.4. Feedstock Considerations.....	25
2.5. Strategies for production of mcl-PHAs.....	27
2.5.1. Strategies for Maximum Volumetric Productivity	28
2.5.2. Strategies for Improved Substrate Yields from MCFAs and LCFAs.....	32
2.6. Extracellular Lipase for Triacylglyceride Consumption.....	34
2.7. Biosynthesis and Monomer Composition of mcl-PHAs from Fatty Acids.....	35
2.8. Properties of PHAs.....	41
2.9. Functional modifications of mcl-PHAs.....	46
2.10. Cross-linking of mcl-PHAs.....	51
2.11. Conclusions	54
Chapter 3: Materials and Methods.....	55
3.1. Preface.....	55
3.2. Microorganisms and Microbial Culturing.....	55
3.3. Reactor Preparation	56
3.4. Sample Treatment	57

3.4.1. Residual Fatty Acid Sampling	57
3.4.2. Microscopy and Plate Counts	57
3.4.3. Centrifugation, Biomass and Supernatant Treatment	58
3.5. PHA Extraction and Purification.....	58
3.6. Gas Chromatographic Analysis of PHA and Fatty Acids	59
Chapter 4: Optimized oxygen-limited production of medium chain length polyhydroxyalkanoates from long chain fatty acids using <i>Pseudomonas</i> <i>putida</i> LS46	61
4.1. Preface	61
4.2. Introduction	61
4.3. Methods	62
4.3.1. Microorganism, Medium and Substrate	62
4.3.2. Reactor Setup and Preparation	63
4.4. Results	64
4.5. Discussion	66
Chapter 5: Carbon flux to growth or polyhydroxyalkanoate synthesis under microaerophilic conditions is affected by fatty acid chain-length in <i>Pseudomonas putida</i> LS46	71
5.1. Preface	71
5.2. Abstract	74
5.3. Introduction	75
5.4. Materials and Methods	77
5.4.1. Microorganism, Medium, and Substrates	77
5.4.2. Reactor Setup and Preparation	77
5.4.3. Feeding Rates	78
5.4.4. Co-feeding and Prolonged LCFA Cultivation Experiments.....	79
5.4.5. Sample Treatment.....	80
5.4.6. Analysis of Mcl-PHA, Fatty Acids, and Ammonium	80
5.4.7. Carbon Balancing and yield analysis.....	80
5.5. Results	82
5.5.1. Dissolved Oxygen.....	82
5.5.2. Total Biomass and PHA Accumulation in Single Substrate Comparison.....	84

5.5.3. Analysis of NPCM, Residual Fatty Acid and Residual Ammonium Concentrations	84
5.5.4. Co-Feeding and Prolonged Incubation Experiments.....	87
5.5.5. Volumetric Productivity	90
5.5.6. Carbon Balancing and Yield Analysis.....	90
5.5.7. Monomer Composition of PHA	93
5.6. Discussion	94
5.7. Acknowledgements	98
Chapter 6: The Thermal and Mechanical Properties of Medium Chain-Length Polyhydroxyalkanoates Produced by <i>Pseudomonas putida</i> LS46 on Various Substrates.....	
6.1. Preface	99
6.2. Abstract	99
6.3. Introduction	100
6.4. Methods and Materials.....	102
6.4.1. Culturing and PHA Synthesis.....	102
6.4.2. Biomass Processing	102
6.4.3. Analysis of Thermal Properties	103
6.4.4. Analysis of Molecular Weight.....	103
6.4.5. Analysis of Mechanical Properties	103
6.5. Results	104
6.6. Discussion	111
6.7. Acknowledgements	117
Chapter 7: Oxidative Cleavage of Unsaturated Medium Chain Length Polyhydroxyalkanoates (PHA): A post-treatment method to customize PHA polymers	
7.1. Preface	119
7.2. Abstract	119
7.3. Introduction	120
7.4. Methods and Materials.....	122
7.4.1. PHA Synthesis.....	122
7.4.2. Ozonolysis	123

7.4.3. Osmium Tetroxide Catalysed Olefin Cleavage	124
7.4.4. Product Analysis	125
7.5. Results	125
7.5.1. Ozonolysis	125
7.5.2. Osmium Tetroxide Catalysed Olefin Cleavage	129
7.6. Discussion	138
7.6.1. Ozonolysis	138
7.6.2. Osmium Tetroxide Catalysed Olefin Cleavage	139
7.7. Conclusions	141
7.8. Acknowledgements	141
7.9. Supplementary Material	142
Chapter 8: Engineering Significance and Concluding Remarks.....	145
8.1. Engineering Significance	145
8.2. Concluding Remarks	146
References	148

Author's Declaration

I hereby declare that I am the sole author of this thesis. This is a true copy of the thesis, after revisions suggested by my examiners.

I understand that my thesis may be made electronically available to the public.

List of Abbreviations

3-HA	3-Hydroxyalkanoic acid
ΔH_m	Melt enthalpy
ATCC	American type culture collection
ATP	Adenosine triphosphate
C	Carbon
C-mol	Carbon atom molar
C4 (3-HB)	3-hydroxybutyrate
C5 (3-HV)	3-Hydroxyvalerate
C6 (3-HHx)	3-hydroxyhexanoate
C7 (3-HHp)	3-hydroxyheptanoate
C8 (3-HO)	3-hydroxyoctanoate
C8:1	3-hydroxyoct-5-enoate
C10 (3-HD)	3-hydroxydecanoate
C10:1	3-hydroxydec-7-enoate
C12 (3-HDD)	3-hydroxydodecanoate
C12:1	3-hydroxydodec-6-enoate,
C12:2	3-hydroxydodec-6,9-dienoate
C14 (3-HTD)	3-hydroxytetradecanoate,
C14:1	3-hydroxytetradec-5-enoate
C14:2	3-hydroxytetradec-5,8-dienoate
C14:3	3-hydroxytetradec-5,8,11-trienoate
C _{dm}	Cell dry mass
CFU	Colony forming units

CoA	Coenzyme A
CuAAC	Copper-catalyzed azide-alkyne [3+2] cycloaddition
Đ	Dispersity (M_w/M_n)
DCM	Dichloromethane
DMF	Dimethyl formamide
DMS	Dimethyl sulfide
DO	Dissolved oxygen
DSC	Differential scanning calorimeter
E	Elongation-at-break
EM	Elastic modulus
FADH ₂	Flavin adenine dinucleotide
GC	Gas chromatograph
GC-MS	Gas chromatograph – mass spectrometer
GPC	Gel permeation chromatography
HPLC	High performance liquid chromatography
K _{La}	Volumetric oxygen mass transfer coefficient
LB	Luria-Bertani broth
LCFAs	Long chain fatty acids
Lcl	Long chain-length
LPM	Liters per minute
M _n	Number average molecular weight
M _w	Weight average molecular weight
m-CPBA	meta-chloroperoxybenzoic acid
MCFAs	Medium chain fatty acids
Mcl	Medium chain-length

MeOH	Methanol
MMA	Methyl methacrylate
MUFAs	Monounsaturated fatty acids
NADH	Nicotinamide adenine dinucleotide
NADPH	Nicotinamide adenine dinucleotide phosphate
n.d	Not determined
NPCM	Non-PHA cell mass
OTR	Oxygen transfer rate
PBS	Phosphate-buffered saline
PEG	Polyethylene glycol
PHA	Polyhydroxyalkanoate
PHB	Polyhydroxybutyrate
PHBV	Polyhydroxybutyrate- <i>co</i> -valerate
PHBU	Polyhydroxybutyrate- <i>co</i> -undec-10-enoate
pi	post inoculation
PMMA	Polymethyl methacrylate
PHO	Polyhydroxyoctanoate
PHOU	Polyhydroxyoctanoate- <i>co</i> -undec-10-enoate
PS	Polystyrene
PTFE	Polytetrafluoroethylene
PUFAs	Polyunsaturated fatty acids
RAFT	Reversible addition-fragmentation chain transfer
Rpm	Rounds per minute
Scl	Short chain-length
SFAs	Saturated fatty acids

T	Tensile strength
T _d	Degradation temperature
T _g	Glass transition temperature
T _m	Melting temperature
t-BuOH	tert-butyl alcohol
TAGs	Triacylglycerides
TGA	Thermogravimetric analysis
USFAs	Unsaturated fatty acids
UV	Ultraviolet
VFA	Volatile fatty acid
Vol	Volume
Y _{X/C}	NPCM yield from carbon
Y _{X/N}	NPCM yield from nitrogen
Δ-#	Carbon position of unsaturation from carboxylic acid (C1)
Ω-#	Carbon position of unsaturation from fatty acid terminus
μ	Specific growth rate
μ _{max}	Maximum specific growth rate

List of Tables

Table 2.1. Monomer composition of mcl-PHAs produced by <i>Pseudomonas spp.</i> from fatty acids.	38
Table 2.2. Tensile properties resulting from longer-side chains, unsaturated side chains and cross-linking of mcl-PHAs produced using various feedstocks.	46
Table 2.3. Functional modification of unsaturated mcl-PHAs	48
Table 3.1. PHA monomer analysis by gas chromatography.	60
Table 5.1. Mixed substrate flask cultivation of <i>P. putida</i> LS46.	73
Table 5.2. Determination of appropriate specific growth rate for exponential feeding of octanoic acid to <i>P. putida</i> LS46.	83
Table 5.3. Comparison of key process performance indicators during mcl-PHA production by <i>P. putida</i> LS46 from LCFAs or octanoic acid as the sole carbon source, or when co-fed in C-mol equivalent proportions.	89
Table 5.4. Final monomer compositions of mcl-PHA polymers synthesized from LCFAs and octanoic acid by <i>P. putida</i> LS46. Values are expressed as mol percent of the total monomers detected by gas chromatography and measured at 16 h pi.	94
Table 6.1. Growth and PHA production by <i>P. putida</i> LS46 on varying carbon substrates. *Oleic acid, linoleic acid, and linolenic acid are 90%, 60%, and 70% technical grades, respectively.	107
Table 6.2. Thermal and tensile properties of mcl-PHAs. T _g : Glass transition temperature T _M : Melting Temperature T _D : Degradation Temperature ΔH _M : Melt Enthalpy T: Tensile Strength E: Elongation at break. EM: Elastic Modulus. N/A – Not applicable (No melt). n.d. – Not Determined. The standard deviations are made from a minimum of three tensile strips.	109
Table 6.3. Compilation of mcl-PHA average molecular weights produced from various substrates using <i>Pseudomonas spp.</i> M _n : Number-average molecular weight. M _w : Weight-average molecular weight Đ: Dispersity. Numbers marked by “*” were calculated by the author using the two reported values.	113
Table 6.4. Thermal properties of mcl-PHAs produced by <i>Pseudomonas spp.</i> using various feedstocks. T _g : Glass transition temperature T _M : Melting Temperature T _D : Degradation Temperature ΔH _M : Melt Enthalpy	115
Table 7.1. Monomer compositions of mcl-PHAs produced from hydrolyzed vegetable oils by <i>P. putida</i> LS46. Below, the composition of major FFA peaks comprising Canola and Flax FFAs.	123
Table 7.2. Experimental reaction conditions. The bold conditions did not yield a film but resulted in a fragrant, black liquid.	130
Table 7.3. Expected monomer products from unsaturated mcl-PHAs after OsO ₄ cleavage.	133

List of Figures

Figure 2.1. The general repeating structure of poly-3-hydroxyalkanoates	24
Figure 2.2. Biosynthetic pathway for mcl-PHA synthesis from fatty acid substrates.	37
Figure 4.1. Exponential feeding of LCFAs derived from canola oil to a 5L working volume of <i>P. putida</i> LS46. Biomass concentration (●), PHA concentration (□) and PHA content (Δ). The dashed lines represent onset of oxygen limitation (— —) which remained at DO=0% for the remainder of the experiment. A change in feeding (— ●) was initiated. The reactor conditions were repeated providing standard deviations of the two reactors.	65
Figure 4.2. The linear rate of biomass production after reaching oxygen-limiting equilibrium during low-mixing (▲), high-mixing (■) and high-mixing + O ₂ supplementation (●) canola LCFA cultivations.	66
Figure 4.3. Modelling decay of specific biomass accumulation rate after onset of oxygen-limitation based on Figure 4.1. Linear (■), “+”-quadratic (x), “-”-quadratic (●), exponential (▲), exponential quadratic (○) rates of decline. The exponential quadratic equation was $y=0.8e(0.04x^2 -0.471x)$	69
Figure 4.4. Theoretical biomass obtained from modelled specific growth rate decline after onset of oxygen-limitation (Figure 4.3.) compared to experimental values (◆) (Figure 4.1.). Linear (■), “+”-quadratic (x), “-”-quadratic (●), exponential (▲), exponential quadratic (○) rates of decline.	70
Figure 5.1. Comparison of <i>P. putida</i> LS46 grown as a fed-batch at $\mu = 0.25 \text{ h}^{-1}$ on LCFAs (filled) or octanoic acid (unfilled). (A) Biomass (circles) and dissolved oxygen (squares). (B) Intracellular PHA content (circles) and total PHA concentration (squares). (C) Non-PHA Cell Mass (D) Residual carbon substrate (circles) and residual ammonium (squares)	86
Figure 5.2. Prolonged cultivation of <i>P. putida</i> LS46 with LCFAs (filled), octanoic acid (unfilled) and a co-feed (half-filled). (A) The non-PHA cell mass demonstrating a substrate-dependent response of <i>P. putida</i> LS46 in response to oxygen limitation. (B) Biomass and PHA production from the C-mol equivalent octanoic acid and LCFA co-feed.	88
Figure 5.3. Yield analysis for octanoic acid grown cultures (A) and LCFA-grown cultures (B) under oxygen excess conditions (0-4 h) and oxygen limited conditions (6-12 h and 12 h onward). Error bars represent standard deviations between biological replicates.	92
Figure 6.1. The 3-Hydroxyalkanoate monomer compositions and molecular weights produced by <i>P. putida</i> LS46 on varying carbon substrates.....	105

Figure 6.2. First heat thermogram overlay of mcl-PHAs obtained from various carbons substrates. Legend inset.	110
Figure 7.1. Proposed method for oxidative cleavage using ozone of unsaturated mcl-PHA.....	124
Figure 7.2. Proposed method for oxidative cleavage using osmium tetroxide of unsaturated mcl-PHA.	124
Figure 7.3. Ozonolysis products from oleic acid. □, DCM and DMS; ▣, DCM, and NaBH ₄ ; ■, DCM/MeOH and DMS; ▤, DCM/MeOH and NaBH ₄ ; ▥, Oleic Acid. *Putative peak assignments.....	126
Figure 7.4. Reduction in unsaturated monomers in mcl-PHA cultivated from flax fatty acids after timed ozonolysis. ■, Saturated PHA monomers; □, Unsaturated PHA monomers.....	127
Figure 7.5. A) and B) Ozonolysis product of unsaturated mcl-PHAs from flax LCFAs in DCM; C) Precipitation of PHA polymer from the DCM/MeOH solution. .	129
Figure 7.6. FTIR spectrum of modified PHA produced by <i>P. putida</i> LS46 from flax fatty acids. ■, Flax PHA; ▣, Thermally cross-linked flax PHA; ▤, Ozonated flax PHA.....	129
Figure 7.7. Gas chromatogram of flax mcl-PHAs (red) and their OsO ₄ cleavage products (blue).	132
Figure 7.8. Gas chromatogram of canola mcl-PHAs (red) and their OsO ₄ cleavage products (blue).	132
Figure 7.9. Proposed unsaturated OsO ₄ -catalysed partial cleavage product of polyunsaturated mcl-PHAs detected by gas chromatography.	134
Figure 7.10. GC-MS fragmentation products of methanolysed polyhydroxyoctanoate numbered by relative abundance.....	136
Figure 7.11. Possible eV cyclization of mcl-PHA OsO ₄ -catalysed cleavage products prior to further fragmentation during GC-MS.	137
Figure 7.12. The ¹ H-NMR (300 MHz, CDCl ₃) of mcl-PHA produced by <i>P. putida</i> LS46 provided A) decanoic acid, B) Canola LCFAs and C) Canola LCFAs followed by the osmium tetroxide catalyzed cleavage reaction.	143
Figure 7.13. The ¹³ C-NMR (75 MHz, CDCl ₃) of mcl-PHA produced by <i>P. putida</i> LS46 provided A) canola LCFAs and B) Flax LCFAs followed by the osmium tetroxide catalyzed cleavage reaction.	144

List of Copyrighted Material with Permission

Permission was received directly from Taylor and Francis Group to re-distribute information presented in sections of Chapter 2, originally published as:

1. Dartiailh C, Cicek N, Sorensen JL, Levin DB. 2021. Production and modification of PHA polymers produced from long-chain fatty acids. Chapter 11, In, “The Handbook of Polyhydroxyalkanoates (PHAs): Volume 1”. M. Koller (Ed.), University of Graz, NAWI Graz, and ARENA, Austria. CRC Press. Taylor & Francis Group. ISBN: 9780367275594.

Permission was granted for use of this publication in Chapter 5 from Springer-Nature through the Copyright Clearance Centre Rightslink®.

2. Blunt W, Dartiailh C, Sparling R, Gapes D, Levin DB, Cicek N. Carbon flux to growth or polyhydroxyalkanoate synthesis under microaerophilic conditions is affected by fatty acid chain-length in *Pseudomonas putida* LS46. *Appl Microbiol Biotechnol.* 2018. 102(15):6437-6449. doi: 10.1007/s00253-018-9055-9.

Permission to redistribute the work presented in Chapter 6 was obtained due to Open Access publication under a Creative Commons CC-BY License. The original article was published in *Frontiers in Bioengineering and Biotechnology*.

3. Dartiailh C, Blunt W, Sharma PK, Liu S, Cicek N, Levin DB. The Thermal and Mechanical Properties of Medium Chain-Length Polyhydroxyalkanoates Produced by *Pseudomonas putida* LS46 on Various Substrates. *Front Bioeng Biotechnol.* 2021. 8:617489. doi: 10.3389/fbioe.2020.617489.

Acknowledgements

This thesis is dedicated to my wife, Sarah. Without you, I would never have undertaken nor completed this endeavour. You have always been my partner and greatest support. I envy your enthusiasm and ambition, and always admire your resourcefulness. I cannot express enough gratitude for being my wife and helping me become who I am today. Of Georges and Amelia, while they have significantly lowered my thesis output, they have filled my heart and made the journey worthwhile. I'm going to finish this thesis, then put on my shoes, then we can go meet Tati for some ICE CREAM.

I'd like to thank the many colleagues and students who occupied the lab and my mind. You made things easier and more difficult, enjoyable and stressful, always presented new challenges and I'm all the better for it. To Warren Blunt with whom I constantly talked shop, I hope from this point forward our friendship can continue without speaking "microaerophilic".

Thanks to my mentors for the last decade: David Levin, Nazim Cicek and David Rourke. I appreciate that you were always welcoming, understanding, interesting and inspirational. These projects only existed because of you and without your guidance I would still be doing lab work (I refuse to give Covid all the credit), running another bioreactor iteration when I should have been writing. Again, Thank you.

Chapter 1: Thesis Overview

1.1. Thesis Objectives

The focus of this thesis is on the production of medium chain length (mcl) polyhydroxyalkanoate (PHA) polymers from long-chain fatty acids (LCFAs). LCFAs, the major components of vegetable oils and animal fats, can provide attractive cost savings for mcl-PHA production. However, there is variability in polymer production based on microbial feedstock. Utilizing LCFAs for mcl-PHA production lengthens the average monomer length and increases unsaturation in the polymer sidechains. The resulting changes to polymer properties require further characterization for specific applications. Unsaturated mcl-PHAs are reactive and can auto-oxidize, but this characteristic is also an avenue for further polymer modification. An overview of published works pertaining to the scope of this thesis are reviewed in Chapter 2. The methods and materials common to multiple research chapters are described in Chapter 3. *P. putida* LS46, like many PHA producers, carries a *phaZ* gene which encodes for a PHA depolymerase. The experimental results discussed below attempt to focus on PHA accumulation rates of the system which would be the sum of the rate of PHA production and its rate of degradation.

The first step in this research was to optimize high cell density cultivation of mcl-PHAs in bioreactors to produce high yields of polymer from LCFAs. In this manner, mcl-PHAs from a variety of LCFAs could be produced for testing of their chemical, thermal and mechanical properties. This also provided sufficient mcl-PHA quantities for further experimentation for both thesis objectives and collaborative efforts under the Fiber Composite and Biomatrix Genomics (FiCoGen) project funded by Genome Canada (2015 to 2018) to utilize mcl-PHAs biocomposites. The response of *Pseudomonas putida* LS46

to the microaerophilic environments encountered during high cell density cultivation using LCFAs in Chapter 4 was further investigated in Chapter 5. This fundamental research to determine microbial growth and PHA production rates in response to oxygen limitation helps direct high cell density optimizations that don't rely on carbon-limited feeding strategies to delay reactor failure.

To assess the effect of the type of LCFAs used on mcl-PHA properties, *P. putida* LS46 was cultivated under similar conditions with a wide-variety of substrates in Chapter 6. In this manner, the substrate effect on mcl-PHAs biosynthesis could be better understood and a correlation between monomer compositions and thermophysical properties could be obtained. Unsaturation in mcl-PHAs have a drastic effect on the polymer's ability to crystallize, and as a result, most LCFAs will produce a polymer that does not crystallize. These PHAs remain an amorphous liquid above their glass transition temperature (T_g), until they auto-oxidize into a cross-linked network. This property of mcl-PHAs made them most suitable for the FiCoGen project where an improvement in elasticity and toughness was observed in cellulose sheets embedded with epoxy containing 5% mcl-PHAs from flax fatty acids.

Finally, strategies for oxidative cleavage of unsaturated sidechains from mcl-PHAs produced from LCFAs was investigated. It was hypothesized that by removing the double-bond and shortening the average monomer sidechain would make the polymers crystallizable again. The pendant oxygen moiety could also introduce hydrogen bonding to the polymer resulting in higher crystallinity and potentially amphiphilic polymers. Furthermore, this reaction could be a route towards further polymer modification through click chemistry.

1.2. Thesis Structure

This thesis is separated into chapters that proceed from microbial cultivation to biopolymer properties and through to post-production modifications. Some of the material presented has been disseminated through journal papers or book chapters. Each of the following chapters will begin with a preface to provide context for the work's presence in the scope of the thesis and to recognize published works.

Chapter 2: Literature Review

2.1. Preface

This chapter introduces the production, properties and modifications of polyhydroxyalkanoates (PHAs) providing literature background for the research chapters. Sections 2.2, 2.4-2.7, 2.9, and 2.10 were published as Chapter 11 in *The Handbook of Polyhydroxyalkanoates* (2021) 1:291-314 titled *Production and Modification of PHA Polymers Produced from Long-Chain Fatty Acids*.

2.2. Introduction to Polyhydroxyalkanoates

Polyhydroxyalkanoates are microbial storage polyesters produced to sequester carbon in response to nutrient-limiting environments. Upon depletion of an external carbon source, the polymer may later be consumed as a source of energy (ATP) and reducing power (NADH/NADPH). Some PHAs have similar characteristics to a range of petroleum-derived polymers (Madison and Huisman, 1999), and can be produced using renewable resources. PHAs are biodegradable due to a breadth of microorganisms that produce external PHA depolymerases or non-specific lipases which result in environmental decomposition (Doi et al., 1990; Jendrossek et al., 1993; Jendrossek and Handrick, 2002; Knoll et al., 2009; Chuah et al., 2013). Another important characteristic of PHAs are their biocompatibility, making them suitable for medical applications (Bonartsev et al., 2007). Taken together, PHAs provide sustainable alternatives for current plastic materials. Formed by the enzymatic (PhaC) condensation of hydroxyalkanoate-CoA monomers, PHA polymers are polyesters consisting of a linear backbone, minimally composed of 3-carbon repeating units, with side chains of varying lengths (Lageveen et al., 1988). Short chain-length (scl-) PHAs range in length from three to five carbons (C3-C5), and medium chain-

length (mcl-) PHAs contain monomers from six to fourteen carbons (C6-C14)(Lee, 1996; Hazer and Steinbüchel, 2007). Long chain-length (lcl-) PHAs are longer than C14, but have only been produced in trace quantities during mcl-PHA production (Steinbüchel and Valentin, 1995; Kim et al., 2007).

2.3. Biosynthesis of PHAs

The basic structure of PHA polymers is shown in Figure 2.1. Microbial biosynthesis of PHA is commonly categorized as scl-PHA or mcl-PHA. The *phaCAB* operon encoding a β -ketoacyl-CoA thiolase, an acetoacetyl-CoA reductase and a PHA synthase converts microbial metabolic intermediates to scl-PHAs. Mcl-PHA biosynthesis occurs through two main pathways: the *de novo* fatty acid biosynthesis pathway or the fatty acid degradation pathway (Eggink et al., 1992; Huijberts et al., 1994; Madison and Huisman, 1999), which will be further discussed in Section 2.7. Notable exceptions include isolated or engineered strains capable of scl-*co*-mcl-PHA biosynthesis and production of 4-hydroxybutyrate or 5-hydroxyvalerate monomers (Steinbüchel and Lütke-eversloh, 2003).

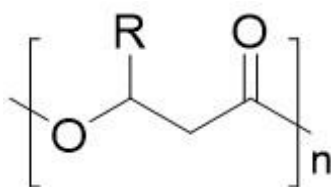


Figure 2.1. The general repeating structure of poly-3-hydroxyalkanoates

PHA production varies by species and depends on which enzymes are present, the specificities and affinities of those enzymes, the provided substrate and the culturing conditions. This is particularly the case with mcl-PHA production which relies on the microorganism's central fatty acid metabolism, can involve multiple different monomer-offering enzymes and have low PHA synthase 3-hydroxyalkanoate (3-HA) specificity

(Kraak et al., 1997; Kim et al., 2007). Ultimately, the differences in monomer composition results in PHAs with varying thermal and mechanical properties.

The strain and substrate also affect the polymer yield. Polyhydroxybutyrate (PHB) accumulating microorganisms can store PHA polymers intracellularly to over 90% of the cell dry mass (cdm), whereas mcl-PHA producing microorganisms can accumulate polymers to 70% of the cdm from octanoic acid, and when grown on long chain fatty acids (LCFAs), are only accumulated up to 50% of the cdm.

2.4. Feedstock Considerations

The production cost of PHAs remain a limitation to broader commercial applications. While research has focused on reducing costs in all facets of the production, extraction, and purification processes, the costs and effects of various substrates have drawn the most attention. The poor substrate yield of *in vivo* systems drives up the production-associated cost. Although the estimated substrate cost for scl-PHA production was reduced to 22% of the total cost when using methane at thermophilic temperatures (Levett et al., 2016), the estimates for substrate cost of elastomeric mcl-PHA production can exceed 50% of the total cost (Choi and Lee, 1997; Koller et al., 2017; Blunt et al., 2018b).

Long chain fatty acids are the main components of vegetable oils and a promising source of cheap, renewable substrates for PHA production (Song et al., 2008). LCFAs are highly reduced and provide ATP as well as reducing equivalents to the cell when metabolized. Worldwide vegetable oil production in 2012 eclipsed 150 million tons (Enferadi Kerenkan et al., 2016), and food processing has been estimated to produce over one million tons of waste vegetable oils (Chhetri et al., 2008). LCFAs can be used as inexpensive substrates for scl-PHA production with high-yield and intracellular content.

However, the scl-PHAs from LCFAs will remain saturated due to the biosynthetic route in which double-bonds are removed in the fatty acid degradation pathway prior to monomer production, and do not contain any functional moieties (Koçer et al., 2003; Ciesielski et al., 2015). Saturated PHAs can be modified through reaction of the polymer ends or free radical mechanisms (Hazer and Steinbüchel, 2007), regardless of the substrate used for their synthesis. The literature has emphasized functionalization of mcl-PHAs from LCFAs, as the unsaturated moieties of some LCFAs can be retained to obtain olefinic mcl-PHAs. The theoretical yield of mcl-PHA from LCFAs is relatively high. The estimated theoretical substrate yield from the LCFAs of canola oil was $0.72 \text{ g mcl-PHA} \cdot \text{g}^{-1}$ substrate (Blunt et al., 2018a).

LCFAs can be composed of saturated fatty acids (SFAs) and unsaturated fatty acids (USFAs). The USFAs can further be classified as monounsaturated (MUFAs) or polyunsaturated (PUFAs) (Chowdhury et al., 1970; Awogbemi et al., 2019). The fatty acid composition of vegetable oils varies with crop and cultivar (Ramos et al., 2009; Gruzdiene and Anelauskaite, 2010), but since fatty acids are largely incorporated into mcl-PHA from fatty acid degradation while conserving the olefin position (Eggink et al., 1992; De Waard et al., 1993), they can be classified by their unsaturation level for the sake of predicting mcl-PHA composition. The composition of vegetable oils can have high proportions of SFAs (coconut, palm), MUFAs (olive, canola), or PUFAs (soybean, flax) (Bart et al., 2010). The predominant monomers in mcl-PHA are C8 and C10, and as a result, low incorporation of olefin moieties occur from predominant $\Delta 9$ -monounsaturated fatty acids (oleic acid), whereas the ω -3 unsaturation of linolenic acid found in polyunsaturated fatty acids can be expected in all monomers C8 and longer (Casini et al., 1997).

Mcl-PHAs produced from octanoic, nonanoic, or decanoic acids have been described as elastomeric materials similar to polyethylene (Antonio et al., 2000). The incorporation of vinyl moieties reduces the crystallinity of these polymers, such that they become completely amorphous with sufficient unsaturation (de Koning et al., 1994). LCFAs cannot be used as a low-cost substrate replacement if the polymer has drastically different properties. However, these polymers can be re-assessed for alternative applications and olefin moieties provide opportunities for polymer modification.

2.5. Strategies for production of mcl-PHAs

PHAs are stored as intracellular granules, and high production rates of polymer require high cell titers. Strategies to improve cell titer include high mixing rates while maintaining high dissolved oxygen (DO) concentrations, often by sparging with pure oxygen or pressurizing the bioreactor (Sun et al., 2007; Follonier et al., 2012). Induction of PHA accumulation has been linked to increased intracellular NADH and acetyl-CoA when growth is limited (Ren et al., 2009). Nitrogen-, phosphate-, sulfur-, magnesium-, and oxygen-limitation have all been used to successfully promote PHA synthesis (Lee et al., 2000b; Koller and Braunegg, 2015). Further improvement of intracellular PHA content has been observed under dual limitation of nitrogen and oxygen (Kim et al., 1997). Contrary to two-phase growth and PHA accumulation models, growth-associated mcl-PHA has been demonstrated at controlled specific growth rates (μ), when the rate of cell replication is controlled at a given exponential rate, suggesting the requirement for nutrient-limitation is strain- and substrate-dependent (Sun et al., 2009). Approaches for reducing PHA production costs focus on maximizing PHA productivity and substrate yield.

2.5.1. Strategies for Maximum Volumetric Productivity

Stirred-tank bioreactors of various discontinuous or continuous operational configurations have been applied to maximize the volumetric productivity ($\text{g PHA} \cdot \text{L}^{-1} \cdot \text{h}^{-1}$), thereby lowering the cost of PHA production. High biomass titers are required for optimum production rates since PHAs are intracellular products, and inhibitory concentrations of medium components limit the productivity of simple batch reactors (Ramsay et al., 1991). Therefore, strategies for fed-batch and continuous PHA production have been developed, which will be briefly summarized here, with a focus on LCFA-based PHA production, as more comprehensive reviews of PHA bioreactor operation have recently been published (Kaur and Roy, 2015; Koller and Braunegg, 2015; Blunt et al., 2018b; Koller, 2018).

Optimized fed-batch bioreactors have used various feeding regimes to provide the carbon substrate and other nutrients to maximize volumetric productivity, and experimentally have provided the highest volumetric productivities (Blunt et al., 2018b). Fed-batch reactors have been more frequently operated using a two-phase feeding regime to first maximize cell biomass titer before an induction phase for PHA accumulation. A significant challenge in fed-batch processes is determining nutrient delivery to maintain concentrations between limiting and inhibitory levels, as optimized feeding may reduce the impact of other fed-batch challenges (i.e. heat and mass transfer, foaming etc.).

Substrate has been delivered for biomass production based on predicted specific growth rates or calculated cumulative substrate consumption using predetermined yield coefficients (Sun et al., 2006; Maclean et al., 2008). Alternatively, response-based substrate delivery has been implemented for pH (Lee et al., 2000b), dissolved oxygen concentration

(Kellerhals et al., 1999; Lee et al., 2000b; Shang et al., 2008), or carbon dioxide evolution (Sun et al., 2006; Andin et al., 2017). Ultimately, due to the low solubility and diffusional limitations of oxygen into the medium, all of these regimes will approach a maximum biomass titer for any reactor configuration due to limited dissolved oxygen (Vendruscolo et al., 2012). Substrate and nutrient delivery modifications are required for the PHA induction phase as the maximum biomass titer is approached.

Pseudomonas species with growth-associated mcl-PHA have been optimized through carbon-limited control of the specific growth rate. In processes using medium chain fatty acids (MCFAs), such as nonanoic acid, a reduced specific growth rate lowered the oxygen uptake rate such that higher biomass was achieved before the onset of oxygen-limited conditions, when nonanoic acid build-up became toxic (Sun et al., 2009). Carbon-limited growth using a quadratic-decaying exponential feed strategy that switched to a linear feed rate, experimentally modeled to optimize growth rate while avoiding oxygen-limitation, resulted in the highest reported volumetric productivity of mcl-PHAs ($2.3 \text{ g PHA} \cdot \text{L}^{-1} \cdot \text{h}^{-1}$) (Maclean et al., 2008).

High cell density mcl-PHA production from LCFAs in fed-batch are limited to a few reports, all of which have distinct growth and PHA production phases. Concomitantly, two fed-batch systems were reported using oleic acid. The highest reported volumetric productivity of mcl-PHA from LCFAs was achieved using a combination of oleic acid delivery methods to maintain the maximum specific growth rate (μ_{max}), first by monitoring optical density, then by switching to DO-control followed by pH-control. Following the depletion of phosphate, PHA accumulation rates increased sharply leading to a final PHA

content of 51.4 weight percent (wt%) in $141 \text{ g}\cdot\text{L}^{-1}$ of biomass for a final volumetric productivity of $1.91 \text{ g PHA}\cdot\text{L}^{-1}\cdot\text{h}^{-1}$ (Lee et al., 2000b).

A similar DO-control fed-batch reactor using oleic acid, but employing nitrogen-limitation, resulted in a lower mcl-PHA volumetric productivity of $0.57 \text{ g PHA}\cdot\text{L}^{-1}\cdot\text{h}^{-1}$, which is partly due to lower biomass obtained, but also because of much lower PHA content. Curiously, the PHA content reached its maximum early into the cultivation through growth-associated PHA synthesis, long before nitrogen-limitation prevented further cell division. Importantly, oleic acid cultivation could be scaled-up into a 30 L reactor with similar results to a 2 L reactor (Kellerhals et al., 2000).

A DO-control fed-batch system for high cell density using phosphorous limitation was used to promote PHA accumulation on corn oil hydrolysate. This resulted in a volumetric mcl-PHA accumulation rate of $0.68 \text{ g PHA}\cdot\text{L}^{-1}\cdot\text{h}^{-1}$ (Shang et al., 2008). Recently, a fed-batch approach with oleic acid controlled through nitrogen-limitation to maintain a low growth rate and couple growth to PHA accumulation, was reported to improve the PHA content and carbon yield. In this system, a biomass of $125.6 \text{ g}\cdot\text{L}^{-1}$ containing 54.4 wt% mcl-PHA was obtained, but the productivity was lower than that reported by Lee et al. [37] due to the length of cultivation (Andin et al., 2017). Finally, the monomer composition and thermal properties of mcl-PHAs using waste rapeseed oil differed with the method of substrate delivery. Pulse-feeding resulted in higher intracellular polymer concentration but lower C12 monomer content, crystallinity and molecular weights than a continuous feed (Mozejko and Ciesielski, 2014).

Continuous-feed PHA production has been developed using a single bioreactor (single-stage continuous) or with the addition of subsequent reactors to separate the growth

and PHA accumulation phases (dual-stage or multi-stage continuous) (Koller, 2018). A continuous-feed bioreactor may not achieve the same maximum biomass titer or PHA content as a fed-batch reactor, but by maintaining a high steady-state concentration of PHA long-term, continuous PHA production can theoretically result in the highest PHA productivities with simpler feeding control and lower operating costs (Preusting et al., 1993; Hartmann et al., 2010).

Dilution rates between 0.1 h^{-1} and 0.3 h^{-1} are optimal for maximizing volumetric productivity. Lower dilution rates increased the PHA content while higher dilution rates could result in cell wash-out (Ramsay et al., 1991; Preusting et al., 1993; Huijberts and Eggink, 1996; Hazenberg and Witholt, 1997; Jung et al., 2001; Hartmann et al., 2006). Nitrogen-limitation is the most prevalent condition for controlling growth rate and promoting PHA synthesis (Hazenberg and Witholt, 1997; Jung et al., 2001), however oxygen-limitation and dual-nutrient limiting conditions have been reported (Huijberts and Eggink, 1996; Durner et al., 2000, 2001). Single-stage, continuous-feed mcl-PHA cultivation resulted in a volumetric productivity of $0.17 \text{ g PHA} \cdot \text{L}^{-1} \cdot \text{h}^{-1}$ (Preusting et al., 1993), and this was subsequently improved up to $0.76 \text{ g PHA} \cdot \text{L}^{-1} \cdot \text{h}^{-1}$ by increasing the concentration of nitrogen and improving oxygen transfer rates to maintain higher cell density (Hazenberg and Witholt, 1997).

A two-stage continuous-feed process for production of mcl-PHA from octane optimized high cell density production in the first stage, which fed into a second reactor with conditions suitable for PHA production. In this manner, the highest continuous volumetric productivity was reported at $1.06 \text{ g PHA} \cdot \text{L}^{-1} \cdot \text{h}^{-1}$ (Jung et al., 2001). From LCFAs, a single-stage cultivation using oleic acid was optimized to $0.69 \text{ g PHA} \cdot \text{L}^{-1} \cdot \text{h}^{-1}$

under oxygen limitation (Huijberts and Eggink, 1996). While the monomer composition of PHA was not affected by growth rate from octanoate (Ramsay et al., 1991; Durner et al., 2000), the use of oleic acid resulted in a mild shift towards longer monomer composition at low dilution rates, without effect on molecular weights of the PHA products (Huijberts and Eggink, 1996). While the theoretical potential of continuous cultivation has yet to be realized, continuous-feed PHA production has proven invaluable for its ability to study effects of growth rate, substrate and nutrient limitation on factors such as monomer compositions, PHA content, yields, molecular weight and thermal properties.

2.5.2. Strategies for Improved Substrate Yields from MCFAs and LCFAs

The substrate costs are estimated to account for the largest proportion of the overall techno-economic assessment (Chanprateep, 2010; Jiang et al., 2016). High volumetric productivities must be balanced with high-substrate yield to minimize production cost. The maximal mcl-PHA yield from LCFAs varies depending on the substrate and monomer composition, but estimates have been reported between 0.58 and 0.72 g g⁻¹, which compares to 0.98 g g⁻¹ from octanoic acid (Hazenberg and Witholt, 1997; Andin et al., 2017; Blunt et al., 2018a). The overall PHA yields are typically much lower when taking into consideration other process yields such as biomass production and maintenance (Ramsay et al., 1991; Follonier et al., 2012).

Optimizations for high intracellular PHA content were necessary to improve the overall mcl-PHA substrate yield, and also significantly reduced the PHA extraction and purification costs. (Hazenberg and Witholt, 1997; Choi and Lee, 1999b). This was confirmed in continuous-feed bioreactor operation as nitrogen-limited conditions with lower dilution rates resulted in improved mcl-PHA substrate yield (Durner et al., 2000).

The experimental carbon yield was improved by step-wise decrease in nitrogen feed during the nitrogen-limitation phase, to couple growth with mcl-PHA production (Andin et al., 2017). Furthermore, strategies to fulfill the substrate requirement for non-PHA biomass, maintenance, and respiration using cheaper substrates have been developed, greatly improving the overall mcl-PHA yield from the more expensive substrate. The overall mcl-PHA yield from octanoate was improved (0.4 g g^{-1}) by providing glucose during the exponential growth and adding octanoate during the nutrient limitation of the PHA accumulation phase, however PHA content was sub-optimal (Kim et al., 1997).

A similar approach was scaled-up with glucose and nonanoic acid, which resulted in a higher PHA content to yield mcl-PHA at 0.56 g g^{-1} from nonanoic acid. PHA accumulation began without lag upon addition of nonanoic acid, supporting the concept of phase-fed fatty acids (Davis et al., 2015). To further improve on this approach, acrylic acid can be provided to inhibit the fatty acid degradation pathway preventing the use of fatty acids for biomass production. A continuous reactor containing glucose and nonanoic acid reported an increase in PHA yield from nonanoic acid from 0.5 to 0.90 g g^{-1} with the addition of acrylic acid (Jiang et al., 2012). Similarly, in a carbon-limited fed-batch, a volumetric productivity of $1.8 \text{ g L}^{-1} \text{ h}^{-1}$ was reported with an overall mcl-PHA yield from nonanoic acid of 0.78 g g^{-1} (Jiang et al., 2013). Since mcl-PHA production has a high affinity for C8, C9, and C10 monomers, the use of acrylic acid with fatty acids of the same length can effectively produce mcl-PHA (Qi et al., 1998). Partial knock-out of the fatty acid degradation pathway was effective at producing high C14 monomer content from tetradecanoic acid (Liu and Chen, 2007). Ultimately, blocking the fatty acid degradation pathway may not be effective for increasing the mcl-PHA yield from LCFAs, certainly not

without drastically changing the monomer composition and production kinetics. Two-reactor systems promise cost-savings through improved substrate yields since no growth occurs in the second, PHA-accumulating reactor (Hartmann et al., 2010). This was demonstrated by an overall mcl-PHA yield of 0.63 g g^{-1} from octane in the second stage, nearly reaching the maximum theoretical yield of 0.66 g g^{-1} (Hazenbergh and Witholt, 1997).

2.6. Extracellular Lipase for Triacylglyceride Consumption

Many *Pseudomonads* do not have the extracellular lipase enzymes required for the metabolism of vegetable oils. The growth of these strains from vegetable or animal sources of triacylglycerides (TAGs) required chemical (hydrolysis) or enzymatic (lipases) pre-treatment (Povolo et al., 2012; Jiang et al., 2016). However, *P. aeruginosa*, *P. resinovorans*, *P. chlororaphis*, and other isolated *Pseudomonas sp.* strains have been reported to grow directly from TAGs (Ashby and Foglia, 1998; Song et al., 2008; Impallomeni et al., 2011; Povolo et al., 2012; Sharma et al., 2017a). Growth and PHA synthesis directly from TAGs is important because it reduces pre-processing steps. It has been reported that the lipase activity is relatively low in *P. resinovorans* (Lee et al., 2012). Fed-batch cultivation of *P. resinovorans* using olive oil deodorizer distillate had a μ_{\max} of 0.19 h^{-1} (Cruz et al., 2016), compared to higher rates of 0.55 h^{-1} reported by *P. putida* KT2440 (Follonier et al., 2012). The apparent decrease in growth rate for *P. resinovorans* is not necessarily detrimental for PHA productivity when considering high productivities at set growth rates of 0.2 h^{-1} (Sun et al., 2009), if the cost benefits of growth from TAGs offset productivity loss. Genes encoding the lipase precursor protein (LipA) and lipase chaperone protein (LimA), which together confer the ability to grow and synthesize PHA directly from TAG substrates have been cloned and expressed in *P. putida* KT2442. Total

biomass of the recombinant bacteria was the same whether cultured with free fatty acids or TAGs, indicating that the lipase activity enabled direct catabolism of the TAGs (Solaiman et al., 2001).

2.7. Biosynthesis and Monomer Composition of mcl-PHAs from Fatty Acids

Medium chain-length polyhydroxyalkanoates can be synthesized from a wide-range of substrates primarily by species of *Pseudomonas* (López et al., 2015). Mcl-PHA synthesis relies on the microorganism's central fatty acid metabolism, in which fatty acid degradation is the major pathway for mcl-PHA production from LCFAs, although this has also been shown to work in concert with fatty acid biosynthesis pathways (Huijberts et al., 1992, 1994). LCFAs are longer than the monomers typically incorporated into mcl-PHAs, and as such undergo several rounds of fatty acid degradation. Each round of fatty acid degradation produces an FADH₂ and NADH and releases acetyl-CoA, which shortens the fatty acid by two carbons (Figure 2.2). Therefore, continued fatty acid degradation is preferred for energy production while the cells are actively dividing, but PHA production rates increased upon onset of conditions limiting to cell growth (Blunt et al., 2017).

Intermediates of fatty acid degradation can be converted to (*R*)-3-hydroxyacyl-CoA for polymerization, a process that requires no expenditure of ATP or NADH (Fiedler et al., 2002; Andin et al., 2017). Thereby, LCFAs can be more directly converted into mcl-PHA than substrates that are unrelated to the 3-hydroxyalkanoate subunits that make up PHA polymers (i.e. carbohydrates), resulting in higher yields (Blunt et al., 2019). Table 2.1 summarizes the monomer compositions of mcl-PHAs produced from various fatty acids and demonstrates that the activities and specificities of enzymes involved in PHA

production vary considerably among *Pseudomonads* given similar substrate and culture conditions.

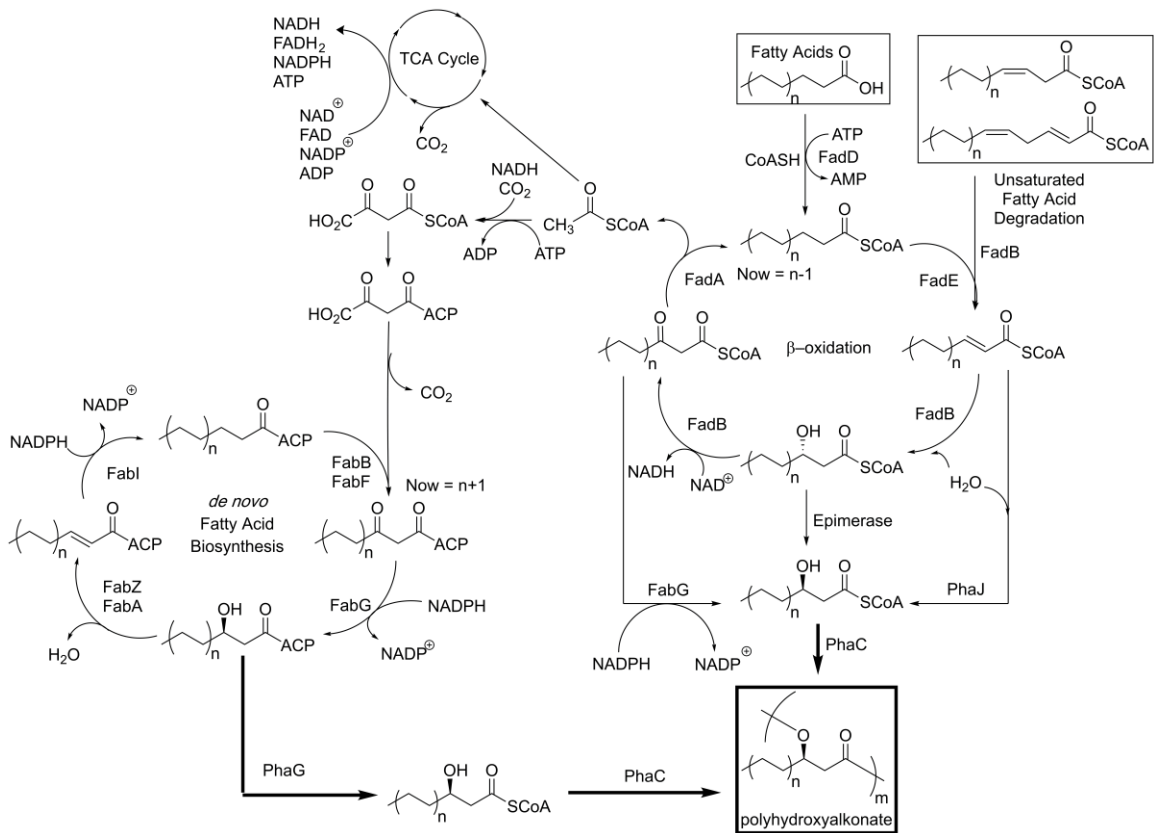


Figure 2.2. Biosynthetic pathway for mcl-PHA synthesis from fatty acid substrates.

Table 2.1. Monomer composition of mcl-PHAs produced by *Pseudomonas spp.* from fatty acids.

Substrate	Microorganism	Monomer Composition (mol %)													References
		C ₄	C ₆	C ₈	C _{8:1}	C ₁₀	C _{10:1}	C ₁₂	C _{12:1}	C _{12:2}	C ₁₄	C _{14:1}	C _{14:2}	C _{14:3}	
Octanoic acid (C ₈)	<i>P. putida</i> KT2442	-	6	92	-	2	-	-	-	-	-	-	-	-	(Huijberts et al., 1994)
Decanoic acid (C ₁₀)	<i>P. putida</i> KT2442	-	5.3	52.3	-	42.3	-	-	-	-	-	-	-	-	(Eggink et al., 1992)
Palmitic Acid (C ₁₆)	<i>Pseudomonas sp.</i> DR2	-	3.4	18.7	-	35.6	-	37.0	-	-	-	-	-	-	(Song et al., 2008)
Petroselenic (C _{18:1})	<i>P. putida</i> KT2442	-	5.1	45.2	-	33.1	-	12.7	Tr	-	3.9	Tr	-	-	(De Waard et al., 1993)
Oleic Acid (C _{18:1})	<i>P. putida</i> KT2442	-	4.4	33.5	-	32.2	-	14.4	Tr	-	-	15.5	-	-	(De Waard et al., 1993)
Oleic Acid (C _{18:1})	<i>P. aeruginosa</i> 27853	-	4	55	-	27	-	8	-	-	6	-	-	-	(Impallomeni et al., 2011)
Oleic Acid (C _{18:1})	<i>P. aeruginosa</i> 42A2 (30 °C)	-	-	24.3	-	30.8	-	3.8	24.2	-	-	3.7	13.1	-	(Fernández et al., 2005)
Oleic Acid (C _{18:1})	<i>P. aeruginosa</i> 42A2 (37 °C)	-	-	2.2	-	39	-	4.7	25.6	-	-	2.1	26.5	-	(Fernández et al., 2005)
Oleic Acid (C _{18:1})	<i>P. Resinovorans</i> B-2649	3.5	7	37	-	33	-	10	-	-	1	8	-	-	(Lee et al., 2012)
Linoleic Acid (C _{18:2})	<i>P. putida</i> KT2442	-	5.6	38.9	-	22.7	-	-	16.9	-	-	-	15.9	-	(De Waard et al., 1993)
Erucic Acid (C _{22:1})	<i>P. aeruginosa</i> 27853	-	3	43	-	36	-	10	-	-	-	8	-	-	(Impallomeni et al., 2011)
Nervonic Acid (C _{24:1})	<i>P. aeruginosa</i> 27853	-	4	28	-	43	-	14	-	-	-	11	-	-	(Impallomeni et al., 2011)
Coconut Oil	<i>P. Resinovorans</i> B-2649	-	8	37	-	35	-	17	-	-	3	-	-	-	(Ashby and Foglia, 1998)
Canola Fatty Acids	<i>P. putida</i> LS46	-	5.4	41.4	-	26.7	-	9.1	3.6	-	9.3	8.6	-	-	(Blunt et al., 2018a)
Soybean Oil	<i>P. Resinovorans</i> B-2649	Tr	8	29	Tr	30	2	5	9	2	2	2	8	-	(Ashby and Foglia, 1998)
Flax Fatty Acids*	<i>P. putida</i> KT2442	-	4.7	23.3	11.4	16.9	9.3	3.9	3.2	~5.5	Tr	2.7	~5.5	~13.6	(Casini et al., 1997)
Linseed Oil	<i>P. aeruginosa</i> 42A2	-	0.4	33.7	5.6	24.3	7.0	4.9	1.4	4.8	0.4	6.4	2.8	8.3	(Bassas et al., 2008)

Tr – Trace. *Values have been assigned as approximate as C_{12:2} and C_{14:2} were lumped as 11% and the 13.6% of C_{14:3} included some C_{16:3}.

Three classes of monomer-supplying enzymes have been hypothesized to convert fatty acid degradation intermediates to (*R*)-3-hydroxyacyl-CoA for PHA synthesis: hydratases, reductases, and epimerases. Hydratases, encoded at least four different *phaJ* genes, convert enoyl-CoA to (*R*)-3-hydroxyalkanoate, which have been confirmed to supply monomers in recombinant hosts (Figure 2.2) (Fukui and Doi, 1997; Tsuge et al., 2003; Davis et al., 2008). Reductases, encoded by *fabG*, were confirmed to convert 3-ketoacyl-CoA to (*R*)-3-hydroxyacyl-CoA in recombinant hosts (Taguchi et al., 1999; Ren et al., 2000). Epimerases, encoded by *fadB* in *Escherichia coli*, as part of the multi-enzyme complex of fatty acid degradation, convert (*S*)-3-hydroxyacyl-CoA to (*R*)-3-hydroxyacyl-CoA (DiRusso, 1990). The putative epimerase was proposed to become more active in response to a knock-out of the (*S*)-3-hydroxyacyl-CoA dehydrogenase, which prevents further fatty acid degradation (Steinbüchel, 2001), and the existence of granule-bound epimerase activity is a possible explanation for *in-vitro* polymerization of PHA from (*S*)-3-hydroxyacyl-CoA (Kraak et al., 1997). However, PHA monomer-supplying epimerase activity has not been observed in *Pseudomonas spp.* (Fiedler et al., 2002).

The activities and specificities of these monomer-supplying enzymes vary among acyl length (Tsuge et al., 2003), and since the expression levels of these monomers can be expected to change with microbial strain and stress-response, the monomer composition of mcl-PHAs may depend on the monomer-supplying enzymes to a greater extent than the specificity of the PHA synthase (Lageveen et al., 1989). However the PHA synthase genes, *phaC1* and *phaC2*, have been shown to have varying monomer specificities (Qi et al., 1997). A knock-out of the native PHA synthases of *Pseudomonas sp.* resulted in a combination of scl-PHA and mcl-PHA monomers when provided an alternative PHA synthase (Sharma et al., 2017b). *E. coli* was provided with the *fabG* monomer-providing enzyme, which resulted in mcl-PHA when provided an mcl-*phaC*, but

produced PHB-*co*-PHHx given an *scl-phaC* (Taguchi et al., 1999). Both these examples indicate that the monomer-supplying enzymes provided a variety of monomer lengths, and the selectivity was due to the PHA synthase. Ultimately, the monomer composition is dependent on a variety of factors, but *mcl*-PHA is produced with a preference of C8 and C10 monomers due to enzyme specificities, as shown in Table 2.1.

Despite the aforementioned monomer preferences, the low substrate specificity of *mcl*-PHA synthases accounts for the incorporation of over 150 monomer types (Steinbüchel and Lütke-oversloh, 2003; Kim et al., 2007). The monomer composition of *mcl*-PHAs will differ by species and is determined both by the substrate and the culturing conditions. The length of fatty acid influences PHA monomer length (Impallomeni et al., 2011), and functional groups may be incorporated into *mcl*-PHAs from the substrate (Kim et al., 2007). The functional moieties in LCFAs can be retained during *mcl*-PHA production depending on their position in the substrate (De Waard et al., 1993; Solaiman et al., 2001; Impallomeni et al., 2011).

The double-bonds of MUFAs and PUFAs are removed as the chain is shortened using the fatty acid degradation pathway. The enzyme *cis*-3,*trans*-2,*enoyl*-CoA isomerase is responsible for removing the odd-carbon double-bonds, while even-numbered double-bonds (such as the Δ 12 olefin group of linoleic acid) are removed by 2,4-*dienoyl*-CoA reductase (De Waard et al., 1993). In this way, one may predict the position of double-bonds in the PHA polymer based on the substrate provided and the monomer length. For instance, 15.5 mol% of *mcl*-PHA synthesized by *P. putida* KT2442 grown with oleic acid (Δ 9) was monounsaturated, as the olefin was maintained in C14 monomers, compared to no retained olefins from petroselenic acid (Δ 6). Growth on linoleic acid (Δ 9, Δ 12) tripled the unsaturation of PHA as both olefins were maintained in the C14, and one olefin still remained at C12 (De Waard et al., 1993). Moreover, PHA produced from linolenic

acid ($\Delta 9$, $\Delta 12$, $\Delta 15$) produced highly unsaturated PHA containing mono-(C8,C10), di-(C12) and poly-(C14) unsaturated monomers (Casini et al., 1997). Table 2.1 illustrates that the average monomer length and mol% of unsaturated monomers increased proportionally with the length and unsaturation of the substrate. Hydroxyl and epoxy moieties have also been observed in mcl-PHA, when *P. aeruginosa* 44T1 was provided with castor or euphorbia oil (Eggink et al., 1995). Mcl-PHAs have incorporated halogen, hydroxyl, carboxyl, thiol, epoxy, aromatic and branched moieties, to name a few, using the appropriate fatty acids (Steinbüchel and Valentin, 1995; Steinbüchel and Lütke-egersloh, 2003; Kim et al., 2007). These functional properties provide the basis for modification of unsaturated mcl-PHAs, but their inclusion also broadens the applicable chemical modifications.

Culture conditions affect the polymer composition due to a shift in the central fatty acid metabolism. As the fatty acids in the bacterial membrane change in length and unsaturation in response to incubation temperature, so too does the mcl-PHA composition (Huijberts et al., 1992). From LCFAs, lower incubation temperature resulted in a shift towards longer monomers with higher unsaturation. As the unsaturated monomers were not consistent with the LCFAs, it was inferred that temperature increased the incorporation of mcl-PHA monomers from *de novo* fatty acid synthesis. The same study also demonstrated a drastic shift in monomer composition based on changing from nitrogen-limitation to phosphate-limitation (Haba et al., 2007). All the above factors ultimately affect the thermal and mechanical properties of mcl-PHAs.

2.8. Properties of PHAs

PHAs exhibit a wide range of polymer properties. The monomer composition, average molecular weight, phase, orientation and crystallinity contribute to the thermal and mechanical properties of PHA polymers. As discussed above, the factors that will determine these properties

include the: microorganism, substrate, culture conditions and processing conditions (Bugnicourt et al., 2014).

Bacteria synthesize and accumulate PHA polymers as energy storage molecules. Higher molecular weight polymers would have greater energy potential. Since PHAs are insoluble in water, they exert negligible osmotic pressure, and thus, selection may favour high molecular weight polymers over multiple oligomers (Madison and Huisman, 1999; Marchessault and Yu, 2005) The effects of temperature, pH and substrate concentration during cultivation on molecular weights of mcl-PHAs were investigated when grown on sodium octanoate. Lower temperatures (down to 15 °C) slowed PHA synthesis but resulted in polymers with higher molecular weight. The pH had no significant effect on polymer molecular weight, although slightly acidic conditions negatively affected production. Higher substrate concentrations had negative effects on PHA accumulation and the molecular weight (Hori et al., 1994). Mozejko and Ciesielski demonstrated that substrate delivery affects molecular weight. Waste rapeseed, when continuously fed, resulted in a semi-crystalline polymer, displaying a higher molecular weight than the amorphous polymer obtained when the substrate was pulse-fed.

Mcl-PHAs are produced at lower number-average molecular weights (M_n) and higher polydispersity than PHB (Liu and Chen, 2007). The M_n of mcl-PHAs is highest when produced from saturated fatty acids such as octanoic acid and coconut oil, whereas molecular weights are lower from longer, unsaturated fatty acids from soybean and flax oils. Double-bonds have little effect on substrate metabolism, but are hypothesized to increase polymer chain termination which resulted in smaller number average molecular weights with increasing unsaturated fatty acid content from coconut to soybean oil (Ashby et al., 1998a). The same trends were not observed with increasing olefin concentrations in PHOU (Schmid et al., 2007), or with increasing substrate

lengths (Impallomeni et al., 2011). Therefore, it is difficult to predict molecular weights based on the provided substrate, without considering culturing conditions and microbial strain.

The average molecular weight of the polymer has several effects on the polymer properties (Kalpakjian and Schmid, 1985). As observed with other common polymers, an increase in polymer molecular weight results in greater tensile strength, impact strength, and increased melting temperature (Nicholson et al., 1999). These same observations are expected to hold true for PHA polymers. PHB has been reported to have increasing mechanical strength with increasing molecular weight (Tsuge, 2016). Brittleness is a drawback of PHB, but PHB with higher molecular weight was reported to be less brittle (Madison and Huisman, 1999), an expected behaviour which improves polymer performance. To be suitable for some plastic processing techniques, such as film extrusion, it will be necessary to achieve high molecular weights of PHA (Bugnicourt et al., 2014). A final consideration is that with increasing molecular weight, an expected decrease in biodegradability will be observed (Tokiwa et al., 2009).

The degree and rate of crystallization also affects the physical properties of PHA polymers. Crystallinity determines the melting point and the viscoelastic properties of PHAs and is dependent upon monomer composition. PHA synthesis is stereo-selective, such that an isotactic polymer is produced with all monomers having (R)-stereochemistry (Schmid et al., 2007). The result is a repetitive polymer with monomers in the same configuration, which enables the formation of crystal structures. While PHB is highly crystalline (Bugnicourt et al., 2014), the level of crystallinity drops with a greater degree of disorder caused by copolymers, longer side-chains, and unsaturated subunits (Kellerhals et al., 2000). PHBV is still over 50% crystalline (Laycock et al., 2014), while the crystallinity of PHN drops to 25% (Marchessault et al., 1990). PHAs containing enough unsaturation in the side-chains exhibit no crystallinity and remain completely amorphous

(Kellerhals et al., 2000). Increasing the proportion of dominant monomer improved crystallinity, and the resulting mechanical properties, of PHO and PHN (Jiang et al., 2012). Efforts to produce homopolymers with alternate dominant monomers through genetic engineering and cultivation control have yields near homopolymers from C5 to C14. At monomer lengths where crystallinity is observed, an increase in dominant monomer proportion resulted in higher melt enthalpy (Liu et al., 2011; Wang et al., 2011; Abe et al., 2012).

The rate of crystallization of PHO produced by *P. oleovorans* was observed when incubated at -20 °C, 0 °C, and 20 °C after melting. Although the fastest crystallization rate was observed between 0 °C to 5 °C, the melting temperature and maximum heat of fusion increased with higher crystallization temperature. Continued incubation at 20 °C resulted in annealing effects, which increased the melt enthalpy and melt point onset. These annealing effects result in sharper melt points. Likewise, tensile strength improved with higher crystallinity (Gagnon et al., 1992). Larrañaga et al. (2014) reported similar results for PHO with incubation temperatures of 0 °C, 23 °C and 37 °C. Crystallization at 37 °C resulted in lower tensile strength, contrary to observation of Gagnon et al. (1992) (Larrañaga et al., 2014). The proposed orientation of crystalline regions in the PHO polymer is a backbone helix structure, but close packing of side-chains is still unclear (Marchessault et al., 1990). Increased crystallinity results in slower biodegradation whereas amorphous polymers are loosely packed, making them more exposed to enzymatic degradation (Tokiwa et al., 2009).

Comparing previously reported thermal data, there is a trend of decreasing glass transition temperature with longer monomer units (Wang et al., 2011; Abe et al., 2012). Although the glass transition can also be affected by the presence of double-bonds in the side-chains (Schmid et al.,

2007), no clear correlation is observed (de Koning et al., 1994; Ashby and Foglia, 1998; Icoz, 2008).

Scl-PHAs, particularly PHB, are highly crystalline polymers which have high tensile strength and elastic modulus but are brittle with low elasticity. Comonomers of 3-HV and 3-HHx have a plasticizing effect on scl-PHAs, along with other potential co-monomers (i.e. 3-HO, 4-HB etc.)(Marchessault and Yu, 2005; Anjum et al., 2016). The tensile properties of various mcl-PHAs are reported in Table 2.2. Mcl-PHA synthesized by bacteria grown on octanoic acid was reported with tensile strength equivalent to PHB and with far greater elongation-to-break ratio and drastically reduced elastic modulus. The mcl-PHAs produced from LCFA feedstocks display decreased tensile strength, and with high unsaturated subunit content the polymers are amorphous and sticky, making them unable to be tested. However, when mcl-PHA polymers with high unsaturated subunit content were cross-linked, they displayed a drastic increase in tensile strength and elastic modulus, with a much shorter elongation-to-break ratio. This result is consistent behaviour of polymer cross-linking (Kalpakjian and Schmid, 1985). Polyunsaturated mcl-PHAs were produced from flax oil, and after cross-linking through auto-oxidation, resulted in the highest tensile strength of any mcl-PHA (Table 2.2)(Ashby et al., 2000).

PHAs have a wide range of native properties based solely on crystallization behaviour differentiated by polymer sidechains. The mechanical and barrier properties can be adjusted to best represent a variety of conventional plastics through bioproduction considerations. Continuing efforts aim to reduce production costs using inexpensive substrates and through biosynthetic engineering, while maintaining desirable material properties. However, this is not always possible, therefore the next sections will discuss possible polymer modifications to provide enhanced material properties to PHAs.

Table 2.2. Tensile properties resulting from longer-side chains, unsaturated side chains and cross-linking of mcl-PHAs produced using various feedstocks.

<i>PHA Polymer Feedstock</i>	<i>T</i> (MPa)	<i>E</i> (%)	<i>Young's</i> <i>Modulus (MPa)</i>	<i>Reference</i>
<i>Octanoic Acid*</i>	16.3	318	14.6	(Larrañaga et al., 2014)
<i>PHB*</i>	16.4	4	1317.4	(Liu and Chen, 2007)
<i>15% C10</i>	8.7	188.7	3.6	(Liu and Chen, 2007)
<i>39% C10</i>	11.3	125	11.5	(Liu and Chen, 2007)
<i>31% C14</i>	7.57	275.1	31.73	(Liu and Chen, 2007)
<i>49% C14</i>	3.15	107.7	34	(Liu and Chen, 2007)
<i>Coconut</i>	2.5	242	2.0	(Ashby et al., 1998b)
<i>Tallow</i>	3.0	320	1.7	(Ashby et al., 1998b)
<i>Soybean</i>	N/A	N/A	N/A	(Ashby et al., 1998b)
<i>Coconut - Irradiated</i>	5.1	360	2.6	(Ashby et al., 1998b)
<i>Tallow - Irradiated</i>	4.9	360	3.0	(Ashby et al., 1998b)
<i>Soybean - Irradiated</i>	0.7	25	3.1	(Ashby et al., 1998b)
<i>Linseed – Epoxidized (25 days)</i>	4.8	54.2	12.9	(Ashby et al., 2000)
<i>Linseed – Epoxidized (75 days)</i>	17	65.7	132.4	(Ashby et al., 2000)
<i>Linseed – Epoxidized (100 days)</i>	20.7	29.2	510.6	(Ashby et al., 2000)
<i>Linseed – Autoxidized (75 days)</i>	20.3	8.7	703.3	(Ashby et al., 2000)
<i>Linseed – Autoxidized (100 days)</i>	25	4.4	767.8	(Ashby et al., 2000)
<i>PHBU</i>	8.5	88.8	367.5	(Levine et al., 2015)
<i>PHBU_{50%} - Crosslinked</i>	11.2	120.3	258.3	(Levine et al., 2015)
<i>PHBU_{98%} - Crosslinked</i>	26.2	95.2	205.5	(Levine et al., 2015)
<i>Polypropylene*</i>	40	100	1900	(Levine et al., 2015)
<i>Low Density Polyethylene*</i>	10	620	200	(Levine et al., 2015)
<i>Silicone Rubber*</i>	7.6	N/A	8	(Levine et al., 2015)
<i>Polylactic Acid*</i>	28	6	1200	(Levine et al., 2015)

*Comparative reference polymers. Tensile strengths (T), Elongation at break (E).

2.9. Functional modifications of mcl-PHAs

The incorporation of vinyl-moieties into mcl-PHAs reduce their crystallinity, ultimately weakening their mechanical properties, but also imparting functionality to the polymer.

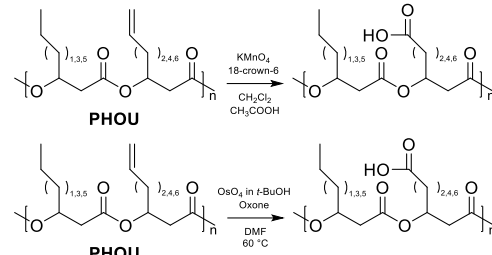
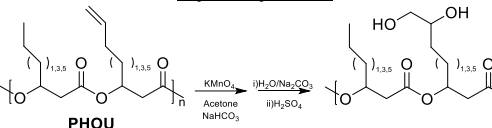
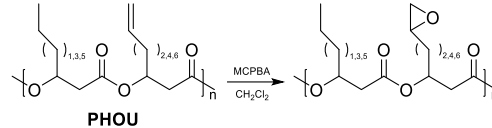
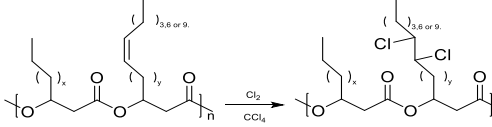
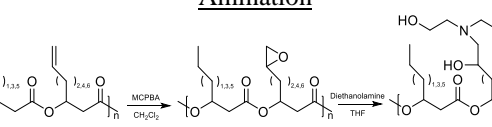
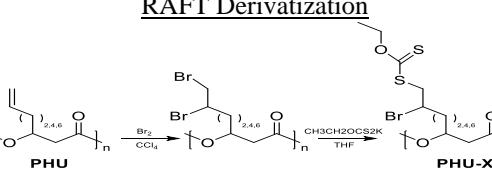
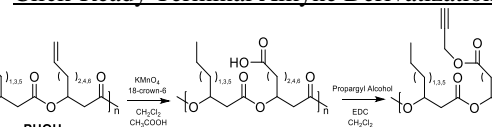
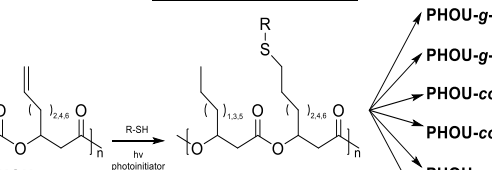
Chemical modifications have imbued unsaturated mcl-PHAs with strength or with new properties targeted at niche biomedical applications. The remainder of this chapter discusses the modification of mcl-PHAs to attain novel properties.

Mcl-PHAs with vinyl-moieties inherited from MUFAs and PUFAs can be tailored by choice of microorganism and culture conditions, but most simply by the substrate delivery (Table 2.1). Vegetable oils vary in their fatty acid composition, and co-feeding strategies can be applied

to control the relative unsaturation (Blunt et al., 2018a). LCFAs appear to increase chain termination during mcl-PHA polymerization resulting in lower molecular weights with increasing unsaturation (Ashby and Foglia, 1998). The glass transition temperatures and melting point decrease with higher unsaturation in the LCFA substrate (Park et al., 1998). Commonly, 10-undecenoic acid is provided for mcl-PHA (PHU) production with terminal vinylic carbons in the side-chains (Kurth et al., 2001; Follonier et al., 2015). Varying the feed ratio of octanoic acid and 10-undecenoic acid resulted in polyhydroxyoctanoate-*co*-undecenoate (PHOU) with unsaturated monomer concentration equal to the substrate ratio, and no effect on molecular weight. When co-feeding octanoate with 10-undecenoate in a continuous steady-state bioreactor, lower dilution rates increased the relative concentration of aliphatic monomers while molecular weights were not affected by growth rate (Hartmann et al., 2006). Increased feed ratios of 10-undecenoic acid resulted in decreased glass transition temperature and melting temperature of the mcl-PHA, and became amorphous with high unsaturation (Hartmann et al., 2006). The same trends of were observed with octane:octene ratios, having a decreasing melt endotherm until completely amorphous at 15 mol% unsaturation (de Koning et al., 1994).

The modification of mcl-PHAs containing side-chain vinyl groups have produced polymers with new properties (Table 2.3). Chlorination across the double-bond drastically elevated the glass transition temperature from -50 °C to 58 °C with melting temperatures more consistent with scl-PHAs than mcl-PHAs, despite hydrolysis resulting in lower molecular weights. The observed changes in these polymers were from sticky to a soft, elastic polymer with moderate chlorine addition. Higher chlorine content in the polymers were described as crystalline and brittle. While crystallinity was not measured in that study, these highly chlorinated polymers were observed well below their glass transition temperatures (Arkin et al., 2000).

Table 2.3. Functional modification of unsaturated mcl-PHAs

Reaction	Described Effect
<p style="text-align: center;"><u>Carboxylation</u></p>  <p style="text-align: center;">PHOU</p> <p style="text-align: center;">PHOU</p>	<p>Increasing carboxylation results in higher hydrophilicity. This functional moiety is also a precursor for other modifications (see “click-ready”). (Kurth et al., 2001; Stigers and Tew, 2003)</p>
<p style="text-align: center;"><u>Hydroxylation</u></p>  <p style="text-align: center;">PHOU</p>	<p>Hydroxylation increased the hydrophilicity of the polymer, becoming insoluble in organic solvents. (Lee et al., 2000a)</p>
<p style="text-align: center;"><u>Epoxidation</u></p>  <p style="text-align: center;">PHOU</p>	<p>Reduced glass transition temperature. Precursor to cross-linking, or for further modification (see “transamination”). (Bear et al., 1997; Park et al., 1998; Ashby et al., 2000)</p>
<p style="text-align: center;"><u>Halogenation</u></p>  <p style="text-align: center;">LCFA mcl-PHA</p>	<p>Higher polymer chlorine content resulted in elevated glass transition and melting temperatures (Arkin et al., 2000). Halogenation provides leaving group for further substitutions (see “RAFT”)</p>
<p style="text-align: center;"><u>Amination</u></p>  <p style="text-align: center;">PHOU</p>	<p>Complete change in solubility from hydrophobic to hydrophilic. Transamination resulted in a significant decrease of molecular weight due to PHA chain-scission. (Sparks and Scholz, 2008)</p>
<p style="text-align: center;"><u>RAFT Derivatization</u></p>  <p style="text-align: center;">PHU</p> <p style="text-align: center;">PHU-Xa</p>	<p>Xanthate substitution of PHA into macro-RAFT agents. RAFT polymerization using <i>N</i>-isopropyl acrylamide produced thermo-responsive, amphiphilic polymers with glass transition temperatures between 58-100 °C. (Toraman and Hazer, 2014)</p>
<p style="text-align: center;"><u>Click-Ready Terminal Alkyne Derivatization</u></p>  <p style="text-align: center;">PHOU</p>	<p>CuAAC-ready mcl-PHAs for diverse applications. Demonstrated improved PEG grafting compared to previous methodology, resulting in improved crystallinity. (Babinot et al., 2012)</p>
<p style="text-align: center;"><u>Thiol-ene Addition</u></p>  <p style="text-align: center;">PHOU</p> <ul style="list-style-type: none"> → PHOU-g-Jeffamine → PHOU-g-(F;PEG) → PHOU-co-SO₃⁻ → PHOU-co-COOH → PHOU-co-OH → PHOU-co-SO₃⁻-g-PEG 	<p>Thiol-ene reaction with PHOU eliminates polymer pre-modification for “clickable” functionalization. Significantly broadens types of functional groups and grafting while avoiding chain-scission of cross-linking. (Le Fer et al., 2012; Babinot et al., 2013; Hazer, 2015; Modjinou et al., 2015; Jain-Beuguel et al., 2019)</p>

Carboxylation and hydroxylation at the terminal vinyl position of PHOU have both been demonstrated to change the solubility of the polymer with no reduction in molecular weight (Lee et al., 2000a; Stigers and Tew, 2003). Increasing unsaturation content in the PHOU resulted in polymers with higher polarity after modification until the polymers were no longer soluble in organic solvent (Lee et al., 2000a; Kurth et al., 2001; Stigers and Tew, 2003). Epoxidation of PHOU was performed without reduction in molecular weight or cross-linking. The glass transition temperature was lower with increased epoxidation, but the polymer remained amorphous. The addition of epoxides provided an avenue for cross-linking or producing amphiphilic polymers (Bear et al., 1997; Park et al., 1998; Ashby et al., 2000). Co-polymer grafting has been achieved via free radical polymerization with the side-chain vinyl moieties of unsaturated mcl-PHAs from soybean fatty acids.

Methyl methacrylate (MMA) initiated by benzoyl peroxide formed a copolymer graft with PHA (PHA-g-PMMA) in which cross-linking could be prevented with the addition of hydroquinone. Soybean mcl-PHA is not in a glassy state and exhibits no crystallinity, but the grafted polymer became hard and brittle, a property inherited by the new glass transition temperature of PMMA. Grafted copolymers were produced with higher tensile strength and elongation at break than either homopolymer (Ilter et al., 2001). Graft polymers were alternatively produced by first activating MMA (or styrene) using an oligo-peroxide to produce activated PMMA and PS respectively. Mixing the activated polymers into unsaturated mcl-PHAs produced PHA-g-PMMA and PHA-g-PS, however the PHA-g-PS cross-linked (Cakmakli et al., 2001). Bromination across the vinyl moieties of unsaturated mcl-PHA followed by xanthate substitution resulted in macro reversible addition-fragmentation chain transfer (RAFT) agents. RAFT

polymerization using N-isopropyl acrylamide produced thermo-responsive, amphiphilic polymers with glass transition temperatures between 58-100 °C (Toraman and Hazer, 2014).

Click chemistry can be applied to the vinyl groups of mcl-PHAs derived from unsaturated fatty acid substrates, which drastically increases the number of modification permutations. Click-ready mcl-PHAs were first produced by converting PHOU to contain terminal R-group carboxylic acids, then by esterification with propargyl alcohol yielding a “clickable” terminal alkyne. The objective was to produce amphiphilic polymers through polyethylene glycol (PEG) grafting. PHA-g-PEG was produced using PEG-azide producing polymers using longer PEG oligomers than could be grafted with previous direct esterification methods, ultimately increasing the molecular weight and crystallinity of this copolymer (Babinot et al., 2010). The terminal alkyne produced enables copper-catalyzed azide-alkyne [3+2] cycloaddition (CuAAC) with molecules containing azide groups.

Instead of modifying mcl-PHAs to introduce click moieties, mcl-PHA have been cultured with terminal azide-groups *in lieu* of vinyl-groups. The resulting mcl-PHAs are CuAAC-ready without need for polymer modification. This was achieved with ω -azidofatty acid substrates delivered to engineered *E. coli* producing mcl-PHA with yield, molecular weights and thermal properties consistent with PHOU production (Pinto et al., 2016). *P. oleovorans* co-fed nonanoate and 11-bromoundecanoic acid produced polymers with terminal bromine groups, which allowed for azide substitution. Instead of a terminal azide, the azide-alkyne reaction could be achieved with terminal alkyne mcl-PHAs produced when co-fed nonanoate and 10-undecynoic acid (Nkrumah-Agyeefi and Scholz, 2017). Furthermore, a strain-promoted cycloaddition was demonstrated eliminating the copper requirement of CuAAC (Pinto et al., 2016; Nkrumah-Agyeefi and Scholz, 2017). Another approach, which employs click-chemistry without metallic catalysts, is thiol-ene

addition. In this case, the desired functional molecules contain pendant thiol moieties, which undergo anti-Markovnikov additions to the side-chain vinyl groups of unsaturated mcl-PHAs. An increase in hydrophilicity without reduction in molecular weight of PHOU and unsaturated mcl-PHA from soybean LCFAs was achieved when hydroxylated and carboxylated in this manner (Hazer, 2015). Polyhydroxybutyrate-*co*-undecenoate (PHBU) was cross-linked using a polythiol (pentaerythritol tetrakis (3-mercaptopropionate)) for the thiol-ene click reaction to increase both the elongation and tensile strength compared to native PHBU (Levine et al., 2016). Pendant sulfonate addition to PHOU resulted dramatic change in solubility, becoming insoluble in organic solvents above 5 mol% sulfonated monomers and self-aggregated into nanoparticle micelles with sizes dependant on sulfonate concentration (Modjinou et al., 2015). Furthermore, employment of thiol-ene reactions have produced various grafted co-polymers from PHOU. Amphiphilic polymers have been designed towards medical application such as drug delivery by grafting using thiol-ene click reactions. Jeffamine[®] grafting onto PHOU increased the hydrophilicity of the polymer (Le Fer et al., 2012). The sequential grafting of fluorinated chains and PEG onto PHOU produced multi-compartment micelles (Babinot et al., 2013). The same procedure substituting fluorinated chains with sulfonated chains produced amphiphilic polymers to be coated onto nano-metal organic frameworks to produce stable hybrid nanoparticles that displayed no cytotoxicity (Jain-Beuguel et al., 2019).

2.10. Cross-linking of mcl-PHAs

Cross-linking of mcl-PHAs involves radical propagation along olefinic moieties, forming a polymer network. Unsaturated mcl-PHAs have been reported to auto-oxidize, and have had cross-linking initiated by reactive peroxides or radiation (de Koning et al., 1994; Ashby et al., 1998a; Hazer et al., 2001; Schmid et al., 2007). Cross-linking is the result of either C-C, ether, or peroxy

bonds, although ether bonds appear to be dominant cross-link during auto-oxidation (Muizebelt et al., 1994; Mallegol et al., 2000). Hydrogen atom abstraction is most likely to occur in the allylic position, at which time the radical reacts with oxygen resulting in a peroxy radical. The peroxy radical can abstract another allylic hydrogen resulting until the reaction is finally terminated (Simic, 1981). The degradation of the hydroperoxide into an epoxide precedes ether bond linkages (Mallegol et al., 2000). The rate of cross-linking can be increased with heat, irradiation, supplementation of oxygen or with increasing unsaturation. Chain scission and cross-linking will occur simultaneously but the ester cleavage requires a much higher activation energy (almost three-fold), therefore cross-linking is promoted before chain scission (Ashby et al., 1998b; Schmid et al., 2007).

Cross-linking of mcl-PHA polymers resulted in markedly different physical and thermal properties. When the octane-based polymer was irradiated, only chain-scission occurred and caused a reduction in molecular weight. Irradiation of a polymer with 15 mol% unsaturated monomers (amorphous) caused cross-linking and the polymer became solid and less sticky. The cross-linked polymers then showed constant dynamic modulus from the glass transition temperatures (-15 to -30 °C) to the onset of thermal degradation (170 °C,) whereas the octane-based polymer showed a significant amount of variation around ambient temperature and softened at 40 °C due to melting. The tear resistance of the cross-linked, amorphous polymer was poor, with much less tensile strength than the crystalline, saturated polymer. However, the cross-linked PHA was still biodegradable (de Koning et al., 1994). Irradiation of mcl-PHAs with 11 mol% monounsaturated monomers synthesized by *P. resinovorans* (NRRL B-2649) from tallow made it slightly stronger and more rigid than its crystalline counterpart. However, further increasing the cross-linking density resulted in a decrease in tear resistance, and the soluble fraction showed

molecular weight reductions up to 70% (Ashby et al., 1998a). Mcl-PHA synthesized from coconut oil (95% saturated), tallow (37% unsaturated oleic acid), and soybean (86% unsaturated or polyunsaturated) fatty acids all displayed increased tensile strength after irradiation.

Mcl-PHA polymers synthesized from soybean oil produced a solid film with higher Young's modulus than the irradiated polymers produced from coconut or tallow feedstocks (Ashby et al., 1998b). Linseed oil derived mcl-PHAs were cross-linked by two methods: chemically induced cross-links with m-CPBA and naturally induced cross-links by exposure to air (auto-oxidation). Chemical treatment with m-CPBA resulted in cross-linking in less than 25 days, and by that time 98% of the polymer was solid and insoluble. Cross-linking by auto-oxidation took between 50-75 days under ambient conditions, but the auto-oxidized PHA had a higher tensile strength and was more brittle than the chemically cross-linked polymers. It was suggested that m-CPBA treatment results in ether cross-links, whereas auto-oxidation resulted in carbon-carbon cross-links conferring more strength to the polymer (Ashby et al., 2000).

PHA films were synthesized by *P. oleovorans* grown with various ratios of octanoic, 10-undecenoic acid, and soybean acids followed by cross-linking treatment. Large variations in tensile strength and elongation at break were observed, such that film characteristics could be tailored by substrate feeding. In all cases, the films were biocompatible but each elicited different magnitudes of inflammation. They concluded that variation in film properties and degradation rates allow for diverse medical applications (Hazer et al., 2009, 2010). A cross-linked network of PHOU-*g*-PEG was produced by UV-irradiation to determine the effect on swelling for drug delivery. The addition of polyethylene glycol (PEG) into the cross-linked polymer reduced tensile strength and elongation to break with increasing PEG concentration and increased the degree of cross-linking and

hydrophilicity. PEG further improved the biocompatibility of mcl-PHAs by reducing platelet and protein interactions (Chung et al., 2003).

2.11. Conclusions

Policy changes towards global consumer sustainability will require a gradual replacement of petrochemical polymers with renewable materials. Currently, bio-based and/or biodegradable bioplastic production accounts for less than 1% of produced plastics production is expected to increase 36% by 2025. PHAs account for 1.7% of bioplastics produced. (Bioplastics market data, 2020). Driven by consumer demand for renewable and biodegradable polymers, particularly to replace single-use plastics, applications for PHAs are expected to increase (Bugnicourt et al., 2014; Chen et al., 2021). A number of challenges have prevented the replacement of conventional plastics with PHAs including higher production costs, processing difficulties and property deficiencies for given applications (Wang et al., 2014).

LCFAs from plant oils can be used for rapid microbial growth with high mcl-PHA yields and reduce the cost of production (Lee et al., 2000b; Ciesielski et al., 2015). LCFAs produce mcl-PHAs with longer and more unsaturated monomer compositions resulting in variability in polymer properties. The LCFA composition and the culturing methods can be adjusted to produce tailored mcl-PHA compositions (Solaiman et al., 2001; Mozejko and Ciesielski, 2014). The unsaturated moieties of mcl-PHAs have provided opportunities for further modification including hydroxylation, copolymer grafting, cross-linking and click-chemistry (Ashby et al., 2000; Hazer and Steinbüchel, 2007; Babinot et al., 2010). The following experimental chapters of this thesis will explore the production of mcl-PHAs from LCFAs, the effects of unsaturated moieties on polymer properties and the effects of cleavage of the unsaturated sidechains.

Chapter 3: Materials and Methods

3.1. Preface

This chapter outlines the methods repeatedly employed throughout the body of thesis research. Methods that are specific to individual procedures will be described in subsequent chapters.

3.2. Microorganisms and Microbial Culturing

Pseudomonas putida LS46 (International Depository Authority of Canada Accession Number 181110-03) (Sharma et al., 2012) was used for production of PHAs. *P. putida* LS46 was revived from glycerol stock cultures (stored at $-80\text{ }^{\circ}\text{C}$) in Luria-Bertani broth (LB). Typically, a plate would be streaked and incubated for 48 h for short-term storage at $-4\text{ }^{\circ}\text{C}$. Either a colony would be picked, or the original LB sampled at 1% (vol/vol⁻¹), and sub-cultured in LB shaken at $30\text{ }^{\circ}\text{C}$ overnight prior to preparation of the experimental inoculum. Minimal growth medium (Ramsay et al., 1990) contained 6.7 g/L Na₂HPO₄, 1.5 g/L KH₂PO₄, 1 g/L (NH₄)₂SO₄, 0.2 g/L MgSO₄·7H₂O, 60 mg/L FeNH₄Citrate, 10 mg/L CaCl₂ and 1 mL of 1000X stock of trace elements (2.78 g/L FeSO₄·7H₂O, 1.98 g/L MnCl₂, 2.81 g/L CoSO₄·7H₂O, 0.17 g/L CuCl₂·7H₂O, 1.47 g/L CaCl₂·2H₂O, and 0.29 g/L ZnSO₄·7H₂O). This minimal broth was used for both inoculum and experimental conditions and adjusted to pH 7. All culturing occurred at $30\text{ }^{\circ}\text{C}$. Typical concentrations of 80-160 carbon atom equivalent millimolar (C-mM) of substrate were added to minimal medium Reagent grade chemicals were used for medium production (Sigma Chemical Co., St. Louis, MO; Fisher Scientific, Toronto, ON). Technical grades of oleic, linoleic and linolenic acid were used to compare the effect of unsaturated fatty acids. 90% oleic acid (Aldrich Chemistry) contained contaminant linoleic and saturated fatty acids. 60% linoleic acid (Acros Organics) contained largely oleic acid contamination. 70% linolenic acid (TCI) contained mostly

linoleic and oleic acid contaminants. Food-grade vegetable oils were hydrolyzed to their respective LCFAs. The purchased flax oil was cold-pressed. The hydrolysis was carried out by saponification using 250 g of NaOH and 500ml of water to 1 L of vegetable oil while gently mixing until solidified. A 200 mL solution of 50% H₂SO₄ was slowly added to release the free fatty acids. Additional H₂SO₄ solution would be added gradually as required to completely convert the solid soap into FFAs. A separatory funnel was used to separate the glycerol containing aqueous solution from the free fatty acids and any unreacted TAGs. The composition (wt%) of canola LCFAs was 4.7% palmitic acid, 2.1% steric acid, 67.1% oleic acid, 16.8% linoleic acid and 6.1% linolenic acid. The composition (wt%) of flax LCFAs was 6.7% palmitic acid, 4.7% steric acid, 21.1% oleic acid, 15.1% linoleic acid and 52.4% linolenic acid. Culturing was performed in 100-, 250-, 500-, or 1000-mL baffled flasks using a shaking incubator or in a 7 L bioreactor.

3.3. Reactor Preparation

The 7 L and 15 L reactors were equipped with a Rushton impeller, three baffles, an electrochemical DO electrode, and a pH electrode. All bioreactors, control tower, probes and accessory equipment were purchased from Applikon Biotechnology (Foster City, CA). The medium (without substrate) was added to the reactor prior to autoclaving for 1 h at 121°C. The reactor was then cooled to 30 °C and stabilized with air overnight to allow polarization of the DO electrode.

The Applikon ez-Control tower provided control and data recording of pH, temperature and dissolved oxygen. The pH was maintained at 6.5 by addition of 4 M NaOH through automated peristaltic pumps for all single substrate experiments. Temperature was maintained at 30 °C with heating jacket or by pumping ice water through the cooling sleeve. The DO electrode was allowed to polarize overnight, and calibration was performed at the same temperature (30°C), aeration rate

and agitation rate as was maintained during the experiment. A two-point calibration was carried out by gassing the reactor with N₂ at 500 mL min⁻¹ until the electrode current was stable at 0 mA, then aeration was turned on at 6 LPM. After the electrode current had stabilized, this was assigned a value of 100% of air saturation at 30 °C. It was assumed that the solubility of O₂ in the medium at 30 °C was 6.77 mg L⁻¹ (Vendruscolo et al., 2012). Since the slope of a one-point calibration was found to be in good agreement with the described two-point calibration, one-point calibrations (at operating conditions) were subsequently performed.

3.4. Sample Treatment

3.4.1. Residual Fatty Acid Sampling

This modified method for sampling residual fatty acid was performed in the late stages of this work. Previous sampling methods (Chapter 3, Section 3.4.3.) assayed the supernatant for residual substrate but due to the immiscible nature of LCFAs, the inability to homogeneously transfer and sample the supernatant became a major source of error. Instead, Polytetrafluoroethylene (PTFE)-lined screw-capped vials were prepared with 1 mL CHCl₃ prior to culturing. Upon withdrawing a sample of culture, 1 mL was immediately placed into a vial, shaken, and left overnight. The organic layer could then be transferred for transesterification (Chapter 3.5). This method resulted in smaller deviation and residual carbon concentrations closer to theoretical values (data not shown).

3.4.2. Microscopy and Plate Counts

A Nikon Ti-U inverted light/fluorescent microscope (Mississauga, ON) was used for cell and PHA visualization. Intracellular PHA content could be observed by staining with a lipophilic dye. A 0.1% solution of Nile Blue in ethanol was added to 200 µL of culture. Prior to microscopy,

the cells were washed and re-suspended in water. The cells were then wet-mounted and observed under green light (636 nm)(Sharma et al., 2017a).

When required, plate counts were performed to corroborate calculated non-PHA cell mass (NPCM) determined by GC. The percent increase in colony count was compared to the percent increase in calculated NPCM at timepoints throughout a reactor experiment to ensure that biomass readings were not artificially increased by unknown extracellular products. Serial dilutions (10^{-5} to 10^{-8}) were performed in PBS and a lawn was streaked onto triplicate LB agar plates. The plates were incubated at 30 °C for 48 h and counted to determine the concentration of colony forming units (CFU/mL).

3.4.3. Centrifugation, Biomass and Supernatant Treatment

A 25-40 mL sample of culture was centrifuged at $16,000 \times g$ for 10 minutes. The supernatant was stored at -20 °C and the pellet was washed with PBS buffer before being re-suspended in diH₂O and transferred to pre-weighed aluminum dishes. The biomass was dried at 60 °C for 24 h and the aluminum dishes re-weighed to determine cdm. The supernatant was vortexed to approach homogeneity and aliquots removed for measurement of residual ammonium and fatty acid concentrations. For fatty acid analysis, 1 mL sample was transferred into screw-capped vials for transesterification (Chapter 3, Section 3.5). For ammonium analysis, 5 mL of 5 X – 20 X sample dilutions were prepared and measured by flow injection with spectrophotometer (Lachat Instruments, CO) recordings at 630 nm to monitor the reaction to indophenol blue (Blunt et al., 2017).

3.5. PHA Extraction and Purification

Twenty to fifty grams of dried biomass was enveloped in tissue paper and placed in the chamber of a Soxhlet apparatus (various sizes equipped with 250 mL to 1L round bottom flasks.

Acetone, but sometimes chloroform or dichloromethane (DCM), were added to the Soxhlet flask and heated to a boil for 4 h to extract PHAs. The extract was titrated with cold methanol (MeOH) until precipitation of PHAs was observed, repeated, and washed with MeOH (Eggink et al., 1995).

3.6. Gas Chromatographic Analysis of PHA and Fatty Acids

PHA was converted to methyl ester monomers by methanolysis of 5 mg of dried biomass (Brandl et al., 1988). Fatty acids were converted to methyl esters using the same procedure, with one of the above (Section 3.4) sampling methods. In a screw-cap vial with PTFE liner, solutions of 1 mg/mL benzoic acid (internal standard) in chloroform and 15% H₂SO₄ in MeOH were added in 1 mL volumes to the sample/standard and heated to 80 °C for a minimum of 4 h. After cooling, 1 ml of water was added and left to separate overnight. The organic fraction was transferred to gas chromatography (GC) vials for analysis using an Agilent 7890 gas chromatograph with an Agilent DB-23 (122-2332E) polysiloxane high-polarity column, a flame ionization detector and equipped with a CombiPal autosampler (CTC Analytics, Zwingen, CH). The column temperature began at 60 °C for two minutes and then ramped by 15 °C/min to 270°C while maintaining 1ml/min flow of inert gas (helium). The retention times would vary over time and with refreshed columns, but are roughly represented in Table 3.1. Response factors for each monomer compared to the benzoic acid internal standard were derived from 3-hydroxy-methyl esters purchased from Sigma-Aldrich (St. Louis, MO). The response factors were regularly updated but are roughly represented in Table 3.1. In this manner, PHA monomer composition and PHA intracellular content could be determined from biomass samples. GC-MS was used to confirm the retention times of unsaturated PHA monomers, and their response factors were assumed to be the same as their saturated counterpart. Gravimetric PHA content analysis was consistent with the PHA content determined using these response factors (data not shown). Response factors for the determination for residual

fatty acids were performed with the same reagent grade fatty acids as provided for culturing and using a Supelco 37 Component FAME Mix from Millipore Sigma (Oakville, ON).

Table 3.1. PHA monomer analysis by gas chromatography.

3-Hydroxyacyl Methyl Ester	Retention Time (min)	Retention Factor
C4 ME	6.22	5.56
C5 ME	6.99	4.01
C6 ME	7.80	1.16
C7 ME	8.52	1.81
C8 ME	9.34	1.38
C8-1 ME	9.61	1.38
C9 ME	9.95	1.31
C10 ME	10.68	1.27
C10-1 ME	10.97	1.27
C12 ME	11.85	1.22
C12-1 ME	11.93	1.22
C12-2 ME	12.26	1.22
C14 ME	12.86	1.59
C14-1 ME	13.01	1.59
C14-2 ME	13.24	1.59
C14-3 ME	13.55	1.59

Chapter 4: Optimized oxygen-limited production of medium chain length polyhydroxyalkanoates from long chain fatty acids using *Pseudomonas putida* LS46

4.1. Preface

This first chapter on experimental research outlines the efforts to produce mcl-PHAs from LCFAs in high cell density cultivations. Bulk polymer production was required to test the material properties of mcl-PHAs, and to produce unsaturated mcl-PHAs from LCFAs for chemical modification. Mcl-PHAs from LCFAs were also required to meet the requirements for biocomposite production outlined in the Fiber Composite and Biomatrix Genomics project. Oxygen-limitation was encountered in numerous high cell density cultivation attempts, however the response to those conditions by *P. putida* LS46 using LCFAs was notably different than the literature reports using *Pseudomonas* sp. with MCFAs. Where oxygen-limitation would cease cell growth and MCFAs would quickly become toxic resulting in reactor failure (foaming), cultures of LCFAs continued to grow and produce PHA production in absence of the toxicity effect and a differential response to oxygen limitation based on substrate. The following results describe how oxygen-limiting PHA production using LCFAs might theoretically be the most productive.

4.2. Introduction

Regulations on single-use plastics have been implemented in 127 countries (Chen et al., 2021), and manufacturing industries are pledging for increased sustainability through reduction, recycling and substitution with sustainable polymers (Berg et al., 2020).

Medium chain length PHAs have improved the elasticity compared to scl-PHAs and are promising for their barrier properties (Tortajada et al., 2013; Tappel et al., 2014).

The cost of PHA production compared to conventional petroleum-derived polymers is a limitation to commercial applications. The lowest cost estimations for PHB production range from 2-6 US\$/kg (Choi and Lee, 1997; Levett et al., 2016; Koller et al., 2017), however mcl-PHAs have lower reported polymer yields, lower volumetric productivities and are most-often produced from MCFAs which would significantly increase the estimated production cost. Various strategies for improving PHA yield and productivity have been described through high cell density cultivation (Ienczak et al., 2013; Blunt et al., 2018b; Koller, 2018). Waste feedstocks have been investigated to reduce the cost of mcl-PHA production, but consideration to monomer composition changes due to substrate structure must be taken (Nikodinovic-Runic et al., 2013; Ciesielski et al., 2015). LCFAs are promising feedstocks for mcl-PHA production since they are a related substrate that provide good polymer yields and are ubiquitous commercial bi-products (Kellerhals et al., 2000; Fernández et al., 2005; Kang et al., 2017). High cell density cultivations of mcl-PHAs from LCFAs have been performed in fed batch with volumetric productivities up to $1.93 \text{ g L}^{-1} \text{ h}^{-1}$ (Kellerhals et al., 2000; Lee et al., 2000b; Ruiz et al., 2019). The objective of this study was to assess high cell density fed-batch production of mcl-PHAs using LCFAs under oxygen limiting conditions for PHA accumulation.

4.3. Methods

4.3.1. Microorganism, Medium and Substrate

This method is discussed in Chapter 3, Section 3.2. Specifically, the minimal medium was modified to for an increased starting ammonium sulfate concentration to 1.5 g/L. Bioreactor experiments were initiated by the addition of 5% (vol vol⁻¹) inoculum. All experiments were conducted with canola LCFAs.

4.3.2. Reactor Setup and Preparation

This method is described in Chapter 3, Section 3.3. The highest cell density was obtained in a 15 L bioreactor with 5 L working volume using 14% ammonium hydroxide to maintain pH and residual nitrogen concentrations. A solution of 4 M H₂SO₄ was also prepared for pH control. Aeration consisted of 5 L/min air and the one-point dissolved oxygen calibration was performed. Mixing cascaded from 250 rpm to 1000 rpm to maintain dissolved oxygen at 40%. Up to 5 L/min oxygen supplemented the aeration when the dissolved oxygen level could no longer be maintained by mixing speeds. Canola LCFAs were fed exponentially from 4 h post inoculation (pi) using a $\mu = 0.5 \text{ h}^{-1}$ determined to approach the μ_{max} experimentally measured in previous batch reactors. Visual observation of centrifuged sample determined that LCFAs were abundant at 12 h pi at which time the ammonium hydroxide was switched to 4 M sodium hydroxide and substrate feeding was halted.

The results obtained using the bioreactor methods outlined above were compared to results in bioreactors with lower volumetric oxygen mass transfer coefficients ($k_{\text{L}}a$) to model the rate of biomass production after the onset of oxygen limitation. The comparative reactors were performed in 7 L bioreactor with 3 L working volumes and 6 L/min air without supplemental oxygen (consistent headspace and air sparging volumes at smaller scale). These conditions are differentiated by cascading mixing from 300-1000 rpm (unreported results) or fixed mixing rate of 500 rpm (Chapter 5) with feeding from 4 h pi using $\mu = 0.5 \text{ h}^{-1}$.

Using the experimental data obtained from these two high cell density reactors, models were produced to predict the reduction in required feeding rates after the onset of

oxygen-limiting equilibrium. The models observe a reduce in specific biomass accumulation rate (h^{-1}) which incorporates the feeding requirement for the accumulation of PHA production. The feeding models began with the experimental substrate delivery based on a biomass accumulation rate of 0.8 h^{-1} and decayed over six hours, then length of time observed between oxygen limitation and nitrogen limitation (observed after removing ammonium from base in pH control), at which time a rate of 0.2 h^{-1} was observed. With the additional constraints that the feeding rate meets the minimum of 0.2 h^{-1} and does not exceed 0.8 h^{-1} , models for the rate of decay were produced. The models were then used to predict biomass beginning at the onset of limitation and overlaid with experimental data to determine the best fit.

4.4. Results

The high cell density production of *P. putida* LS46 with canola LCFAs using supplemented oxygen reproducibly obtained 53.7 g L^{-1} of cdm at 12 hours post-inoculation (h pi), despite dissolved oxygen having reached 0% by 7 h pi (Figure 4.1). The final mcl-PHA concentration was 15.7 g L^{-1} in 24 h, resulting in a volumetric productivity of $0.65 \text{ g L}^{-1} \text{ h}^{-1}$. The intracellular mcl-PHA content during between 5-13 h pi was $11.9 \pm 2.4 \%$, which rose to 30.4% from 13-24 h pi in response to growth cessation from nitrogen limitation. The continued rate of growth post oxygen-limitation was too rapid to observe a significant increase in intracellular PHA accumulation.

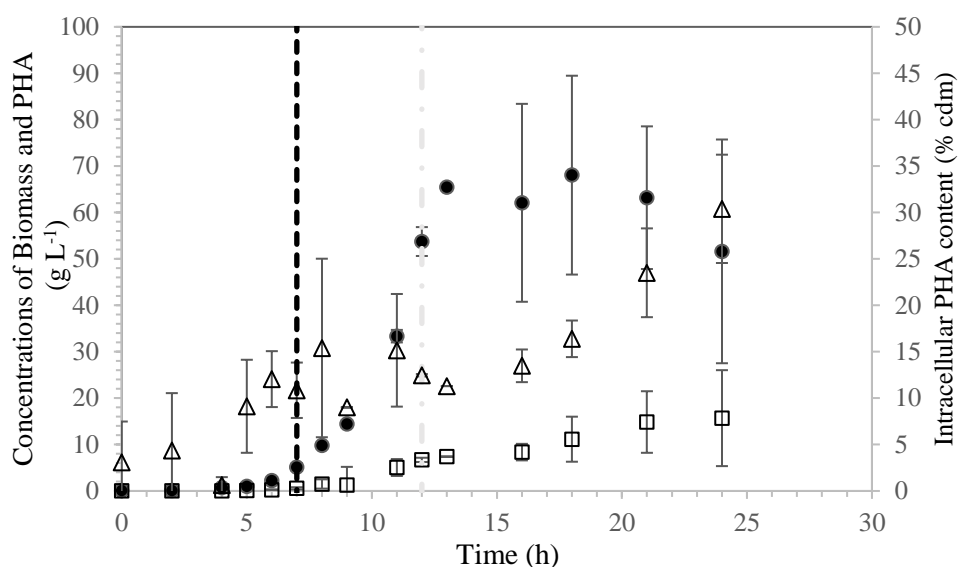


Figure 4.1. Exponential feeding of LCFAs derived from canola oil to a 5L working volume of *P. putida* LS46. Biomass concentration (●), PHA concentration (□) and PHA content (Δ). The dashed lines represent onset of oxygen limitation (— —) which remained at DO=0% for the remainder of the experiment. A change in feeding (— ●) was initiated. The reactor conditions were repeated providing standard deviations of the two reactors.

Unlike the response of *P. putida* LS46 to dissolved oxygen limitation grown on octanoic acid which resulted in immediate reduction in cell growth and increased PHA accumulation rates (Blunt et al., 2017), *P. putida* LS46 continued to produce NPCM under microaerophilic conditions using canola LCFAs. The rate of biomass production after oxygen limitation is almost linear under these conditions. As seen in Figure 4.2, the linear rate of biomass production was dependent on the mass transfer of oxygen. Biomass was produced at $0.48 \text{ g L}^{-1} \text{ h}^{-1}$ with low agitation (500 rpm in 7 L reactor), at $2.25 \text{ g L}^{-1} \text{ h}^{-1}$ with high agitation (1250 rpm in 7 L reactor) and at $8.16 \text{ g L}^{-1} \text{ h}^{-1}$ with high agitation and supplemental oxygen (1000 rpm and $1 \text{ vol vol}^{-1} \text{ O}_2$ in 15 L reactor).

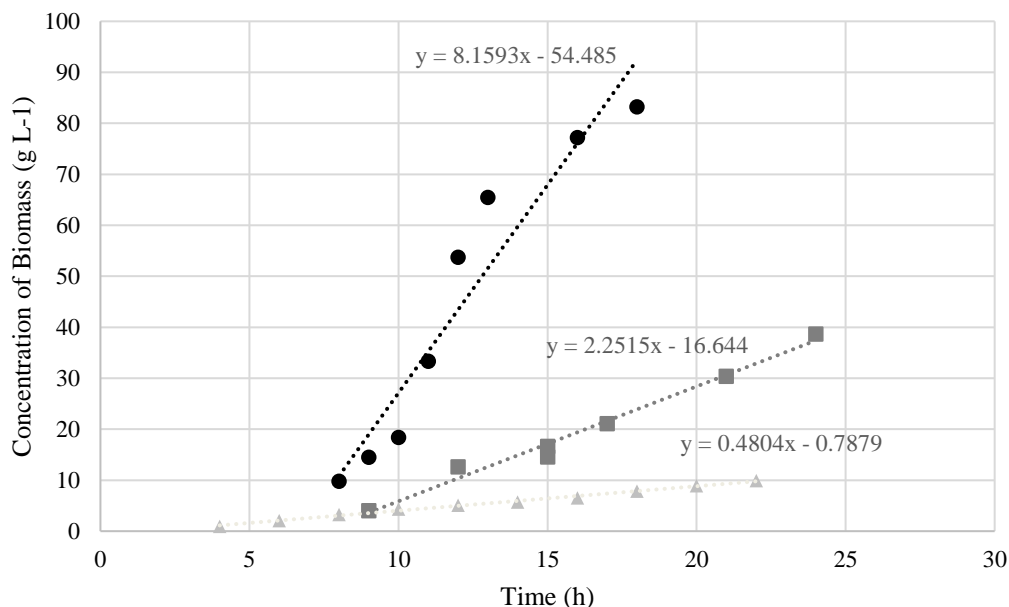


Figure 4.2. The linear rate of biomass production after reaching oxygen-limiting equilibrium during low-mixing (▲), high-mixing (■) and high-mixing + O₂ supplementation (●) canola LCFA cultivations.

4.5. Discussion

Mcl-PHA production from LCFAs have already been optimized for high cell densities and high volumetric productivities (Kellerhals et al., 1999; Shang et al., 2008; Andin et al., 2017). The highest reported volumetric productivity for mcl-PHAs from LCFAs is 1.91 g L⁻¹ h⁻¹ (Lee et al., 2000b). Ultimately, maximizing oxygen delivery with micro-bubblers, agitation and pure oxygen are needed to obtain such a result. However in addition to high k_{LA} , substrate delivery regimes that slow cellular oxygen uptake by limiting the microorganism's specific growth rate have been modelled to maximize the cellular titer by avoiding oxygen limitation and minimize the cultivation time (Maclean et al., 2008; Davis et al., 2015).

The results presented here (Figure 4.1) are interesting not for their productivity, but because they were obtained by maintaining a feeding rate based on $\mu = 0.5 \text{ h}^{-1}$, which quickly became oxygen-limited. Substrate began to accumulate rapidly as the growth rate slowed in response to oxygen limitation, however the culture continued to grow and produce PHAs constrained only by the inherent limitations of the system. Fundamentally, the energy derived from cellular oxygen uptake can be associated with cell growth, cell maintenance and PHA accumulation. At the equilibrium of oxygen-limitation, where cellular oxygen uptake equals the rate of oxygen mass transfer, the energy producing capabilities of the system becomes fixed, which explains the linear biomass production observed in Figure 4.2. Cell titer continues to increase with further growth and the energy requirements for cellular maintenance increase. Biomass increases appeared linear, but the specific growth rate was slowing, and the cells were accumulating higher contents of mcl-PHAs. This PHA accumulation, which can be observed with oxygen limitation (Blunt et al., 2018a), was not observed in the results presented in Figure 4.1 because insufficient reduction in growth rate had occurred in the narrow timeframe prior to the induction of nitrogen limitation. Eventually, as cell titer increases and cellular oxygen uptake per cell is reduced, cellular maintenance will require all the energy produced, and the intracellular PHA content should near its theoretical maximum for this system. This will come at the expense of carbon yield requiring reactor termination at the optimum mcl-PHA yield to maximize intracellular PHA content.

Limitation of oxygen will always be the final constraint to achieving maximum titer of mcl-PHAs. Cultivation strategies typically avoid oxygen limitation with slower growth rates to achieve higher titers. The data presented here could be used to model a system that

allows oxygen limitation for maximum biomass and PHA accumulation and minimizes rate reductions brought on from carbon or nitrogen limitation. The main drawback of this approach is that the dO_2/CO_2 off-gas concentrations are the most valuable real-time signals for assessing the state of the system, which do not fluctuate when oxygen uptake matches its mass transfer. Optical density becomes unreliable with homogenized LCFAs and supernatant fouling. The cultivations observed in Figure 4.1 continued with only visual assessments of biomass pellet and excess LCFAs. They were terminated with changes to feeding based on unreliable performance metrics, otherwise cell titer and productivity could have been increased. Further improvements require a better comprehension of system performance after dissolved oxygen is undetectable. Figure 4.3 attempts to model theoretical reductions in the specific biomass accumulation rate (cell+PHA) after onset of oxygen limiting conditions, adapted from some of the carbon-limited strategies employed by Maclean et al. 2008. The model begins feeding based on a specific biomass accumulation rate of 0.8 h^{-1} for *P. putida* LS46 from LCFAs exceeds the experimental μ of *P. putida* LS46 during this time ($\mu = 0.50 \text{ h}^{-1} \pm 0.05$), however the feeding model only begins after at 4 h pi to observe any possible lag based on the response of dissolved oxygen, so $\mu = 0.8 \text{ h}^{-1}$ ensures excess feeding is sustained until the model needs to adapt for oxygen limitation. The theoretical biomass obtained from these equations were plotted next to the experimental data in Figure 4.4. The exponential decay in specific biomass accumulation rate best describes the experimental data, however further cultivation would likely require models that decay to $\mu = 0.5 \text{ h}^{-1}$ and further for experimental data to fit. These models were adapted to fit this experimental setup, for the purpose of determining feeding rates for future cultivations under these conditions.

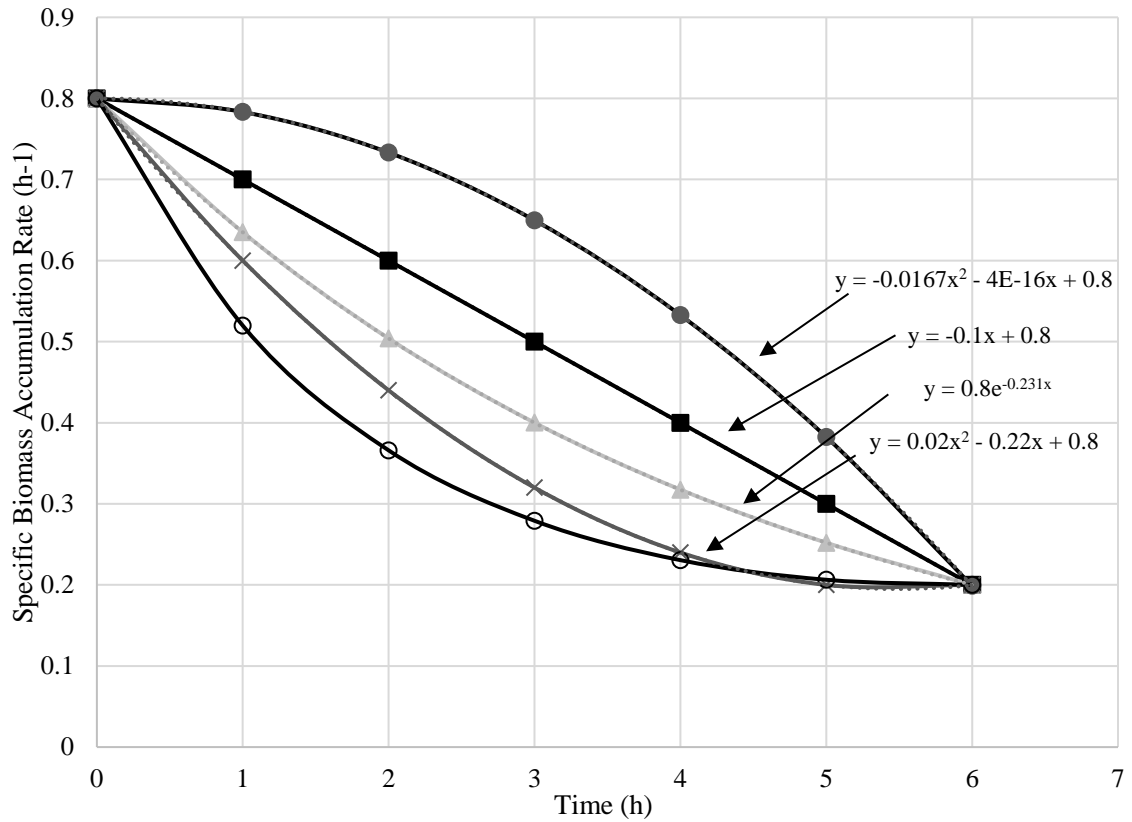


Figure 4.3. Modelling decay of specific biomass accumulation rate after onset of oxygen-limitation based on Figure 4.1. Linear (■), “+”-quadratic (x), “-”-quadratic (●), exponential (▲), exponential quadratic (○) rates of decline. The exponential quadratic equation was $y=0.8e(0.04x^2 -0.471x)$.

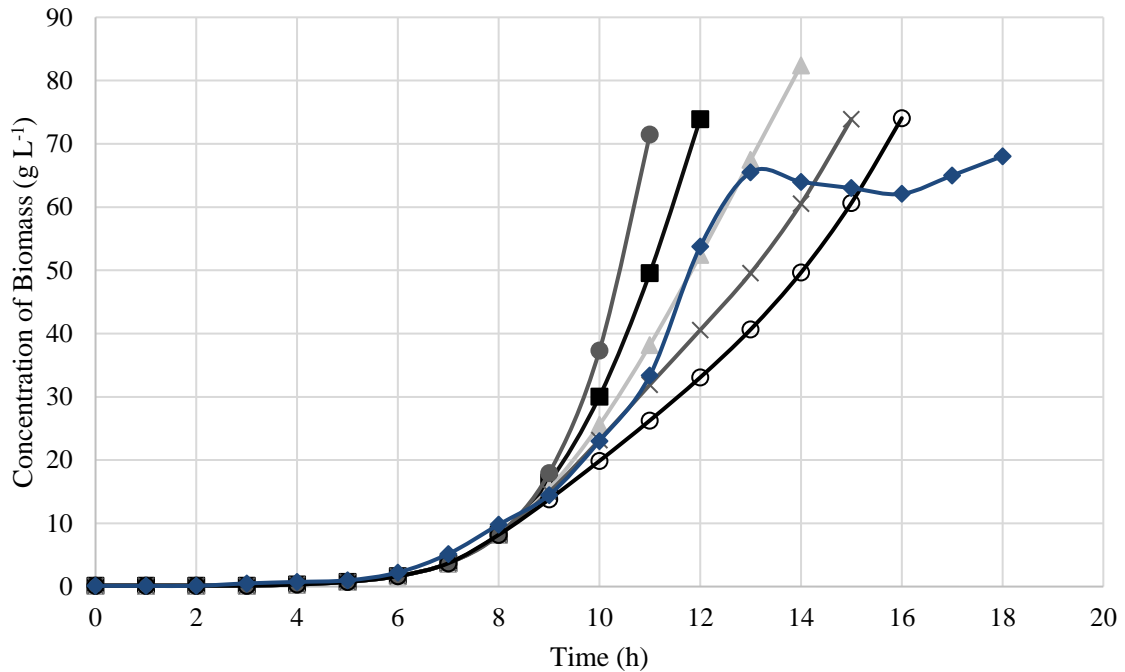


Figure 4.4. Theoretical biomass obtained from modelled specific growth rate decline after onset of oxygen-limitation (Figure 4.3.) compared to experimental values (◆) (Figure 4.1.). Linear (■), “+”-quadratic (×), “-”-quadratic (●), exponential (▲), exponential quadratic (○) rates of decline.

This approach of high cell density production of mcl-PHAs has not been previously reported and determining the real-time performance metrics after onset of oxygen-limitation was a design-limitation. Further exploration of this system could produce models adaptable for a bioreactor system of any given k_{LA} . In this way, feeding strategies can be developed to maximize cell titer, substrate yield and productivity and properly employ dual limitation without proper real-time feedback. FTIR methods can be applied for rapid and quantitative analysis of intracellular PHA content (Hong et al., 1999; Arcos-Hernandez et al., 2010), which could direct process termination for optimum PHA content and maximize the substrate yield.

Chapter 5: Carbon flux to growth or polyhydroxyalkanoate synthesis under microaerophilic conditions is affected by fatty acid chain-length in *Pseudomonas putida* LS46

5.1. Preface

In the previous chapter, the challenges of predicting cell growth and PHA production during oxygen limitation during high cell density fed-batch on LCFAs were described. The cellular response to oxygen-limitation required further understanding to predictively model systems for high volumetric productivity. The solubility of oxygen into water is considerably lower than any other medium component which presents a challenge to any high cell density cultivation, compounded further with increasing scale. High cell densities are required to improve the productivity of mcl-PHA production, leaving only two options: avoid oxygen-limitation through pre-emptive nutrient-limitation or utilize oxygen-limitation for mcl-PHA production. The latter was not well studied and, since dissolved oxygen is the clearest real-time experimental feedback, required an improved experimental understanding to determine feed rates during the PHA accumulation phase at high cell densities. It became clear that *P. putida* LS46 had various responses to oxygen-limitation based on substrate, unlike the relatively predictable PHA accumulation phase from depletion of other nutrients. Therefore, the following series of experiments were designed with Warren Blunt, who was already investigating the effects of microaerophilic environments on mcl-PHA production, to better understand these effects for improved bioprocess control of mcl-PHA production.

Co-feeding was previously performed using LCFAs and octanoic acid in flasks to determine if any preference in substrate or change in monomer composition could be

observed (Table 5.1) with methods described in Chapter 3.2. The co-feeding data obtained in flasks indicated that co-feeding could result in higher biomass than when solely produced on octanoic acid; and higher intracellular PHA content and C8 monomer content than when solely produced on LCFAs. This initiated the in-depth analysis of co-feeding and the response to oxygen limitation on carbon flux in the chapter below.

The following chapter was published in *Applied Microbiology and Biotechnology* 2018 102(15): 6437-6449. This publication was a formal co-authorship with Warren Blunt. The tasks of experimental design, sampling, sample processing/analysis, and manuscript preparation were shared equally. My contributions were to design the LCFA and co-feeding experiments and a process to hydrolyze canola oil to free fatty acids, perform the LCFA and co-feeding experiments and provide insight on monomer composition and product characteristics of the mcl-PHAs. Warren Blunt provided programming, automation, and on-line bioreactor monitoring; performed the octanoic acid experiments and performed the mass balancing and yield analysis.

As it was not reported in the published manuscript, the values for biomass coefficient from ammonium sulfate ($Y_{X/N}$) was 1.93 g/g. The biomass coefficient from octanoic acid ($Y_{X/C}$) was 0.72 g/g. These values were determined experimentally. Feeding of LCFAs from canola oil was calculated to be carbon equivalent (C_{mol}/C_{mol}) to the feeding of octanoic.

Table 5.1. Mixed substrate flask cultivation of *P. putida* LS46.

	Biomass (g L ⁻¹)	PHA Content (% cdm)	Monomer Composition (mol %)				Residual Substrate (g L ⁻¹)	
			C6	C8	C10	C12	Octanoic	Oleic
<i>Oct:Can</i> 12h (20:20e mM)	1.7 +/- 0.13	21.4 +/- 2.3	7.3 +/- 0.10	85.3 +/- 0.35	6.0 +/- 0.27	1.3 +/- 0.08	1.6 +/- 0.76	1.6 +/- 0.24
<i>Oct:Can</i> 18h (20:20e mM)	2.7 +/- 0.22	41.2 +/- 1.6	7.5 +/- 0.11	84.3 +/- 0.28	6.9 +/- 0.34	1.3 +/- 0.11	0.6 +/- 0.18	1.6 +/- 0.28
<i>Oct:Can</i> 24h (20:20e mM)	3.8 +/- 0.07	55.6 +/- 3.6	7.2 +/- 0.10	82.5 +/- 0.65	8.6 +/- 0.55	1.6 +/- 0.18	0.2 +/- 0.11	1.0 +/- 0.19
<i>Oct:Can</i> 36 h (20:20e mM)	4.1 +/- 0.12	65.9 +/- 3.1	7.3 +/- 0.26	79.3 +/- 1.17	10.9 +/- 0.96	2.5 +/- 0.37	0.0 +/- 0.42	0.4 +/- 0.01
<i>Oct:Can</i> 12h (20:20e mM)	1.6 +/- 0.16	16.8 +/- 2.4	7.3 +/- 0.05	85.2 +/- 0.51	6.1 +/- 0.38	1.3 +/- 0.08	1.5 +/- 0.70	1.3 +/- 0.06
<i>Oct:Can</i> 18h (20:20e mM)	2.7 +/- 0.30	42.9 +/- 4.5	7.4 +/- 0.44	84.2 +/- 0.66	7.1 +/- 0.28	1.3 +/- 0.05	0.7 +/- 0.39	1.1 +/- 0.06
<i>Oct:Can</i> 24h (20:20e mM)	3.6 +/- 0.37	58.4 +/- 2.8	7.3 +/- 0.09	81.8 +/- 0.50	9.2 +/- 0.30	1.7 +/- 0.11	0.1 +/- 0.03	0.5 +/- 0.38
<i>Oct:Can</i> 36h (20:20e mM)	4.0 +/- 0.09	60.0 +/- 0.9	7.3 +/- 0.42	80.4 +/- 0.57	10.2 +/- 0.64	2.2 +/- 0.19	0.0 +/- 0.06	0.4 +/- 0.05
Octanoic 12h (40 mM)	0.0 +/- 0.34	12.1 +/- 0.6	8.6 +/- 0.48	84.9 +/- 4.33	4.5 +/- 3.46	1.9 +/- 1.26	4.2 +/- 1.74	n.a.
Octanoic 18h (40 mM)	0.6 +/- 0.28	11.1 +/- 4.1	9.0 +/- 0.47	86.4 +/- 1.68	3.2 +/- 1.34	1.4 +/- 0.62	2.5 +/- 0.41	n.a.
Octanoic 24h (40 mM)	0.9 +/- 0.20	16.9 +/- 2.3	9.0 +/- 0.20	87.0 +/- 0.77	2.6 +/- 0.71	1.3 +/- 0.28	2.8 +/- 1.07	n.a.
Octanoic 36h (40 mM)	2.2 +/- 1.09	51.0 +/- 19.0	8.3 +/- 0.65	89.3 +/- 1.78	1.7 +/- 0.87	0.7 +/- 0.38	0.8 +/- 0.96	n.a.
Canola 48h (60 mM)	2.95 +/- 0.52	33.4 +/- 5.8	5.4 +/- 0.2	41.4 +/- 0.6	26.7 +/- 5.1	9.1 +/- 1.2	n.a.	n.d.

*Italicized substrate was used for inoculum growth. n.a. – not applicable. n.d. - not determined. e – c-mol equivalent.

5.2. Abstract

Economical production of mcl-PHA is dependent on efficient cultivation processes. This work describes growth and mcl-PHA synthesis characteristics of *Pseudomonas putida* LS46 when grown on MCFAs (octanoic acid) and lower-cost LCFAs, derived from hydrolyzed canola oil, in microaerophilic environments. Growth on octanoic acid ceased when the oxygen-uptake rate was limited by the oxygen-transfer rate, and mcl-PHA accumulated to 61.9% of the cdm. From LCFAs, production of NPCM continued at a rate of $0.36 \text{ g L}^{-1} \text{ h}^{-1}$ under oxygen-limited conditions, while mcl-PHA accumulated simultaneously to 31% of the cdm. The titer of NPCM from LCFAs at 14 h pi was double that obtained from octanoic acid in bioreactors operated with identical feeding and aeration conditions. While the productivity for octanoic acid was higher by 14 h, prolonged cultivation on LCFAs achieved similar productivity but with twice the PHA titer. Simultaneous co-feeding of each substrate demonstrated the continued cell growth under microaerophilic conditions characteristic of LCFAs, and the resulting polymer was dominant in C8 monomers. Furthermore, co-feeding resulted in improved PHA titer and volumetric productivity compared to either substrate individually. These results suggest that LCFAs improve growth of *P. putida* in oxygen-limited environments and could reduce production costs since more NPCM, the cellular factories required to produce mcl-PHA and the most oxygen-intensive cellular process, can be produced for a given oxygen transfer rate.

5.3. Introduction

Medium chain-length polyhydroxyalkanoates are bio-polyester polymers synthesized by primarily *Pseudomonas* species, under nutrient-limited conditions as a means of storing carbon and energy (Anderson and Dawes, 1990; López et al., 2015; Anjum et al., 2016). While these polymers may have value as renewable and biodegradable alternatives to traditional petroleum-based polymers, current cost estimates range from three to fifteen-fold higher than polyethylene or polypropylene (Możejko-Ciesielska and Kiewisz, 2016; Kourmentza et al., 2017), and must be reduced to facilitate widespread application.

Since the carbon source for PHA production has been reported to account for a significant proportion of the production costs (Choi and Lee, 1997; Koller et al., 2017), it is imperative to find inexpensive and readily available feedstocks. Long chain fatty acids (LCFAs) are a promising candidate for PHA production because the theoretical yield of polymer (3-hydroxydecanoate) from LCFAs (i.e. oleic acid) via β -oxidation is relatively high (Chanprateep, 2010). There is a significant amount of waste LCFAs available as TAGs or free fatty acids from the food-processing and biodiesel production industries (Chhetri et al., 2008; Du et al., 2012; Nikodinovic-Runic et al., 2013). Both LCFAs and TAGs are carbon-rich waste streams that create significant disposal challenges due to high biochemical oxygen demand and their hydrophobicity and insolubility in aqueous medium (Ravindran and Jaiswal, 2016; Wallace et al., 2017). In North America and other temperate regions, waste sources of LCFAs (including biodiesel and hydrolyzed cooking oil wastes) are typically derived from plant oils like canola and soybean (Song et al., 2008; Nikodinovic-Runic et al., 2013). These contain a mixture of fatty acids, predominantly

C16:0, C18:0, C18:1 and C18:2 fatty acids (Fu et al., 2014). Fatty acids are degraded to acetyl-CoA and acyl-CoA intermediates using the β -oxidation cycle, producing reduced electron carriers NADH and FADH₂. The PHA synthase has low substrate specificity, which allows incorporation of various acyl-CoA monomers into the polymer (Kim et al., 1997). The predominant mcl-PHA monomer units from fatty acids are eight and ten carbons in length, but LCFAs have been reported to produce PHA polymers containing longer as well as unsaturated monomer units (De Waard et al., 1993; Haba et al., 2007).

In addition to using low-cost carbon feedstocks, improving productivity through cultivation techniques or mode of bioreactor operation is crucial to the sustainability of PHAs (Kaur and Roy, 2015; Koller et al., 2017). To date, the highest productivities for both scl- and mcl-PHA production have been achieved through fed-batch strategies, in which cells are grown to high cell densities with high polymer content in short cultivation times (Wang and Lee, 1997; Lee et al., 2000b; Maclean et al., 2008). However, these high cell density cultures are inevitably limited by the oxygen transfer rate (OTR) from the introduced gas into the liquid phase resulting in environments with low dissolved oxygen. Previously, it was shown that in such microaerophilic environments with excess ammonium, *P. putida* LS46 accumulates mcl-PHA to 57.3% of the cdm in 14 h from 20 mM octanoic acid, and that the polymer synthesis rate was improved as the k_{La} was reduced (Blunt et al., 2017). While that work showed that oxygen-limited mcl-PHA production could be a viable mcl-PHA production strategy, the results were limited to octanoic acid and productivity was limited by batch cultivation. This work aims to build on previous work by identifying if the previous response observed under oxygen limitation could be extended to other fatty acids, and specifically lower-cost LCFAs, or if it was a unique

manifestation of mcl-PHA synthesis from octanoic acid. The objectives of this work are therefore to: 1) compare growth and PHA synthesis characteristics from LCFAs and octanoic in fed-batch cultivations with low DO which are likely to persist in high cell density cultures and large-scale bioreactors; and 2) examine the effect of co-feeding both substrates to improve mcl-PHA productivities and/or yields.

5.4. Materials and Methods

5.4.1. Microorganism, Medium, and Substrates

This method is discussed in Chapter 3, Section 3.2. Specifically, the minimal medium was modified to for an increased starting ammonium sulfate concentration to 1.5 g/L. Experiments were initiated by the addition of 5% (vol vol⁻¹) inoculum. In all experiments the addition of LCFAs, whether adding an initial concentration to a flask or bioreactor, or during fed-batch experiments (described below) was C-mol equivalent to the addition of octanoic acid.

5.4.2. Reactor Setup and Preparation

All reactor experiments were conducted in a 7 L glass, round-bottom reactor with a 3 L initial working volume. The reactor was prepared as described in Chapter 3, Section 3.3. Aeration rate (6 LPM) and agitation rate (500 rpm) were fixed during the experiments.

The k_{La} was determined in the absence of cells in 3 L Ramsay medium (no substrate added) by the dynamic out-gassing method (Garcia-Ochoa et al., 2010). Briefly, the reactor (under operating conditions) was gassed with N₂ at 500 mL min⁻¹ until the DO signal was stable. Subsequently, aeration was turned on at 6 LPM and the DO response was measured and recorded in LabBoss software in five-second intervals. It was assumed that the probe response could be modeled as first order, and the response time was determined to be 24

sec, as previously described (Blunt et al., 2017). The corresponding k_{LA} was determined to be $54 \pm 3 \text{ h}^{-1}$. Carbon dioxide in the off-gas was measured with either an HPR 40 dissolved species membrane inlet mass spectrometer (MIMS, Hiden Analytical, Warrington, UK) or a BlueInOne Cell O_2/CO_2 sensor (Bluesens Gas Sensor, GmbH, Germany). The MIMS setup and calibration procedures have been previously described elsewhere (Blunt et al. 2014).

5.4.3. Feeding Rates

During initial attempts at optimizing fed-batch cultivations, several trials on octanoic acid were conducted using a variety of exponential feeding rates and high k_{LA} values resulting from use of a mixing cascade up to 1200 rpm. When those trials were compared to growth on LCFAs using a relatively fast feeding rate ($\mu = 0.5 \text{ h}^{-1}$), it was observed that under similar oxygen-limited conditions, *P. putida* LS46 produced significantly higher total biomass and NPCM. Because of this observation, the feeding of carbon and nitrogen sources was modeled for a μ of 0.25 h^{-1} (Equation 1). The rate of feeding for carbon and ammonium were calculated according to Equation 2 and Equation 3, respectively. In the case of LCFAs, the carbon feed rate was adjusted to be carbon-mol (C-mol) equivalent to the 0.25 h^{-1} feeding schedule developed for octanoic acid. Although the feeding schedule was based on maintaining a μ of 0.25 h^{-1} , this will not be achieved in practice upon onset of oxygen limitation. The purpose of this model was to observe how each carbon source is utilized when fed at the same rate (i.e. C-mol hour^{-1}) under oxygen-limited conditions.

$$[X(t)] = [X_{t_0}]e^{\mu(t-t_0)} \quad (\text{Eq. 1})$$

$$[C(t)] = \frac{[X_t]e^t - [X_{t_0}]e^{t_0}}{Y_{X/C}} \quad (\text{Eq. 2})$$

$$[N(t)] = \frac{[X_t]e^t - [X_{t_0}]e^{t_0}}{Y_{X/N}} \quad (\text{Eq. 3})$$

Where X = NPCM (g); X_{t_0} = the amount of NPCM present in the bioreactor at the beginning of the time interval (g); t_0 , t the beginning and end of a given time interval (h), respectively. $C(t)$ and $N(t)$ are the required amounts (g) of carbon or ammonia, respectively, fed to the bioreactor in a given time interval; $Y_{X/C}$ and $Y_{X/N}$ are the yield coefficients of NPCM from the carbon source and ammonium (g g^{-1}), respectively. The yield coefficients were derived from previous experimental values (unpublished data). Square brackets indicate concentration.

After an hour delay following inoculation, carbon (either LCFAs or octanoic acid) and a 200 g L^{-1} solution of $(\text{NH}_4)_2\text{SO}_4$ were continually supplied with two titration syringes adapted to three-way valves. The feeding program described above was automated in LabBoss software (Scion, Rotorua, New Zealand). Calibration and operation of this setup has been previously described in greater detail by Blunt et al. (2014). The initial value of X_{t_0} was set as 0.75 g to compare the cell mass production by *P. putida* LS46 cultured with LCFAs versus octanoic acid. All conditions were run in duplicate.

5.4.4. Co-feeding and Prolonged LCFA Cultivation Experiments

To investigate further potential for production of NPCM and/or mcl-PHA under microaerophilic conditions, experiments were conducted using co-feeding and LCFA feeding with prolonged cultivation under identical aeration conditions ($k_{\text{La}} = 54 \text{ h}^{-1}$). To avoid preferential uptake of octanoic acid or LCFAs, the co-feeding experiments were initiated with a 5% (vol vol^{-1}) inoculum from cells grown in LB medium, and washed in sterile PBS solution. Due to technical limitations, NH_4OH was used in place of $(\text{NH}_4)_2\text{SO}_4$ and NaOH for co-feeding experiments to maintain ammonium and pH levels. The co-

feeding experiments were started with 10 mM of octanoic acid and C-mol equivalent LCFAs.

The feeding rates for prolonged co-feeding and LCFAs cultivations were identical (C-mol h⁻¹) to the aforementioned experimental rates (0.25 μ) up to 16 h pi. During co-feeding, each substrate was fed in a 1:1 ratio on a C-mol basis. As the exponential feeding program resulted in highly excess conditions by 16 h pi, feeding rates were decreased for further cultivation. Further cultivation with LCFAs provided substrate and (NH₄)₂SO₄ at linear rates of 1.43 g h⁻¹ and 0.59 g h⁻¹ respectively, while carbon feeding was ceased at 16 h pi in co-feeding experiments. In all experiments, the feeding after 16 h pi was determined to maintain carbon and ammonium in excess without approaching toxic concentrations.

5.4.5. Sample Treatment

After inoculation, 40 mL samples were periodically withdrawn and treated as per Chapter 3, Section 3.4.3.

5.4.6. Analysis of Mcl-PHA, Fatty Acids, and Ammonium

See Chapter 3, Section 3.6 for PHA and fatty acid analysis methods, and Chapter 3, Section 3.3.3. for residual ammonium analysis.

5.4.7. Carbon Balancing and yield analysis

Carbon balances were performed for both substrates following the approach described by Blunt et al. (2017), in which the carbon moles of detected mcl-PHA monomers, NPCM, and CO₂ were compared to the carbon moles of substrate consumed. It was assumed that the chemical composition of *P. putida* NPCM could be approximated as C₄H₇O₂N and having a molecular weight of 101 g mol⁻¹ (Guedon et al., 1999). It was determined that each mole of PHA monomers derived from the octanoic acid polymer

contained 7.9 moles of carbon and had an average molecular mass of 159.4 g mol⁻¹. The corresponding values for carbon content and molecular mass of LCFA PHA were 10.3 C-mol mol⁻¹ and 194.7 g mol⁻¹, respectively. Similarly, the PHA obtained from co-feeding experiments contained 8.2 C-mol mol⁻¹, and had molecular mass of 162.3 g mol⁻¹. These values were obtained as the weighted average of the detected monomers.

The yield of PHA from carbon substrate was calculated as the slope of a plot between PHA titer (g L⁻¹) and substrate uptake (g L⁻¹). The theoretical yield of PHA from octanoic acid and LCFAs were assumed to be 0.98 and 0.72 g g⁻¹, respectively. These values were obtained from the ratio of molecular mass of an average monomer sub-unit (described in the assumptions above) and dividing it by the molecular mass of the carbon substrate. Due to the mixed composition of LCFAs derived from canola oil, it was assumed to have a molecular mass of 271.5 g mol⁻¹. This value was obtained as the weighted average of the molecular masses of the individual fatty acid components detected by GC.

Due to problems determining the concentration of (insoluble) residual LCFAs in the culture medium, the carbon consumption was back-calculated for LCFA cultures by assuming that all carbon could be accounted for through measurement of mcl-PHA monomers, NPCM, and CO₂. The validity of this assumption has been tested through previous High-performance liquid chromatography (HPLC) analysis for soluble end-products in the supernatants of both octanoic acid and LCFA-grown cultures (unpublished data). The efficacy of the back-calculation method was verified using the results from octanoic acid, and it was found that octanoic acid uptake could be estimated within an average margin of error of 10%.

5.5. Results

On the basis of the results shown in Table 5.2, a feeding program of $\mu = 0.25 \text{ h}^{-1}$ was chosen for growth on octanoic acid since higher rates led to rapid accumulation of octanoic acid to inhibitory levels. Stirring was kept constant at 500 rpm to provide consistent OTR throughout both conditions and avoid variations in the response of the DO controller. The following results describe the performance comparison between LCFA and octanoic acid feeds under identical exponential rates (C-mol h^{-1}) with DO as the only growth-limiting variable.

5.5.1. Dissolved Oxygen

The measured DO profiles are shown in Figure 5.1A. The reactor was saturated with air ($\text{DO} = 100\%$ or 6.77 mg L^{-1}) prior to inoculation, after which the culture consumed DO until the electrode read zero current at 4 h pi, despite constant mixing and aeration. After 4 h pi, the oxygen uptake rate should be equivalent to the OTR, which is in turn limited by k_{La} . Previous studies have confirmed that such conditions correspond to DO concentrations less than 0.05 mg L^{-1} (Blunt et al. 2017). The DO remained below detectable limits until the experiment was terminated in the case of growth on LCFAs, or until octanoic acid accumulated to an inhibitory level, which is shown by the rapid rise in DO after 14 h pi.

Table 5.2. Determination of appropriate specific growth rate for exponential feeding of octanoic acid to *P. putida* LS46.

Feeding program	Maximum Biomass g/L cdm	Maximum PHA Content % cdm	End to process h pi	Reason for termination
$\mu=0.5 \text{ h}^{-1}$ from 0h pi with octanoic acid	2.6	13.6	10	Octanoic acid concentration $\geq 50 \text{ mM}$
$\mu=0.5 \text{ h}^{-1}$ from 6 h pi with octanoic acid	3.9	30.3	9	Octanoic acid concentration $\geq 50 \text{ mM}$
$\mu=0.4 \text{ h}^{-1}$ from 4 h pi with octanoic acid	12.4	39.1	16	Octanoic acid concentration $\geq 50 \text{ mM}$
$\mu=0.25 \text{ h}^{-1}$ from 4 h pi with octanoic acid	21.5	41.5	33	Reduction in OD ₆₀₀ of culture
$\mu=0.5 \text{ h}^{-1}$ from 4h pi with LCFAs	46.7	32.8	35	Excess substrate

5.5.2. Total Biomass and PHA Accumulation in Single Substrate Comparison

Figure 5.1A shows the total biomass produced throughout the growth curves for each condition. The two conditions produced similar concentrations up to 4 h pi. After 6 h pi, when exponential growth was finished due to onset of oxygen limitation, the difference in total biomass became increasingly higher for the culture grown on LCFAs compared to octanoic acid. Accumulation of PHA is shown in Figure 5.1B. The mcl-PHA content of octanoic acid-grown cultures was initially $28.0 \pm 6.1\%$ cdm due to carry-over from the inoculum and decreased to $19.2 \pm 3.0\%$ cdm at 4 h pi. The onset of oxygen limitation caused PHA to accumulate to $61.5 \pm 1.4\%$ cdm by 14 h pi, which is expected when the DO was maintained at 1-5% or less in the presence of excess carbon (Blunt et al. 2017). The maximum mcl-PHA titer of $2.5 \pm 0.3 \text{ g L}^{-1}$ (Figure 5.1B). When the substrate was LCFAs, the initial PHA content detected at 0 h pi was $8.5 \pm 5.8\%$ cdm and was similar at 4 h pi when the DO concentration dropped below detectable limits for the electrochemical probe ($12.2 \pm 6.8\%$ cdm). Following onset of oxygen limitation, the cellular PHA content increased to $34.2 \pm 6.1\%$ cdm by 16 h pi. The mcl-PHA titer in *P. putida* LS46 cultured with LCFAs reached $1.9 \pm 0.6 \text{ g L}^{-1}$ cells at 16 h pi.

5.5.3. Analysis of NPCM, Residual Fatty Acid and Residual Ammonium

Concentrations

A contrast in NPCM production was observed for octanoic acid and LCFA cultures following the onset of oxygen-limitation at 4 h pi (Figure 5.1C). The NPCM became relatively constant from 6 h pi in the octanoic acid-grown cultures, after which the majority of the total biomass increase was due to PHA accumulation. When grown on LCFAs, the NPCM increased at a relatively constant rate ($0.36 \text{ g L}^{-1} \text{ h}^{-1}$) for 8 h past the onset of oxygen

limitation, reaching $3.7 \pm 0.1 \text{ g L}^{-1}$. This was more than double the highest value obtained by the culture grown on octanoic acid at 14 h pi ($1.6 \pm 0.1 \text{ g L}^{-1}$).

Figure 5.1D displays the residual octanoic acid and LCFA concentrations. Both substrates were slowly depleted for the first 8 h pi, after which the residual substrate levels began to accumulate. After 14 h pi, octanoic acid had accumulated to inhibitory levels ($\geq 50 \text{ mM}$), and this toxicity likely led to the observed decrease in the NPCM of octanoic-acid fed cultures at 14-16 h pi. When in excess, the LCFAs were observed to form a layer on top of the medium after centrifugation, and the actual concentration of residual LCFAs was difficult to determine. No inhibitory or toxic effects were observed due to excess LCFAs, as was observed with excess octanoic acid. A similar trend was observed with residual ammonium concentrations using both substrates (Figure 5.1D). The residual concentrations of carbon substrate and free ammonium being measured in excess for the entire cultivation period confirmed that oxygen uptake rate was the only growth-limiting factor.

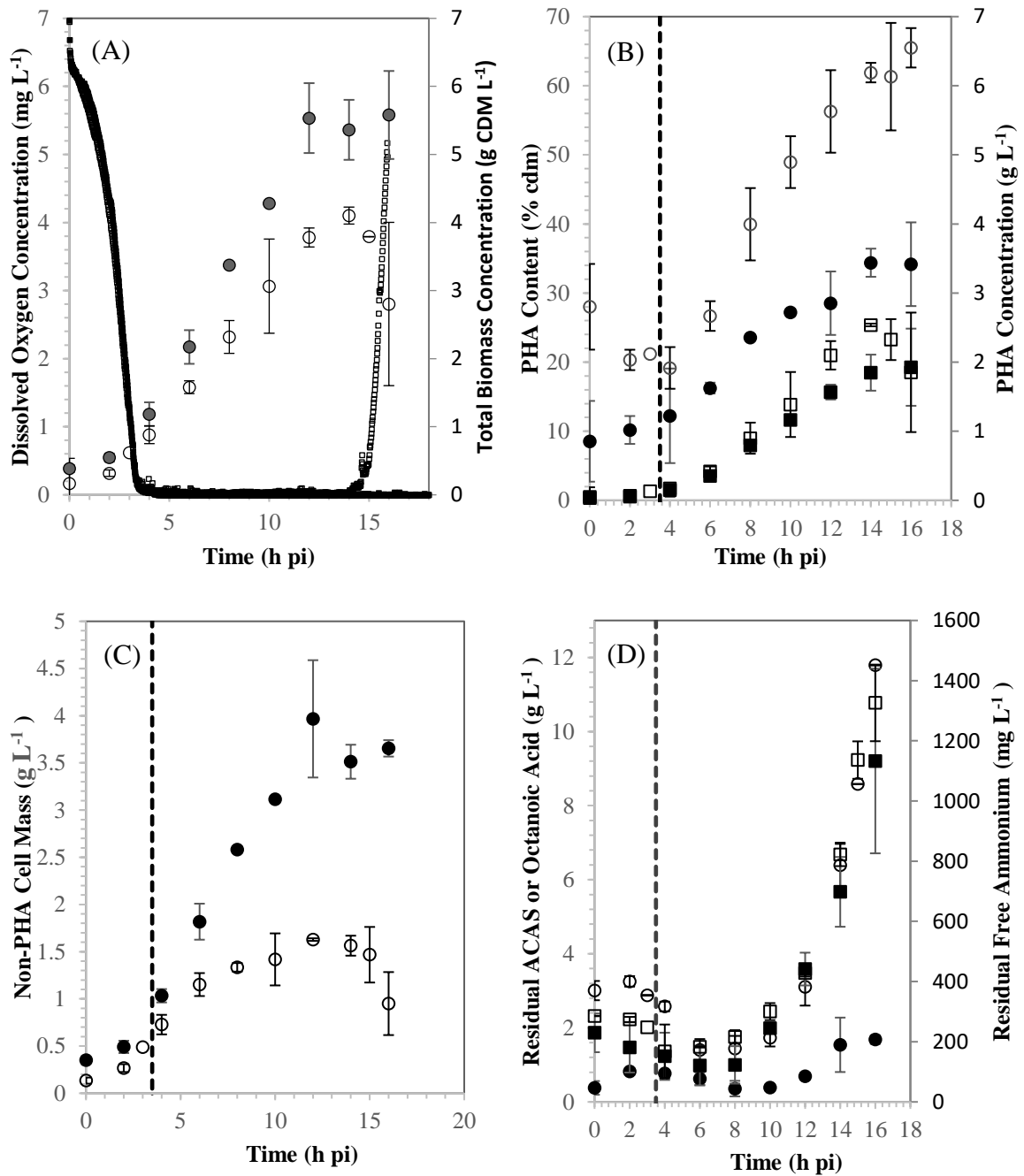


Figure 5.1. Comparison of *P. putida* LS46 grown as a fed-batch at $\mu = 0.25 \text{ h}^{-1}$ on LCFAs (filled) or octanoic acid (unfilled). (A) Biomass (circles) and dissolved oxygen (squares). (B) Intracellular PHA content (circles) and total PHA concentration (squares). (C) Non-PHA Cell Mass (D) Residual carbon substrate (circles) and residual ammonium (squares)

5.5.4. Co-Feeding and Prolonged Incubation Experiments

Due to the higher biomass production and continued growth trends observed over the course of the previous experiments with LCFAs, the cultivations were prolonged with additional feeding to observe further potential capacity of both biomass and PHA production. The NPCM production from these prolonged LCFA experiments is shown in Figure 5.2A. The total biomass, NPCM and PHA content continued to increase after 16 h pi and NPCM finally stabilized near $7.1 \pm 0.4 \text{ g L}^{-1}$ (over four times the maximum NPCM obtained from octanoic acid growth), while the final PHA content reached $38.3 \pm 2.8\%$ cdm at 30 h pi, resulting in a PHA titer of $4.4 \pm 0.8 \text{ g L}^{-1}$ (Table 5.3)

The results for the single substrate experiments indicate that for constant bioreactor conditions, the LCFAs have the potential to produce higher total biomass and NPCM under microaerophilic conditions, but the PHA content of the cells was still lower in comparison to octanoic acid cultures. This led to querying the effect of co-feeding both substrates. The total biomass, PHA content, and PHA titer from the co-feed experiments are shown in Figure 5.2B. By 26 h pi, the total biomass reached $11.7 \pm 0.1 \text{ g L}^{-1}$, containing $54.1 \pm 2.2\%$ PHA, resulting in a PHA titer of $6.3 \pm 0.3 \text{ g L}^{-1}$. The NPCM for the co-feed experiment is shown in Figure 5.2A and is overlaid with other results of the single-substrate experiments for comparison. Over the course of the co-feed cultivation, the NPCM was lower compared to when LCFAs were the sole carbon source and reached at final titer of $5.4 \pm 0.4 \text{ g L}^{-1}$ at 26 h pi (Table 5.3) This value is 3.3 times more than the maximum NPCM titer obtained when octanoic acid was the sole substrate.

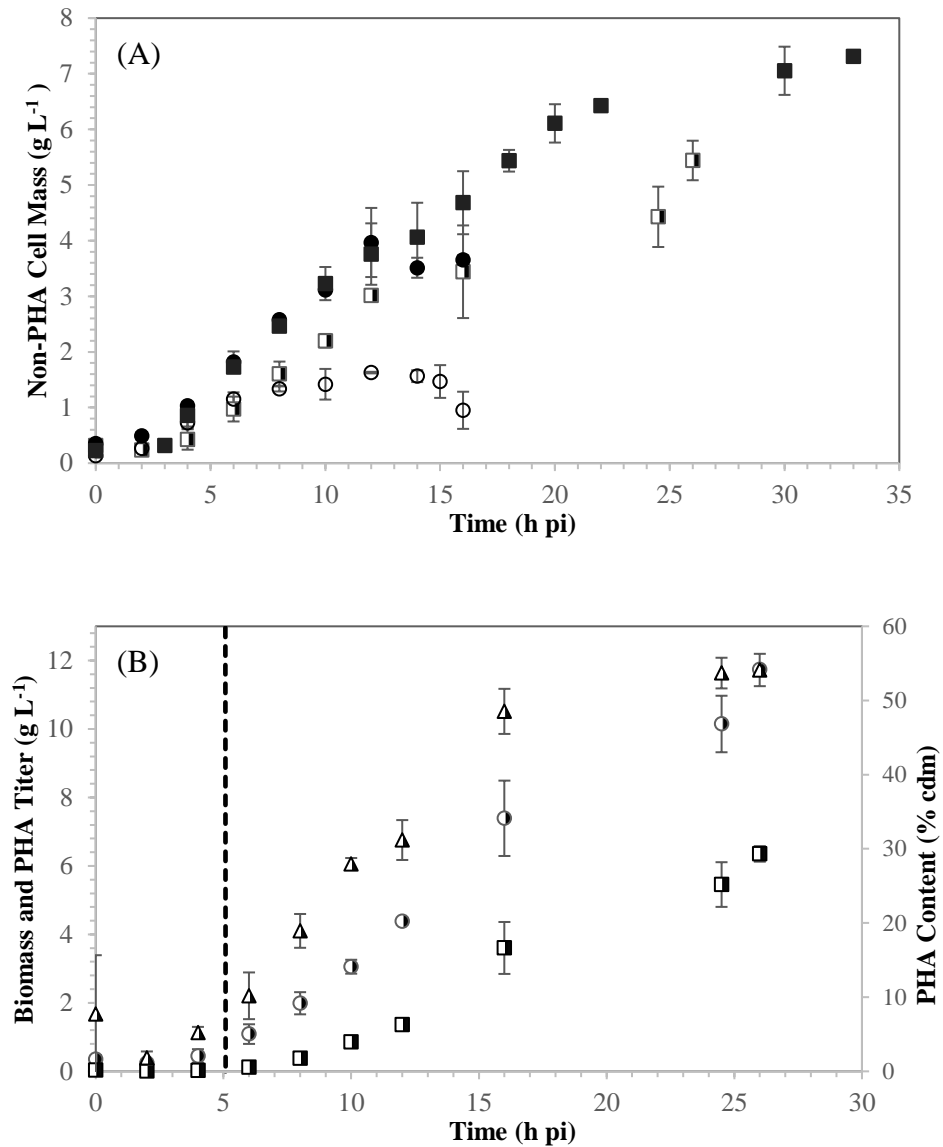


Figure 5.2. Prolonged cultivation of *P. putida* LS46 with LCFAs (filled), octanoic acid (unfilled) and a co-feed (half-filled). (A) The non-PHA cell mass demonstrating a substrate-dependent response of *P. putida* LS46 in response to oxygen limitation. (B) Biomass and PHA production from the C-mol equivalent octanoic acid and LCFA co-feed.

Table 5.3. Comparison of key process performance indicators during mcl-PHA production by *P. putida* LS46 from LCFAs or octanoic acid as the sole carbon source, or when co-fed in C-mol equivalent proportions.

	<u>LCFAs</u>		<u>Octanoic</u>	<u>Co-Feed</u>	
	16 h pi	30 h pi	14 h pi	16 h pi	26 h pi
Biomass (g L ⁻¹)	5.6 ± 0.6	11.5 ± 1.2	4.1 ± 0.1	7.4 ± 1.1	11.7 ± 0.1
NPCM (g L ⁻¹)	3.7 ± 0.1	7.1 ± 0.4	1.6 ± 0.1	3.8 ± 0.3	5.4 ± 0.3
PHA Content (% cdm)	34.1 ± 6.1	38.3 ± 2.8	61.9 ± 1.4	48.5 ± 3.0	54.1 ± 2.2
PHA Titer (g L ⁻¹)	1.9 ± 0.6	4.4 ± 0.8	2.5 ± 0.0	3.6 ± 0.8	6.4 ± 0.2
Vol. Productivity	0.12 ± 0.04	0.15 ± 0.03	0.18 ± 0.00	0.23 ± 0.05	0.24 ± 0.01

5.5.5. Volumetric Productivity

Overall volumetric productivities for each process are summarized in Table 5.3. For the octanoic acid cultivation, volumetric productivity reached a maximum value of $0.18 \pm 0.00 \text{ g L}^{-1} \text{ h}^{-1}$ by 14 h pi. By comparison, lower volumetric productivity was observed in the LCFA cultivation at 14 h ($0.12 \pm 0.01 \text{ g L}^{-1} \text{ h}^{-1}$). With prolonged feeding, the LCFA cultures reached a maximum volumetric productivity of $0.15 \pm 0.02 \text{ g L}^{-1} \text{ h}^{-1}$ after 30 h pi. In the co-feed experiments, the maximum volumetric productivity was $0.24 \pm 0.01 \text{ g L}^{-1} \text{ h}^{-1}$ at 26 h pi.

5.5.6. Carbon Balancing and Yield Analysis

Figure 5.3. shows the carbon flux under oxygen-excess (0-4 h pi) and oxygen-limiting conditions (6-12 h pi and onward) for octanoic acid (Figure 5.3A) and LCFAs (Figure 5.3B). When octanoic acid was the substrate, the main trade-off in carbon flux is between NPCM and PHA. With the onset of oxygen limitation at 4 h pi, the yield of NPCM decreased (0.48 to $0.08 \text{ C-mol C-mol}^{-1}$), while PHA yield increased (0.19 to $0.55 \text{ C-mol C-mol}^{-1}$). Little change was observed in CO_2 yield over time regardless of DO content, which is consistent with previous batch results (Blunt et al. 2017). When LCFAs were the substrate, the onset of oxygen limiting conditions increased the carbon flux to PHA (0.12 to $0.25 \text{ C-mol C-mol}^{-1}$), but the reduction in carbon flux to NPCM (0.60 to $0.39 \text{ C-mol C-mol}^{-1}$) was not nearly as significant as in the case of octanoic acid. Further incubation of the LCFA culture beyond 12 h pi resulted in similar carbon flux to PHA and a reduction in carbon flux to NPCM ($0.30 \text{ C-mol C-mol}^{-1}$) with increased CO_2 production. Since the yield of mcl-PHA from LCFA was well below the calculated theoretical value (0.72 g g^{-1}) it is possible that higher mcl-PHA content was not obtained in the LCFA-grown culture during

the first 16 h (Figure 5.1B) because NPCM also continued to increase, and accounted for a significant portion of the carbon consumed during this period. While the presence of some longer chain and unsaturated monomers suggested that a portion of the mcl-PHA was synthesized from octanoic acid, the estimated maximum yield of mcl-PHA from octanoic acid in the co-feed experiments was observed between 8 h pi and 26 h pi was 0.49 ± 0.05 C-mol C-mol⁻¹ and was comparable to the yield obtained when octanoic acid was the sole carbon source.

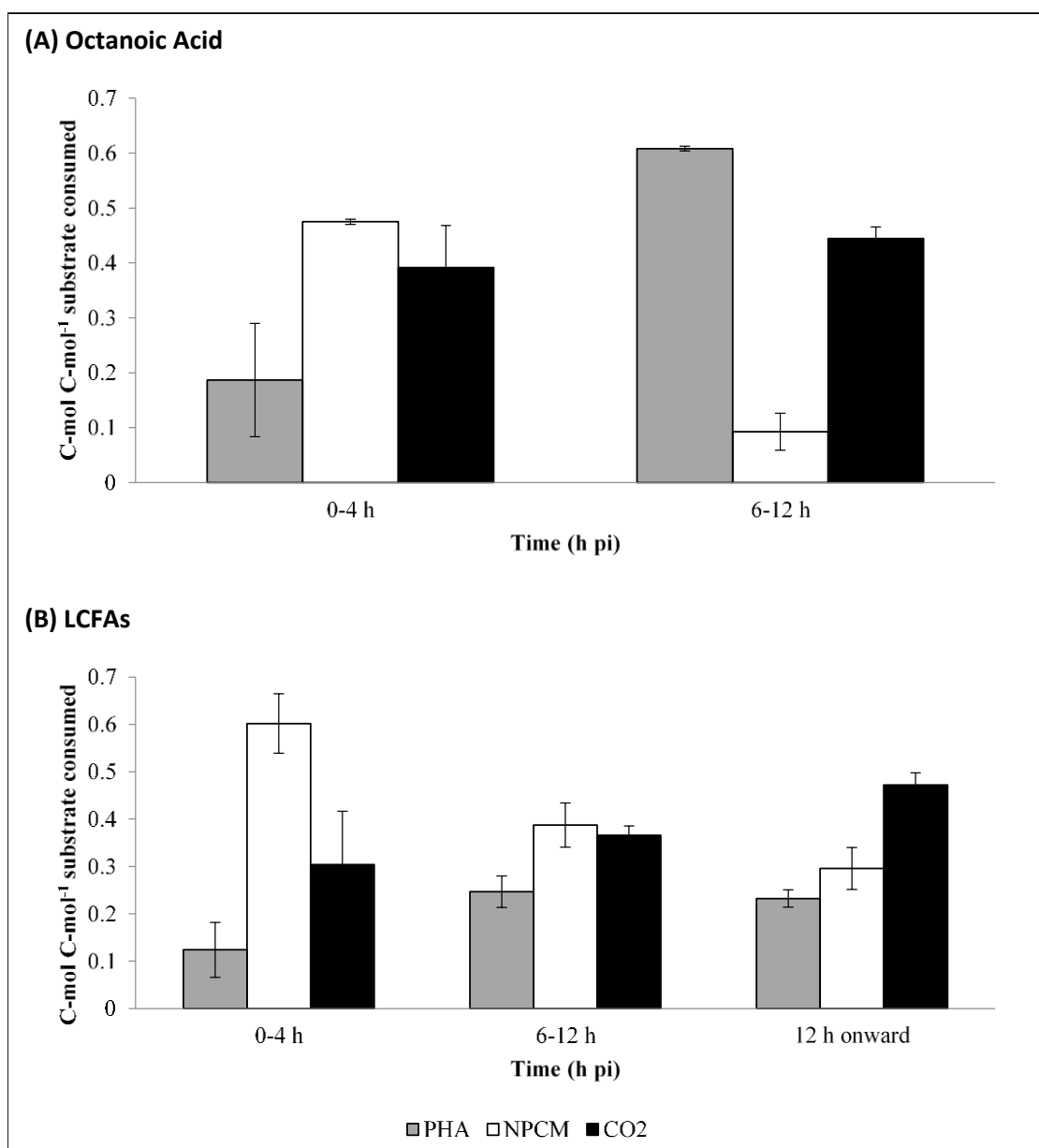


Figure 5.3. Yield analysis for octanoic acid grown cultures (A) and LCFA-grown cultures (B) under oxygen excess conditions (0-4 h) and oxygen limited conditions (6-12 h and 12 h onward). Error bars represent standard deviations between biological replicates.

5.5.7. Monomer Composition of PHA

Monomer composition of the PHAs produced from both octanoic acid and LCFAs are shown in Table 5.4. As indicated, the polymer produced from octanoic acid contained predominantly C8 monomers, which is consistent with the literature (Kellerhals et al., 2000; Elbahloul and Steinbüchel, 2009; Fontaine et al., 2017). Previously, it was reported that oxygen-limitation did not significantly affect the monomer composition mcl-PHA polymers when octanoic acid was the substrate (Blunt et al., 2017). The polymer synthesized from LCFAs consists of a distribution of monomers ranging from C6 to C14, with C8 and C10 as the dominant fatty acids. Further, the LCFA-derived polymers also contained monomers with unsaturated carbon-carbon double-bonds (C12:1 and C14:1). Similar monomer compositions have been reported for mcl-PHAs synthesized by other bacteria using LCFAs as substrates (Huijberts et al., 1992; Kellerhals et al., 2000; Fernández et al., 2005; Fontaine et al., 2017). The mcl-PHAs produced by *P. putida* LS46 from LCFAs remain amorphous, presumably since they contain longer and unsaturated monomers and exhibit a higher degree of disorder. In contrast, mcl-PHA polymers synthesized from octanoic acid crystallize into elastomers. Similar observations have been previously reported (Kellerhals et al., 2000). Co-feeding of octanoic acid and LCFAs produced a polymer dominant in C8 monomers. Comparing the monomer composition of co-feeding against single substrate feeding (Table 5.4), the C8 monomer content was increased while longer monomer lengths were reduced 90% compared to the PHA from LCFAs.

Table 5.4. Final monomer compositions of mcl-PHA polymers synthesized from LCFAs and octanoic acid by *P. putida* LS46. Values are expressed as mol percent of the total monomers detected by gas chromatography and measured at 16 h pi.

Substrate	mol% C ₆	mol% C ₈	mol% C ₁₀	mol% C ₁₂	mol% C ₁₄	mol% C _{12:1}	mol% C _{14:1}
Octanoic	7.8 ± 0.3	89.3 ± 0.1	2.3 ± 0.2	0.6 ± 0.2	0	0	0
LCFAs	5.4 ± 0.2	41.4 ± 0.6	26.7 ± 5.1	9.1 ± 1.2	9.3 ± 1.6	3.6 ± 0.9	8.6 ± 3.9
Co-feed	6.9 ± 0.2	80.7 ± 0.5	9.0 ± 3.4	1.7 ± 0.5	0	0.5 ± 0.0	1.0 ± 0.2

5.6. Discussion

Fed-batch cultures are regarded as the best method for highly productive PHA production (Sun et al., 2007), but producing high cell density cultures can be infeasible at larger scale due to power consumption for aeration, agitation, or use of purified oxygen (Lara et al., 2006). In this study, growth on an equal C-mol basis and under identical, oxygen-limited bioreactor operating conditions resulted in double the NPCM titer from LCFAs compared to cells grown on octanoic acid at 14 h pi. In addition, the yield of NPCM from LCFAs remained relatively high in an oxygen-limited environment at 0.39 C-mol C-mol⁻¹, while the yield of NPCM from octanoic acid was almost negligible at 0.09 C-mol C-mol⁻¹. This suggests that LCFAs may be good substrate to efficiently produce NPCM, or the cell chassis required to accumulate mcl-PHA, particularly when oxygen is limited. However, overall productivity is not only a function of high cell titer, but also requires obtaining a high intracellular PHA content (Choi and Lee, 1999a). While lower volumetric productivity was obtained at 14 h pi for LCFA compared to octanoic acid, similar productivity was obtained by extending the LCFA cultivation to 25 h pi. It is important to note that, despite lower intracellular PHA content, the PHA titer from LCFAs at 25 h pi was more than double the maximum titer obtained from octanoic acid. This shows the potential value of sustained growth of NPCM with simultaneous PHA production under low-DO conditions. A recent study of metabolic flux in N-limited fed batch culture of *P.*

putida KT2440 grown on oleic acid has suggested that residual growth may also improve PHA yield by linking production of reduced cofactors of FADH₂ and NADH to anabolic demand (Andin et al., 2017). Cell growth simultaneous to PHB synthesis was reported not to affect PHB yield and improved the PHB synthesis rate in P-limited fed batch cultures of *C. necator* grown on butyric acid (Grousseau et al., 2013).

The sustained growth rate on LCFAs and PHA synthesis from octanoic acid suggest an opportunity to maximize PHA titer and productivity in low-DO environments thereby reducing operating costs. The data obtained through co-feeding of octanoic acid and LCFAs indicates that both substrates were being consumed simultaneously with continued NPCM production after onset of oxygen limitation. The PHA content of 54.1% was improved over LCFA cultivations and the monomer composition was very similar to that obtained from octanoic acid in terms of C8 content (Table 5.4).

Further optimization of the octanoic acid and LCFA feeding proportions and rates could further improve PHA titer, productivity increase polymer uniformity and improve PHA yield from octanoic acid. In a similar way, phase feeding strategies have used glucose or glycerol as an inexpensive carbon source for the growth phase followed by feeding fatty acids to improve polymer content of the cells (Kim et al., 1997; Mozejko and Ciesielski, 2014; Davis et al., 2015; Fontaine et al., 2017) or to obtain novel monomer compositions (Dufresne et al., 2001; Kurth et al., 2001; Hartmann et al., 2006). The highest yield of PHA from nonanoic acid was achieved by co-substrate growth with glucose in the presence of acrylic acid to prevent fatty acid degradation (Jiang et al., 2012).

Continued NPCM production from LCFAs (compared to octanoic acid) under oxygen-limited conditions is interesting from a redox perspective. Previously it was shown

that in a microaerophilic environment, mcl-PHA is efficiently synthesized from octanoic acid and the polymer consists of predominantly C8 monomers (2 electron oxidation) (Blunt et al., 2017). This was thought to be a possible mechanism to maintain cellular redox through the reduction of a minimal amount of oxygen, while providing some energy conservation through oxidative phosphorylation. When LCFAs are used as the substrate, β -oxidation cycle needs to remain active to shorten oleic acid to C8-C10 (R)-3-hydroxyacyl-CoA monomers (4-5 complete cycles), which appear to be preferentially incorporated by the PHA synthase (Table 5.4). Because *P. putida* lacks any fermentative pathways, the resulting reduced electron carriers (NADH, FADH₂) must be oxidized via electron transport to O₂ (Sohn et al., 2010; Nickel and de Lorenzo, 2013). This could create high NADH/NAD⁺ ratios, a condition previously linked to PHA synthesis (Ren et al., 2009), and result in a major bottleneck for growth in a microaerophilic environment. However, contrary to this expectation, a consistent increase in NPCM was observed in the current study when *P. putida* LS46 was cultured on LCFAs.

Examination of the available literature suggests several possible explanations for this observation: 1) Fatty acids are known to exert considerable toxicity on cells by disruption of the membrane potential and electron transport (Desbois and Smith, 2010; Jarboe et al., 2013). When the substrate is octanoic acid, less carbon is available per proton translocated (compared to oleic acid), and this could cause greater uncoupling of proton-motive force and result in less ATP conserved, and hence less NPCM produced. 2) Transport of fatty acids could be more limiting for one substrate depending on the hydrophobicity of the molecule (Jarboe et al., 2013). 3) LCFAs have been shown to bind to transcription factors (PsrA, FadR) and cause de-repression of genes associated with fatty

acid degradation and electron transport (Dirusso and Black, 2004; Fujita et al., 2007; Kang et al., 2008). This would be expected to cause increased growth and less PHA production, which was recently demonstrated in a PsrA deficient mutant of *P. putida* KT2440 during growth on decanoate (Fonseca et al., 2014). These same observations occurred in this work when LCFAs were present whether as the sole carbon source or when co-fed with octanoic acid. While the mechanism for the observed differences between the two substrates remains unclear, follow-up proteomic or transcriptomic analysis should be done to improve understanding of how the cell may respond at the molecular level to exogenous fatty acids of different chain-lengths.

In conclusion, when grown on free fatty acids, carbon flux in *P. putida* LS46 appears to be greatly influenced by the length of the fatty acid carbon chain, particularly under microaerophilic conditions. In cells cultured with octanoic acid as the sole carbon source, we observed growth arrest and rapid mcl-PHA accumulation when the oxygen uptake rate became limited by the bioreactor OTR. In contrast, we observed continued cell division and lower mcl-PHA accumulation in cells cultured with LCFAs as the sole carbon source under identical conditions. This resulted in over twice the NPCM when grown on LCFAs after 16 h pi of fed-batch cultivation, but with lower intracellular PHA content compared to octanoic acid. With further incubation, the LCFA fed culture produced 4.4 times the maximum NPCM measured in the octanoic acid culture, and achieved similar overall volumetric productivity with much higher mcl-PHA titer, after 30 h pi.

Similar behavior was also observed when the two substrates were co-fed, where NPCM production continued after oxygen limitation resulting in 3.3 times the maximum NPCM titer obtained from using octanoic acid as the sole carbon source. Intracellular PHA

content also improved from 38.4% cdm to 54.1% compared to using LCFA as the sole carbon source. The PHA titer of 6.4 g L^{-1} , and volumetric productivity $0.24 \text{ g L}^{-1} \text{ h}^{-1}$ after 26 h pi of co-feeding were significantly higher than the single substrate conditions. Furthermore, the resulting mcl-PHA was 81% C8, suggesting preferential use of octanoic acid for mcl-PHA synthesis, with growth and maintenance requirements being supplied by LCFA. This data suggests that a greater cell yield for a given aeration input can be obtained when LCFAs are present, a finding which could have important cost-saving implications for design of production processes. Subsequent work will focus on improving productivity of the co-feed cultivation by optimizing feeding rates for improved mcl-PHA content.

5.7. Acknowledgements

The co-authors Daniel Gapes, Richard Sparling, David B. Levin and Nazim Cicek provided guidance on experimental design and manuscript revisions. This study was funded by Genome Canada, through the Genome Applications and Partnership Program (GAPP), and the Natural Sciences and Engineering Research Council (NSERC) of Canada through a Collaborative Research and Development (CRD) grant with Minto BioProducts Ltd. as the industrial partner (grant number CRDPJ-490630-15). The authors disclose they have no conflict of interest. This article does not contain any studies with human participants or animals performed by any of the authors.

Chapter 6: The Thermal and Mechanical Properties of Medium Chain-Length Polyhydroxyalkanoates Produced by *Pseudomonas putida* LS46 on Various Substrates

6.1. Preface

Feedstock for microbial cultivation of mcl-PHAs is the largest process cost and has diverse effects on polymer properties. The thermal and mechanical properties of a polymer will determine their suitability for a particular application. The variability in polymer properties of mcl-PHAs is well represented in the literature, however these effects are often described using varying strains of *Pseudomonas* sp. and varying cultivation conditions. This work was performed to further elucidate the role of feedstock on mcl-PHA biosynthesis and the ultimate role of monomer composition on polymer properties, and to further characterize mcl-PHAs from LCFAs.

The following chapter was published in *Frontiers in Bioengineering and Biotechnology*. 2021. 8:617489. I contributed to experimental designs and execution, data analysis and manuscript preparation. Warren Blunt and Zimo Jin aided with polymer production.

6.2. Abstract

Medium chain-length polyhydroxyalkanoates were produced by *Pseudomonas putida* LS46 cultured with a variety of carbohydrate and fatty acid substrates. The monomer compositions and molecular weights of the polymers varied greatly and was dependent on whether the substrate was metabolized via the fatty acid degradation or the de novo fatty acid synthesis pathways. The highest molecular weights were obtained from medium chain-length fatty acids, whereas low molecular weights were obtained from

longer chain-length and more unsaturated fatty acids or carbohydrates. The differences in monomer compositions and molecular weights due to the choice of substrate did not affect the polymer thermal degradation point. The glass transition temperatures varied from -39.4 °C to -52.7 °C. The melting points, when observed, ranged from 43.2 °C to 51.2 °C. However, a profound substrate effect was observed on the crystallinity of these polymers. Reduced crystallinity was observed when the monomer compositions deviated away from C8-C10 monomer lengths. The highest crystallinity was observed from medium chain-length fatty acids, which resulted in polymers with the highest tensile strength. The polymer produced from octanoic acid exhibited the highest tensile strength of 4.3 MPa with an elongation-at-break of 162%, whereas the polymers produced from unsaturated, long chain fatty acids remained amorphous. A comparative analysis of the substrate effect on the physical-mechanical and thermal properties of mcl-PHAs better clarifies the relationship between the monomer composition and their potential applications, and also aids to direct future PHA synthesis research towards properties of interest.

6.3. Introduction

Polyhydroxyalkanoates are a diverse class of microbially-produced biopolymers known to vary in sidechain length, monomer back-bone length and functional groups (Steinbüchel and Valentin, 1995; Kim et al., 2007). The polymer structure is determined by microbial biosynthetic pathways, and is affected by the microbial species, the carbon substrate and the culturing conditions. This variability has produced PHAs with drastically different polymer properties (Brandl et al., 1988). PHAs have been compared to polypropylene, low-density polyethylene, rubber and adhesives due to the range of observed PHA properties (Anderson and Dawes, 1990; de Koning et al., 1994; Chen, 2010;

Mozejko and Ciesielski, 2014). Possible applications for PHAs include molds and films for replacing single-use plastics, laminates, composites, coatings, adhesives, and biocompatible products for biomedical applications (Madison and Huisman, 1999).

The commercial applications of PHAs have been limited by the comparatively high cost of production against competing petrochemical plastics. Substrate utilization has represented 30-50% of the reported PHA production costs, imparting the need for cheaper waste sources of triacylglycerides and simple sugars (Chanprateep, 2010; Jiang et al., 2016; Favaro et al., 2019). For further cost reduction, culturing conditions are optimized for high volumetric productivity of PHAs using a variety of feeding methods and co-substrates to obtain desired monomer compositions and improve the yield coefficient of carbon for PHA production (Blunt et al., 2018b).

The objective of PHA production is sustainable and renewable plastic products capable of replacing current petroleum-derived plastics that are non-biodegradable and a major source of environmental pollution. The challenge of using waste substrates to reduce PHA production costs is the affected chemical, thermal and mechanical properties of the polymer. The production and properties of medium chain-length PHAs have been studied on a wide range of substrates using various *Pseudomonas* spp. subjected to nutrient-limited minimal medium. Mcl-PHAs have been “tailor-made” based on changes in monomer composition, but better understanding of these effects on thermal and mechanical properties are required to justify a preferred monomer composition for a given application. In this study, the cell mass production, PHA production, polymer subunit composition, and molecular weights of mcl-PHAs synthesized by *P. putida* LS46 were assessed for a suite of carbohydrate and fatty acid substrates. This analysis was conducted to further understand

the effect of substrate type on mcl-PHA biosynthesis, removing the variability of strain and culturing conditions. The corresponding thermal and mechanical properties are reported. This further elucidates the biochemical response to substrate changes by these microorganisms during PHA production, and how the resulting material properties of these mcl-PHAs can direct production design for niche applications.

6.4. Methods and Materials

6.4.1. Culturing and PHA Synthesis

This method is consistent with Chapter 3, Section 3.2. Specifically, 160 C-mM of substrate was added to minimal medium, however substrate toxicity was observed in some conditions. Hexanoic acid, heptanoic acid, octanoic acid and nonanoic acid were provided 120 C-mM (Blunt et al., 2018a), while shorter fatty acids could not be provided in sufficient concentration to effectively synthesize mcl-PHA under these conditions, and were produced with ammonium sulfate and substrate reduced to 0.1 g/L and 16 C-mM (our unpublished data). A 1% inoculum (v/v) to 500 mL baffled experimental flasks with 150 mL working volumes were incubated in a rotary shaker for 30 hours for the determination of chemical and thermal properties. Scale-up of PHA production for the determination of tensile properties was performed using 1 L baffled flasks or in a 7 L bioreactor.

6.4.2. Biomass Processing

See Chapters 3, Sections 3.3, 3.4, and 3.5. Chloroform was the chosen extraction solvent for these experiments since it is most effective in the dissolution of scl-PHAs. In addition, ¹H-NMR and ¹³C-NMR using a Bruker AMX-300 spectrometer (Bruker Biospin AG, Billerica, MA) were used to determine the chemical structure and monomer

composition of purified PHAs. 10 mg of polymer sample was dried over Na_2SO_4 and redissolved in CDCl_3 .

6.4.3. Analysis of Thermal Properties

Differential scanning calorimetry (DSC, TA Instruments Q2000, New Castle, DE) of 5-10 mg of purified PHA samples were analyzed using a heat-cool-heat protocol at a heating rate of 10 °C/min from -60 °C up to 200 °C. Thermogravimetric analysis (TGA) were performed as previously described (Sharma et al., 2017b) from 35 °C to 500 °C at 5 °C under air, after determining that degradation was non-oxidative using argon gas.

6.4.4. Analysis of Molecular Weight

High-performance liquid chromatography using a Waters 1515 with Waters 2414 refractive index detector (Waters Corp., Milford, MA) using an Agilent 5 μm PLgel Mixed-C column and guard column were used to conduct gel permeation chromatography (GPC) at 30°C. A calibration curve was produced using Agilent EasiCal PS-1 polystyrene narrow molecular weight standards (Agilent Technologies, Santa Clara, CA). Purified PHA polymers were diluted to a concentration of 1.5 mg/mL in HPLC-grade chloroform and filter sterilized with 0.45 μm PTFE syringe filters (Fisher Scientific, Toronto, ON). 20 μL samples were injected into the HPLC-grade chloroform mobile phase with a flow rate of 1 mL/min.

6.4.5. Analysis of Mechanical Properties

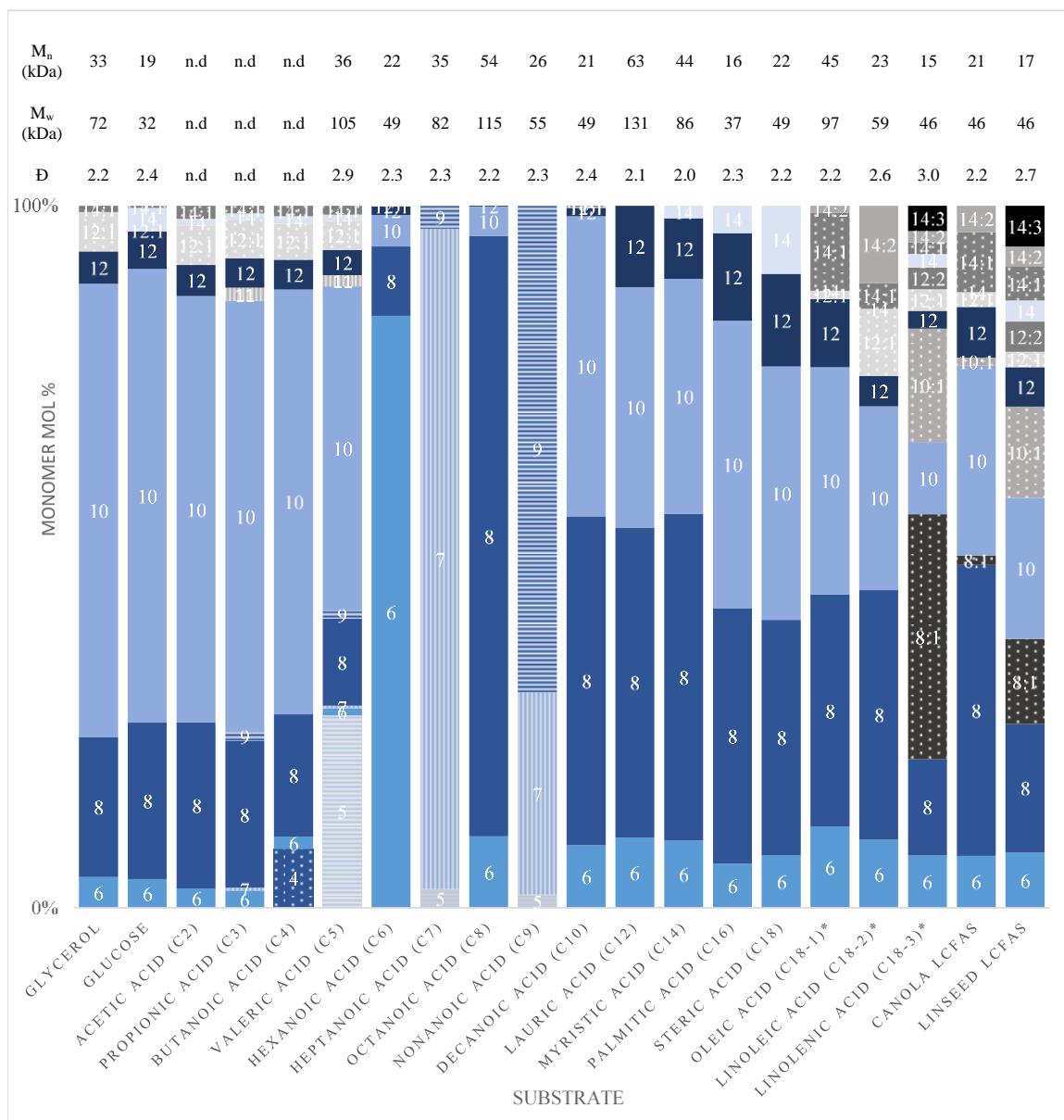
Tensile strips were melt-cast using a “dog-bone” stainless steel form (Precision ADM, Winnipeg, MB) in accordance with ASTM D638-03 (50 mmx10 mmx1 mm, LxWxT) and conditioned as per D618-13 to a relative humidity of 63%. The plates of a Lloyd LS5 tensile tester were separated at a rate of 10 mm/min.

6.5. Results

Figure 6.1 displays the monomer compositions of mcl-PHAs produced from a variety of carbon substrates. Odd-numbered carbon length monomers were only observed from odd-numbered fatty acid substrates. C10 was the dominant monomer from carbohydrates and the volatile fatty acids (VFAs) shorter than hexanoic acid. For the substrates in the range of hexanoic acid to nonanoic acid, the dominant monomer was the same length as the substrate. Even-numbered substrates of eight to eighteen carbons were all preferentially incorporated to C8 and C10 monomers. These results are consistent with the dominant monomers observed with *P. putida* KT2442 by which we can infer that fatty acids longer than valeric acid rely primarily upon the fatty acid β -oxidation pathway for PHA monomer production, while structurally-unrelated substrates rely solely on the fatty acid biosynthesis pathway (Huijberts et al., 1994).

Huijberts et al. (1994) suggested that the main source of longer monomers from hexanoic acid were from an elongation of hexanoic acid with acetyl-CoA, over a completely *de novo* fatty biosynthesis route. Here, the ratio of C8/C10 from hexanoic, and the inclusion of some C9 from heptanoic acid agree with their findings. However, PHA production from propionic acid resulted in only 3.7 mol% of uneven-length monomers longer than the substrate, whereas the remaining 96.3 mol% of monomers were even-length, and longer than the substrate. A similar trend was observed by PHA production from valeric acid, except for the incorporation of C5. PHA production from butanoic acid, with exception to the 8.5 mol% C4 incorporated, resulted in monomer ratios similar to those obtained from glycerol and glucose. This indicates that the main route for PHA

production from substrates shorter than hexanoic acid is by oxidation of the substrates to acetyl-CoA and subsequent *de novo* fatty acid biosynthesis route for PHA production.



The 3-Hydroxyalkanoate monomers are abbreviated by carbon length and number of olefin moieties (ie. 3-hydroxyoctenoate as 8:1). M_n: Number-average molecular weight. M_w: Weight-average molecular weight Đ: Dispersity. n.d. – not determined. * These substrates do not represent pure fatty acids. Oleic acid, linoleic acid and linolenic acid are 90%, 60% and 70% technical grades respectively.

Figure 6.1. The 3-Hydroxyalkanoate monomer compositions and molecular weights produced by *P. putida* LS46 on varying carbon substrates.

Increased fatty acid substrate length resulted in an increased proportion of C12 and C14 monomers. An increase in LCFA unsaturation resulted in a non-proportional increase of unsaturated 3-hydroxyacids. When fatty acid biosynthesis was required for PHA synthesis, small proportions of saturated C12 and C14 monomers along with monounsaturated C12:1 and C14:1 were observed.

The molecular weight data corresponding to the mcl-PHAs produced by these substrates is also tabulated in Figure 6.1. Clear trends in PHA molecular weights based on carbon substrates could not be identified, despite the dispersity of molecular weights being consistent. Low molecular weights with higher dispersity were obtained from highly unsaturated mcl-PHAs.

The intracellular PHA content was highest from MCFAs and lowest in substrates with high proportions of polyunsaturated fatty acids and steric acid, the later likely due to substrate mass transfer limitations (Table 6.1). The NPCM ranged from 0.17 g/L to 2.96 g/L where the lowest titers were obtained from MCFA substrates and the highest obtained from LCFAs. The higher NPCM values obtained from LCFAs could be partially explained by artificial increases due to contaminating substrate not removed during biomass processing, but these results are consistent with previous observation under microaerophilic conditions (Blunt et al., 2018a), which could impact these flask culturing conditions. PHAs produced from VFAs shorter than hexanoic acid resulted in an NPCM range of 0.25 g/L to 0.32 g/L and a PHA content range of 31.4% to 42.2%. The lower cell titer was due to one-tenth medium concentration required due to substrate toxicity.

Table 6.1. Growth and PHA production by *P. putida* LS46 on varying carbon substrates. *Oleic acid, linoleic acid, and linolenic acid are 90%, 60%, and 70% technical grades, respectively.

Substrate	Biomass (g/L)	PHA Content (% cdm)	PHA Titer (g/L)	NPCM (g/L)
Glycerol	3.06 ± 0.38	32.3 ± 8.9	1.01 ± 0.38	2.05 ± 0.01
Glucose	2.24 ± 0.32	20.0 ± 9.0	0.43 ± 0.16	1.81 ± 0.42
Hexanoic Acid (C ₆)	2.31 ± 0.06	69.9 ± 5.2	1.61 ± 0.10	0.70 ± 0.13
Heptanoic Acid (C ₇)	1.18 ± 0.20	74.5 ± 6.4	0.88 ± 0.18	0.30 ± 0.07
Octanoic acid (C ₈)	2.00 ± 0.69	41.8 ± 14.4	0.85 ± 0.22	1.31 ± 0.68
Nonanoic Acid (C ₉)	0.56 ± 0.06	68.7 ± 21.2	0.39 ± 0.16	0.17 ± 0.11
Decanoic Acid (C ₁₀)	2.52 ± 0.32	50.2 ± 10.8	1.29 ± 0.41	1.23 ± 0.10
Lauric Acid (C ₁₂)	2.72 ± 0.16	47.5 ± 5.3	1.29 ± 0.12	1.43 ± 0.20
Myristic Acid (C ₁₄)	2.55 ± 0.12	28.1 ± 6.6	0.72 ± 0.19	1.83 ± 0.17
Palmitic Acid (C ₁₆)	3.51 ± 0.31	41.5 ± 6.7	1.46 ± 0.29	2.05 ± 0.29
Steric Acid (C ₁₈)	3.13 ± 0.21	5.61 ± 2.2	0.18 ± 0.07	2.96 ± 0.20
Oleic Acid (C ₁₈₋₁)*	3.30 ± 0.45	46.7 ± 1.8	1.54 ± 0.27	1.76 ± 0.18
Linoleic Acid (C ₁₈₋₂)*	3.00 ± 0.45	49.2 ± 12.0	1.50 ± 0.56	1.50 ± 0.29
Linolenic Acid (C ₁₈₋₃)*	3.24 ± 0.24	16.0 ± 7.8	0.52 ± 0.25	2.72 ± 0.30
Canola LCFAs	2.85 ± 0.39	20.0 ± 1.3	0.57 ± 0.11	2.27 ± 0.27
Flax LCFAs	2.96 ± 0.34	11.3 ± 0.8	0.34 ± 0.06	2.63 ± 0.28

The crystallinity of mcl-PHAs, as determined by melt enthalpy, was highest in polymers produced from octanoic acid (Table 6.2). Decreases in melting temperature (T_m), glass transition temperature (T_g) and melt enthalpy (ΔH_m) were observed with longer fatty acid substrates and LCFAs lacked any crystallinity, consistent with previous reports (Ashby and Foglia, 1998). Polymers produced from carbohydrates were observed to crystallize into films after solvent evaporation and room temperature, but with low crystallinity and lower glass transition temperature. The melting temperature for the mcl-PHA films ranges from 43.2 °C to 51.2 °C. Upon a cooling and second heat cycles, no melting temperature was observed, unlike PHB and PHBV polymers which observe a similar melting behavior (data not shown). This is due to the slow crystallization behavior of mcl-PHAs (Marchessault and Yu, 2005). Interestingly, polymers produced from valeric

acid displayed no crystallinity, and those from hexanoic acid resulted in very low enthalpy melting at 131.1 °C. The glass transition temperature of mcl-PHA from hexanoic acid and the melt enthalpies of mcl-PHA from MCFAs are distinguishable from the other mcl-PHA thermograms (Figure 6.2). The behavior of mcl-PHA from flax above 70 °C could be the result of thermal polymer cross-linking. The tensile strength (Table 6.2) increased with polymer crystallinity. Mcl-PHAs produced from carbohydrates tore easily as observed with low tensile strength and low elongation-at-break. The polymers produced from octanoic, nonanoic or decanoic acid produced highly elastic polymers with elongation-at-break between 162% and 184%. Octanoic acid polymers had a significantly higher tensile strength than nonanoic or decanoic acid polymers, and lower elongation-at-break percentages. The saturated LCFAs longer than decanoic acid could not be effectively scaled-up in a bioreactor for property analysis. These fatty acids are solid at cultivation temperatures and poor mass transfer results in significant foaming issues with air sparging causing removal of the substrate.

Table 6.2. Thermal and tensile properties of mcl-PHAs. T_g : Glass transition temperature T_M : Melting Temperature T_D : Degradation Temperature ΔH_M : Melt Enthalpy T: Tensile Strength E: Elongation at break. EM: Elastic Modulus. N/A – Not applicable (No melt). n.d. – Not Determined. The standard deviations are made from a minimum of three tensile strips.

Substrate	T_g (°C)	T_M (°C)	T_D (°C)	ΔH_M (J/g)	T (MPa)	E (%)	EM (MPa)
Glycerol	-47.0 ± 0.7	43.2 ± 0.9	n.d.	10.3 ± 1.7	1.0 ± 0.1	20 ± 3.6	17.3 ± 7.2
Valerate (C ₅)	-46.9	N/A	n.d.	N/A	N/A	N/A	N/A
Hexanoic Acid (C ₆)	-29.7 ± 1.1	131 ± 5.6	n.d.	0.27 ± 0.2	N/A	N/A	N/A
Octanoic Acid (C ₈)	-38.1 ± 1.9	51.2 ± 0.9	249 ± 1.3	21.0 ± 0.8	4.3 ± 0.4	162 ± 6.7	25.3 ± 1.8
Nonanoic Acid (C ₉)	-41.3 ± 0.9	47.2 ± 0.4	246 ± 3.1	17.6 ± 3.8	2.6 ± 0.8	184 ± 18	12.6 ± 4.7
Decanoic Acid (C ₁₀)	-44.0 ± 1.1	45.5 ± 1.3	254 ± 6.1	15.2 ± 0.1	2.8 ± 0.4	171 ± 1.4	10.8 ± 0.6
Canola LCFAs	-52.7 ± 0.5	N/A	253 ± 2.3	N/A	N/A	N/A	N/A
Flax LCFAs	-46.9 ± 5.8	N/A	n.d.	N/A	N/A	N/A	N/A

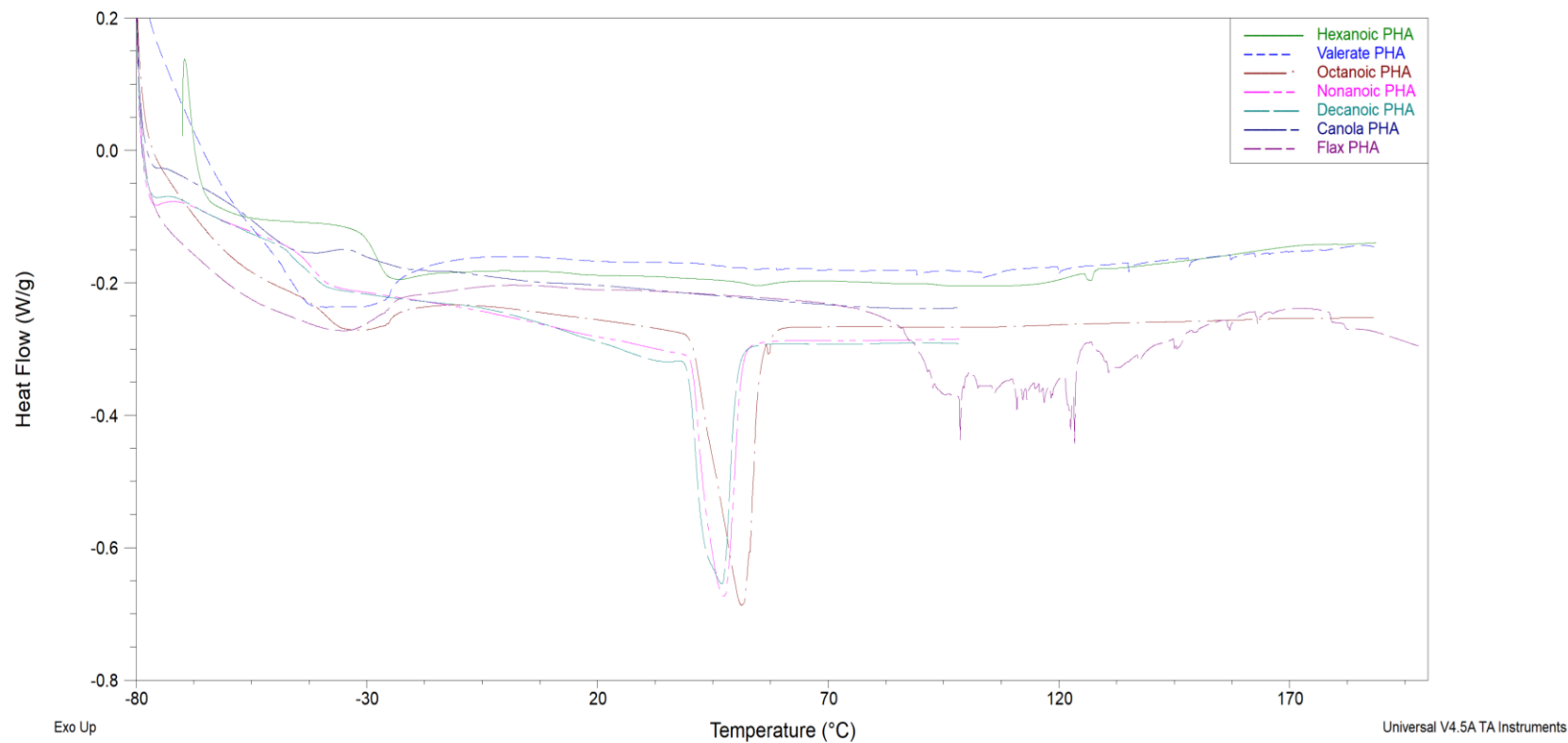


Figure 6.2. First heat thermogram overlay of mcl-PHAs obtained from various carbons substrates. Legend inset.

6.6. Discussion

Mcl-PHA production by *Pseudomonas* spp. across a variety of substrates exhibit a biosynthetic preference for the incorporation of C8, C9 and C10 monomer lengths. *P. putida* KT442 incorporated high C10 from glycerol and glucose substrates and very small fractions of longer monomers were observed with some unsaturation. From decanoate and C18 fatty acid substrates, C8 became the dominant monomer. (Eggink et al., 1992). Similar results were obtained with other *Pseudomonas* spp. across the literature (Ashby and Foglia, 1998; Haba et al., 2007; Bassas et al., 2008; Song et al., 2008; Impallomeni et al., 2011), consistent with the substrate effect on mcl-PHA monomer composition observed in this study (Figure 6.1). Comparing the monomer compositions of various *Pseudomonas* sp. cultivated with oleic acid, the dominant monomer varied between C8 and C10 and significant variability is seen among the other monomers, thus demonstrating the difficulty in comparing properties across the literature for the increased variability attributed to strain and culturing conditions (Eggink et al., 1992; Ashby and Foglia, 1998; Solaiman et al., 2001; Fernández et al., 2005; Conte et al., 2006; Haba et al., 2007; Impallomeni et al., 2011).

The uneven-length monomer compositions from nonanoic acid and heptanoic acid (Figure 6.1) are consistent with those reported by other *Pseudomonas* sp. (Thakor et al., 2005; Sun et al., 2009; Wang et al., 2011). The monomer composition obtained from growth on undecenoic acid suggested a biosynthetic preference for C9 monomers (Hartmann et al., 2006, 2010). The high monomer mol% of C6 and C7 observed from hexanoic acid and heptanoic acid, respectively, is a result of the availability of those

monomers from the β -oxidation pathway and the apparent minor role of the *de novo* fatty acid biosynthesis for PHA production from fatty acids longer than valeric acid.

Unsaturated positions were conserved in the polymer sidechains of sufficient length resulting in saturated, mono- or di-unsaturated C14 monomers from petroselinic (Δ -6), oleic (Δ -9) and linoleic (Δ -9,12) acids respectively. Mono-unsaturated C12 monomers were obtained from linoleic acid. (De Waard et al., 1993). Linolenic acid (Δ -9,12,15) retains the Δ -15 unsaturation down to C8 monomers (Casini et al., 1997). Due to the added olefin and the biosynthetic preference of C8 and C10 monomers, PHAs produced from linolenic acid contain a drastically higher unsaturation content (Figure 6.1). The theoretical ratio of unsaturated moieties is 10.3:2.9:1 for linolenic:linoleic:oleic acids based on the average monomer lengths obtained from *P. putida* LS46 using C18 LCFA substrates; and the observed ratio was 5.3:2.5:1 which was lowered due to the technical grades of the reagents having 70%, 60% and 90% purity respectively.

The molecular weights observed from *P. putida* LS46 under these conditions were smaller but comparable with literature values (Figure 6.1, Table 6.3). The molecular weight of mcl-PHAs was highest when produced from saturated fatty acids such as octanoic acid and lowest from the unsaturated LCFAs. Higher double-bond content results in lower molecular weight. Unsaturated fatty acids are hypothesized to increase polymer chain termination which resulted in smaller number average molecular weights (Ashby et al. 1998a). The molecular weights were unaffected in mcl-PHAs produced with terminal double-bonds (de Koning et al., 1994; Schmid et al., 2007), indicating that chain termination could be caused by steric effects of having kinked sidechains.

Table 6.3. Compilation of mcl-PHA average molecular weights produced from various substrates using *Pseudomonas* spp. M_n : Number-average molecular weight. M_w : Weight-average molecular weight \bar{D} : Dispersity. Numbers marked by “*” were calculated by the author using the two reported values.

<i>PHA Polymer</i>	M_w (kDa)	M_n (kDa)	\bar{D}	<i>Reference</i>
<i>B. Carinata</i> Oil	56	31	1.8	(Impallomeni et al., 2011)
Oleic Acid	57	26	2.2	(Impallomeni et al. 2011)
Nervonic Acid	122	63	1.9	(Impallomeni et al. 2011)
Erucic Acid	114	56	2.0	(Impallomeni et al. 2011)
Dodecanoic acid (15% C12)	100	80	1.25	(Liu and Chen 2007)
Dodecanoic acid (39% C12)	157	108	1.45	(Liu and Chen 2007)
Tetradecanoic acid (31% C14)	83	46	1.82	(Liu and Chen 2007)
Tetradecanoic acid (49% C14)	95	67	1.43	(Liu and Chen 2007)
Glucose + Oleic Acid	630	135	4.6	(Solaiman et al., 2002)
Lard	559	103	5.4	(Solaiman et al. 2002)
Soybean Oil	289	67	4.3	(Solaiman et al. 2002)
Coconut Oil	343	74	4.6	(Solaiman et al. 2002)
Oleic Acid	146	73	2.00	(Ashby and Foglia, 1998)
Tallow	142	82	1.73	(Ashby and Foglia 1998)
Lard	139	84	1.66	(Ashby and Foglia 1998)
Butter Oil	135	82	1.65	(Ashby and Foglia 1998)
Olive Oil	119	72	1.65	(Ashby and Foglia 1998)
Sunflower Oil	112	65	1.72	(Ashby and Foglia 1998)
Coconut Oil	165	101	1.63	(Ashby and Foglia 1998)
Soybean Oil	127	70	1.81	(Ashby and Foglia 1998)
Tallow	415	147	2.8	(Ashby et al., 1998a)
Coconut Oil	449	133	3.38	(Ashby et al., 1998b)
Tallow	269	93	2.89	(Ashby et al. 1998b)
Soybean Oil	121	57	2.13	(Ashby et al. 1998b)
Octanoic acid	211.5	106*	1.99	(Schmid et al., 2007)
90% Octanoic, 10% Undecenoic	164.0	83*	1.98	(Schmid et al. 2007)
50% Octanoic, 50% Undecenoic	206.5	97*	2.13	(Schmid et al. 2007)
25% Octanoic, 75% Undecenoic	185.5	92*	2.02	(Schmid et al. 2007)
Linseed	126	60	2.1	(Bassas et al., 2008)
100% Octane	194	126	1.54*	(de Koning et al., 1994)
5% Octene	223	123	1.81*	(de Koning et al., 1994)
25% Octene	255	109	2.34*	(de Koning et al., 1994)
Soybean Oil/Octanoic Acid (80/20)	155	51	3.07	(Hazer et al., 2009)
Soybean Oil/Octanoic Acid (72/28)	162	63	2.57	(Hazer et al. 2009)
Soybean Oil/Octanoic Acid (50/50)	161	60	2.66	(Hazer et al. 2009)
Soybean Oil/Undecanoic Acid (50/50)	176	63	2.80	(Hazer et al. 2009)
Octanoic Acid/Undecanoic Acid (50/50)	201	64	3.11	(Hazer et al. 2009)
Octanoic Acid	189	51	3.69	(Hazer et al. 2009)
Soybean Oil	130	72	1.80	(Hazer et al. 2009)
Undecanoic Acid	260	135	1.92	(Hazer et al. 2009)

Several conclusions can be postulated about the substrate effect on the thermal data presented in Table 6.2 when also considering the associated molecular weights and monomer compositions (Figure 6.1) and comparing to results across the literature (Table 6.4). The crystallinity of PHAs depends on the length of the monomer sidechains. The crystal structure of scl-PHA chains is disrupted by the conformational requirements of longer mcl-PHA sidechains (Marchessault et al., 1990). The incorporation of C4 and C5 monomers by native *P. putida* LS46 remains low despite using butanoic or valeric acid, instead relying on the *de novo* fatty acid synthesis pathway for mcl-PHA production. The mcl-PHA obtained from valeric acid exhibited no crystallinity in contrast to the crystallinity observed from glucose, confirming that co-polymers of scl-PHA and mcl-PHA are not isomorphic. The C6 dominant mcl-PHA produced from hexanoic acid exhibited a very weak melt enthalpy consistent with the melting temperature of PHV, whereas previous reports indicated no melt point (Marchessault et al., 1990). Homopolymers of C6 and C7 PHA monomers exhibited no crystallinity in one report using mutant *P. putida* KT2442 (Wang et al., 2011), however exhibited melting temperatures of 59 °C and 45 °C respectively using engineered *E. coli*. The x-ray diffraction pattern of a C6 homopolymer indicated an alternative crystal structure to either scl-PHA or mcl-PHA (Abe et al., 2012). Sidechains of 3-4 carbons may be too long for crystal structures with attractive forces between parallel back-bone chains, but too short to form any potential interactions of sidechain close-packing. Alternatively, the unique crystallization of these polymers may not be isomorphic with the wild-type co-monomer composition of mcl-PHA, and the discrepancy between C6 homopolymers.

Table 6.4. Thermal properties of mcl-PHAs produced by *Pseudomonas* spp. using various feedstocks. T_g : Glass transition temperature T_m : Melting Temperature T_D : Degradation Temperature ΔH_M : Melt Enthalpy

<i>PHA Polymer Feedstock</i>	T_g (°C)	T_m (°C)	ΔH_m (J/g)	<i>Reference</i>
Valeric Acid (100% C5)	-15.1	112.3	73.31	(Wang et al., 2011)
Hexanoic Acid (99% C6)	-28.2	N/A	N/A	(Wang et al., 2011)
Heptanoic Acid (100% C7)	-32.1	N/A	N/A	(Wang et al., 2011)
Octanoic Acid (96% C8)	-38.4	66.1	30.2	(Wang et al., 2011)
Octanoic Acid (88% C8)	-40	54	9	(Jiang et al., 2012)
Octanoic Acid (98% C8)	-42	62	15	(Jiang et al., 2012)
Nonanoic acid (70% C9)	-45	46	12	(Jiang et al., 2012)
Nonanoic acid (95% C9)	-48	63	27	(Jiang et al., 2012)
100% Octane	-29	61	23	(de Koning et al., 1994)
95% Octane, 5% Octene	-27	55	11	(de Koning et al., 1994)
75% Octane, 25% Octene	-30	N/A	0	(de Koning et al., 1994)
Octanoic Acid	-33.1	58.1	14.5	(Schmid et al., 2007)
90% Octanoic, 10% Undecenoic	-35.9	50.8	10.2	(Schmid et al., 2007)
50% Octanoic, 50% Undecenoic	-44.6	39.9	0.2	(Schmid et al., 2007)
25% Octanoic, 75% Undecenoic	-49.3	N/A	N/A	(Schmid et al., 2007)
Dodecanoic Acid (15% C12)	-44	53	18	(Liu and Chen, 2007)
Dodecanoic Acid (39% C12)	-43	65	28	(Liu and Chen 2007)
Tetradecanoic Acid (31% C14)	-40	58.1	25.6	(Liu and Chen, 2007)
Tetradecanoic Acid (49% C14)	-40	66.8	25.1	(Liu and Chen, 2007)
<i>B. Carinata</i> Oil	-47	N/A	N/A	(Impallomeni et al., 2011)
Oleic Acid	-52	N/A	N/A	(Impallomeni et al. 2011)
Nervonic Acid	-46	50	16.1	(Impallomeni et al. 2011)
Erucic Acid	-43	50	15.5	(Impallomeni et al. 2011)
Oleic Acid	-44	42	10.7	(Ashby and Foglia, 1998)
Tallow	-45	44	11.4	(Ashby and Foglia, 1998)
Lard	-46	39	9.5	(Ashby and Foglia, 1998)
Butter Oil	-43	44	11.0	(Ashby and Foglia, 1998)
Olive Oil	-45	41	10.7	(Ashby and Foglia, 1998)
Sunflower Oil	-46	41	10.0	(Ashby and Foglia, 1998)
Coconut Oil	-38	48	12.3	(Ashby and Foglia, 1998)
Soybean Oil	-45	N/A	N/A	(Ashby and Foglia, 1998)
Linseed Oil	-51	N/A	N/A	(Bassas et al., 2008)

Monomers of C6 act as effective internal plasticizers for scl-PHA copolymers where some disruption to crystallinity can improve elastic performance (Sudesh et al., 2000). Efforts to increase the monomer mol percentage of C8 or C9 from their respective fatty acids using acrylic acid as a β -oxidation inhibitor, subsequently reducing the presence of C6 or C7 monomers, resulted in increased melting temperatures and enthalpies (Jiang et al., 2012). As previously noted, *Pseudomonas* spp. predominantly produced C8 and C10 monomers from LCFAs. Mutant *P. putida* strains were produced that incorporated higher contents of C12 and C14 monomers resulting in mcl-PHAs with increased sidechain crystallization and elevated melting temperatures (Liu and Chen, 2007; Liu et al., 2011; Abe et al., 2012). The increased content of C12 and C14 monomers in mcl-PHAs produced from glucose or unsaturated LCFAs is unlikely to contribute to their reduced crystallinity, instead the olefin moieties are responsible for the reduction in crystallinity (Ashby and Foglia, 1998). Where terminal olefins did not affect the mcl-PHA molecular weights, increased unsaturation content resulted in drastic reduction in melt enthalpy (de Koning et al., 1994; Schmid et al., 2007).

The mechanical properties of mcl-PHAs were consistent with literature reports for similar substrates (Ashby et al., 1998a; Liu and Chen, 2007; Larrañaga et al., 2014). The tensile strips always broke near the clamps due to the localization of stress from the dog-bone mold which resulted in slightly dampened results. The tensile properties are reflective of the polymer crystallinity. Mcl-PHAs are viscoelastic polymers compared to thermoplastic scl-PHAs associated with the greater motional freedom of sidechain crystallinity (Marchessault and Yu, 2005; Liu et al., 2011). Improved tensile properties can be achieved by manipulating the monomer composition of mcl-PHAs to contain saturated

monomers of C8 or longer. Unsaturated monomers and short length monomers reduce the crystallinity of mcl-PHAs and detract from the viscoelastic film properties. On the other hand, the inclusion of these monomers may be preferential for alternative applications. Mcl-PHAs of low crystallinity are tacky and may find application as biodegradable adhesives (Madison and Huisman, 1999). Unsaturated moieties have also been used to improve tensile properties or produce amphiphilic polymers by co-polymer grafting, cross-linking and through chemical modification (Hazer and Steinbüchel, 2007; Kim et al., 2007).

The results described herein further elucidates the relationship between carbon substrate, the biochemical pathways of *Pseudomonas*, and the resulting polymer properties. Mcl-PHAs of varying monomer compositions were obtained from a suite of carbon substrates indicating that crystallinity, measured by melt enthalpy, was dependent on monomer length and monomer saturation which ultimately determined tensile properties. The diversity in mcl-PHA monomer composition continues to increase through the genetic modification of PHA accumulating microorganisms, culturing conditions and chemical modification of PHAs. Careful consideration of the polymer properties beyond monomer composition is required to direct culturing methods and genetic modifications towards polymers tailored for diverse applications.

6.7. Acknowledgements

Warren Blunt contributed to experimental design, laboratory assistance and manuscript review. Parveen Sharman contributed *P. putida* LS46 and laboratory assistance. Song Liu contribute laboratory infrastructure and experimental design. Nazim Cicek contributed funding, laboratory infrastructure, intellectual input and manuscript

review. David Levin contributed funding, laboratory infrastructure, intellectual input and manuscript review. This study was funded by Genome Canada, through the Genome Applications and Partnership Program (GAPP), and the Natural Sciences and Engineering Research Council (NSERC) of Canada through a Collaborative Research and Development (CRD) grant with Minto BioProducts Ltd. as the industrial partner (grant number CRDPJ-490630-15).

Chapter 7: Oxidative Cleavage of Unsaturated Medium Chain Length Polyhydroxyalkanoates (PHA): A post-treatment method to customize PHA polymers

7.1. Preface

Long Chain Fatty Acids (LCFAs) have been highlighted throughout this thesis as a promising substrate for providing high yields of mcl-PHAs and reducing production costs. As discussed in the previous chapter, mcl-PHAs have low crystallinity and crystallize slowly presenting a processability challenge. The chain length variability and unsaturated monomer content inherit from vegetal sourced LCFAs further reduce crystallinity. While these properties are a draw-back to native film processing, the unsaturated monomers present opportunities for chemical modification. The initial hypothesis was that cleaving the side chains through ozonolysis would remove some of the steric hindrances of the polymer and re-introduce mcl-PHA crystallization. Eventually, a more concerted mechanism was desired and a similar cleavage was proposed using an osmium tetroxide catalyst.

7.2. Abstract

Biodegradable polymeric materials are valuable commodities to produce a sustainable future but need to challenge the current costs, properties and processing simplicity of petroleum-based plastics. The waste streams of vegetable oils could significantly decrease the cost of producing sustainable mcl-PHAs. However, mcl-PHAs from vegetable oil contain unsaturated moieties and lack crystallinity, but have been modified to introduce crystallinity, amphiphilicity, or to produce a cross-linked polymer network. Mcl-PHAs of varying unsaturated monomer content were produced from the

hydrolysed fatty acids of canola or flax oil. Osmium-tetroxide catalysis of olefin cleavage was performed on the mcl-PHAs produced from vegetable oils. The resulting polymer has limited residual unsaturation and higher purity is achieved as contaminant fatty acids are further removed. Shorter, saturated sidechains in mcl-PHAs often result in increased crystallinity and terminal carboxylic acids would increase the hydrophilicity of the polymer. The resulting polymers displayed increased hydrophilicity and crystallinity, compared to mcl-PHAs from either saturated or unsaturated fatty acids.

7.3. Introduction

Polyhydroxyalkanoates are produced by some microorganisms as intracellular granules for carbon storage which provide sustainable alternatives to some conventional thermoplastic and elastomeric polymers. Medium chain length PHAs, consisting of 6-14 carbon 3-hydroxyalkanoate monomers, have been produced by a variety of *Pseudomonas* species with both related and unrelated substrates. Long chain fatty acids can be sustainably sourced and can reduce fermentations costs through reduced substrate cost and good yields. LCFAs are shortened to appropriate 3-HA precursor lengths via the microorganism's central fatty acid degradation pathway and the resulting PHA monomer composition will be determined by the specificities of the biosynthetic machinery and the composition of LCFAs (Solaiman et al., 2001; Impallomeni et al., 2011). Unsaturated moieties are removed during fatty acid degradation from the C3 or C4 position resulting in conserved double-bonds in the sidechains of some lengths of mcl-PHA monomers. PHA unsaturation will increase as the LCFAs become more unsaturated and when the unsaturated moieties are more distally positioned (De Waard et al., 1993; Ashby and Foglia, 1998). Mcl-PHAs produced from flax fatty acid produce some 3-HA monomers with three double bonds, and

due to the Ω -3 unsaturation and the biosynthetic preference to produce C8 and C10 monomers, this results in over ten times the unsaturation compared to oleic acid (Casini et al., 1997; Dartiailh et al., 2021). Tailor-made mcl-PHAs have been produced through co-feeding to modify the abundance and location of olefinic moieties with minor control of monomer lengths (de Koning et al., 1994; Hartmann et al., 2006; Follonier et al., 2015; Blunt et al., 2018a). The effect of unsaturation on mcl-PHAs is a reduced crystallinity likely caused by steric effects of the non-linear side-chains (Ashby et al., 1998a; Kellerhals et al., 2000). PHAs with sufficient unsaturation remain completely amorphous and will eventually cross-link through autooxidation (Ashby et al., 2000; Hartmann et al., 2006; Schmid et al., 2007).

Modifications to mcl-PHAs containing unsaturated side chains have resulted in polymers with enhanced properties. The olefin moieties have been oxidized, reduced, halogenated, grafted and cross-linked to produce mcl-PHAs with improved mechanical properties or increased hydrophilicity (Hazer and Steinbüchel, 2007; Kim et al., 2007). Conversion of mcl-PHAs with terminal olefin moieties to carboxylic acids using potassium permanganate resulted in increased hydrophilicity and formation of suspended nanoparticles for potential site-specific drug delivery (Kurth et al., 2001). More recently, similar carboxylation of mcl-PHAs followed by esterification with propargyl alcohol produced a terminal alkyne ready for further copper-catalyzed azide-alkyne [3+2] cycloaddition click chemistry (Babinot et al., 2010). A greater range of mcl-PHA properties can be achieved through click chemistry through simple, efficient reactions with existing azide co-monomers to tailor crystallinity and amphiphilicity for targeted applications.

Oxidative cleavage of unsaturated olefins have been demonstrated by ozonolysis (Pryor et al., 1991; Cvetković et al., 2008; Omonov et al., 2014; Benessere et al., 2015) or by transition metal-catalyzed cleavage (Travis et al., 2002; Spanning et al., 2014) of oleic acid. Unsaturated mcl-PHA produced from 10-undecenoic acid resulting in terminal side-chain vinyl moieties have been converted into terminal carboxylic acids through osmium tetroxide cleavage (Stigers and Tew, 2003). The objective of this work was to investigate oxidative cleavage of unsaturated mcl-PHA sidechains produced from LCFAs using osmium tetroxide. The oxidative cleavage of unsaturated side chains results in shortening the average side-chain length by elimination of carbon-carbon double bonds, resulting in the removal of kinks and eliminating the steric effects preventing polymer crystallinity. We hypothesize that greater crystallinity and hydrophilicity would be imparted to the modified mcl-PHAs given the effects of terminal side-chain oxidation previously reported and could provide a cost-effective route to producing click-ready mcl-PHAs.

7.4. Methods and Materials

7.4.1. PHA Synthesis

Pseudomonas putida LS46 was cultured as described in Chapter 3, Section 3.2. Saturated mcl-PHAs were produced using octanoic acid and unsaturated mcl-PHAs were produced using hydrolysed food-grade canola or cold-pressed linseed oils, as described in Chapter 3, Sections 3.3.3 and 3.4. Table 7.1 summarized the monomer compositions of unsaturated mcl-PHAs produced for oxidative cleavage reactions.

Table 7.1. Monomer compositions of mcl-PHAs produced from hydrolyzed vegetable oils by *P. putida* LS46. Below, the composition of major FFA peaks comprising Canola and Flax FFAs.

Mcl-PHA	Monomer Mol %											
	C ₆	C ₈	C _{8:1}	C ₁₀	C _{10:1}	C ₁₂	C _{12:1}	C _{12:2}	C ₁₄	C _{14:1}	C _{14:2}	C _{14:3}
Canola PHA	8.5	51.7	2.0	22.3	1.8	4.1	2.0	0.7	Tr	4.1	1.2	1.6
Flax PHA	6.3	29.6	18.8	14.1	12.4	2.2	1.7	5.2	Tr	1.6	0.8	6.2
FFAs	Fatty Acid Weight %											
	C ₁₆		C ₁₈		C ₁₈₋₁		C ₁₈₋₂		C ₁₈₋₃			
Canola FFAs	4.7		2.1		67.1		16.8		6.1			
Flax FFAs	6.7		4.7		21.1		15.1		52.5			

7.4.2. Ozonolysis

Ozonation and successive reduction were performed to cleave olefin groups as proposed in Figure 7.1 with methods adapted from Cvetković et al. (2008). The 50 mg sample was dissolved in 5 mL of either DCM or 1.5:1 of DCM:methanol (MeOH) and the tube placed in a dry ice bath. The test tube contained a stir bar, and the dry ice bath was placed onto a stir plate. Air was passed through a desiccator into the ozone generator at 0.43 amps at a flow rate of 0.5 L/min and bubbled into solution. Following ozonation, air was bubbled into the solution for 5 minutes before addition of 50 µL reducing agent dimethylsulfide (DMS) or sodium borohydride (NaBH₄) was added. The reaction was quenched and washed with 0.2 M H₂SO₄ three times. Solvents were obtained from Fisher Scientific (Toronto, ON.) and reducing agents were obtained from Sigma Aldrich (St. Louis, MO.) Ozonolysis of oleic acid was performed under identical conditions to compare with ozonolysed mcl-PHAs.

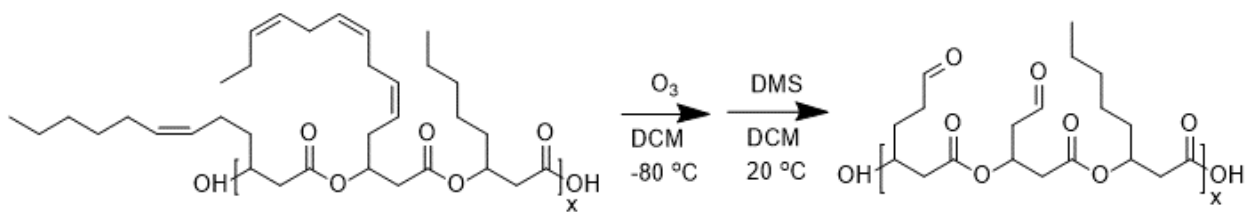


Figure 7.1. Proposed method for oxidative cleavage using ozone of unsaturated mcl-PHA.

7.4.3. Osmium Tetroxide Catalysed Olefin Cleavage

Figure 7.2 outlines the proposed reaction of mcl-PHAs using osmium tetroxide with methods adapted from Stigers and Tew (2002). Oleic acid (100 mg), canola oil (100 mg), mcl-PHA from canola fatty acids (250 mg), and mcl-PHA from flax fatty acids (50 mg) were measured based on molar unsaturation concentrations into 10 mL reaction flasks with 3 mL dimethyl formamide (DMF) equipped with stir bar. OsO_4 (2.5% in t-BuOH; 30 μL) was added and allowed to stir for 10 minutes. Oxone (250 mg) was slowly added, then the reaction flask was stoppered and stirred for 24 hours (h). Sodium sulfite (150 mg) was added and the solution was stirred for 1 h. Ethyl acetate and 1N H_2SO_4 were added and the aqueous layer discarded. The product was washed three times with 1N H_2SO_4 and once with brine prior to drying over sodium sulfate.

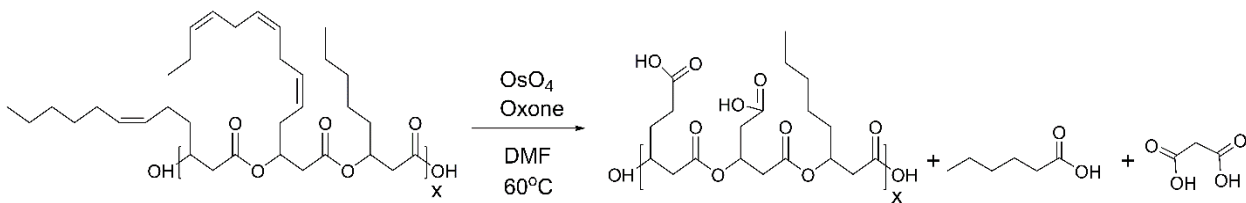


Figure 7.2. Proposed method for oxidative cleavage using osmium tetroxide of unsaturated mcl-PHA.

7.4.4. Product Analysis

The products were tested for solubility in chloroform and methanol. $^1\text{H-NMR}$ and $^{13}\text{C-NMR}$ using a Bruker AMX-300 spectrometer (Bruker Biospin AG, Billerica, MA) were performed to analyze the modified polymer. A 5 mg sample was methanolysed (Brandl et al., 1988) to determine a change in monomer composition by gas chromatography using an Agilent 7890 equipped with flame ionization detector and an Agilent DB-23 column. Standards of oleic acid, linoleic acid, linolenic acid, azelaic acid, 1-nonanol, 1-nonanal, 1-nonanoic acid, 1-hexanoic acid, dimethyl 3-hydroxyglutarate, and glutaric anhydride were methanolysed to identify substrates and products of osmium tetroxide cleavage. Standards of 3-hydroxyhexanoate, 3-hydroxyheptanoate, 3-hydroxyoctanoate, 3-hydroxynonanoate, 3-hydroxydecanoate, 3-hydroxydodecanoate and 3-hydroxytetradecanoate were methanolysed to determine mcl-PHA monomers. All standards were obtained from Sigma Aldrich (St. Louis, MO.). The same Agilent DB23 column and running method were applied to a GC-MS to obtain similar retention times and identify unknown peaks.

7.5. Results

7.5.1. Ozonolysis

Ozonolysis was performed on oleic acid prior to mcl-PHAs as a positive control. The reaction was performed in DCM followed by a dimethyl sulfide or NaBH_4 reductive workup, or in DCM/MeOH followed by DMS or NaBH_4 . The resulting products were analyzed after derivatization with MeOH (Figure 7.3). Under these derivatization conditions, the observed products are expected to be nonanoic acid methyl ester and azelaic acid methyl ester; nonanol and 9-hydroxynonanoic acid methyl ester; and 1,1-

dimethoxynonane and 9,9-dimethoxynonanoic acid methyl esters. Nonanal was observed as two peaks likely due to the incomplete derivatization which produced both the acetal and hemiacetal analogues. Alternative derivatization procedures have been applied for nonanal to improve conversion to 1,1-dimethoxynonane (Tavassoli-Kafrani et al., 2016). The putative presence of hexanal is the product of contaminant linoleic acid. The 9-oxononanoic acid, 9-hydroxynonanoic acid and azelaic acid are poorly represented in the GC analysis, possibly due to their partial solubility in aqueous was conditions.

In all cases, oleic acid was completely consumed in the reaction and aldehydes were obtained. NaBH₄ as a reducing agent resulted in some carboxylic acid or alcohol products depending on the presence of MeOH. DMS had higher fidelity towards the aldehyde products.

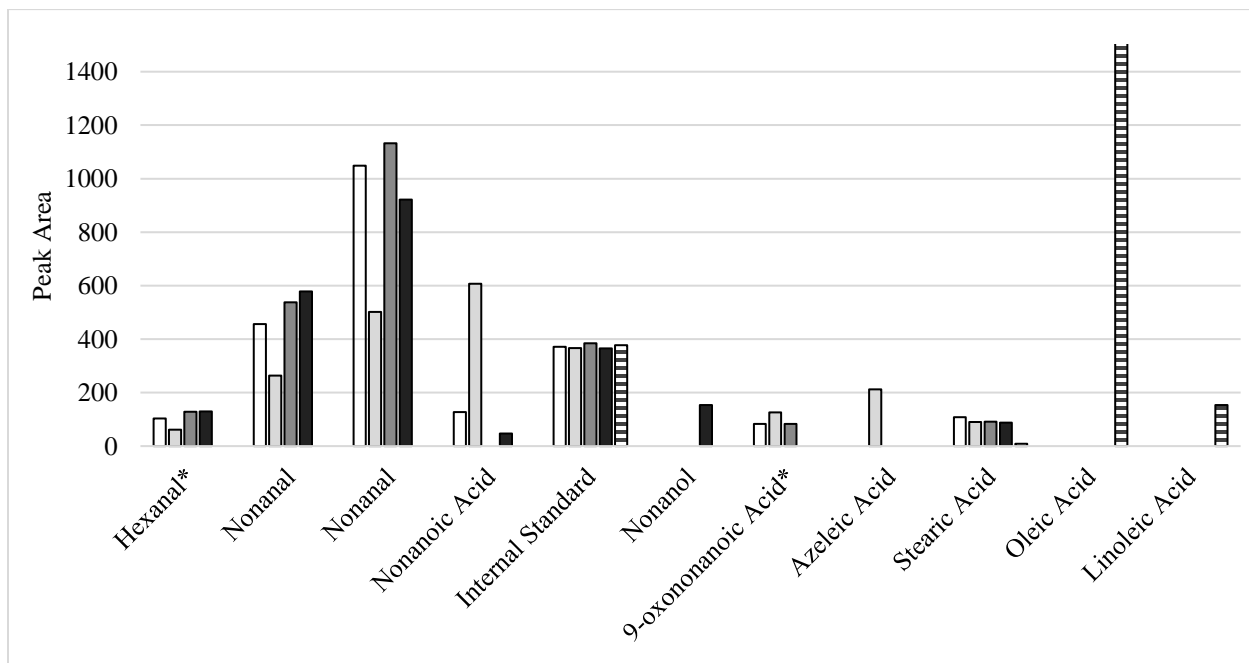


Figure 7.3. Ozonolysis products from oleic acid. □, DCM and DMS; ▣, DCM, and NaBH₄; ■, DCM/MeOH and DMS; ■, DCM/MeOH and NaBH₄; ▤, Oleic Acid. *Putative peak assignments.

The kinetics of ozonolysis of highly unsaturated mcl-PHAs from flax fatty acids were performed in DCM with variable length in ozone exposure time before the addition of DMS (Figure 7.4). Reaction completion was determined by the reduction in unsaturated monomers from PHA using gas chromatography. Under these conditions, 5 minutes of ozonation resulted in 88% disappearance in unsaturated monomers, while 1 minute of ozonation only resulted in a 34% decrease. The presence of 29 distinct new peaks were observed, the primary and secondary ozonolysis products. One possible product, 3-hydroxyglutaric acid, expected from the cleavage of C8-1, C14-1, C14-2 and C14-3 with residual carboxylic acid shares a retention time with C10-1 and therefore correcting for this possibility indicates that the removal of double bonds through ozonolysis neared 98%.

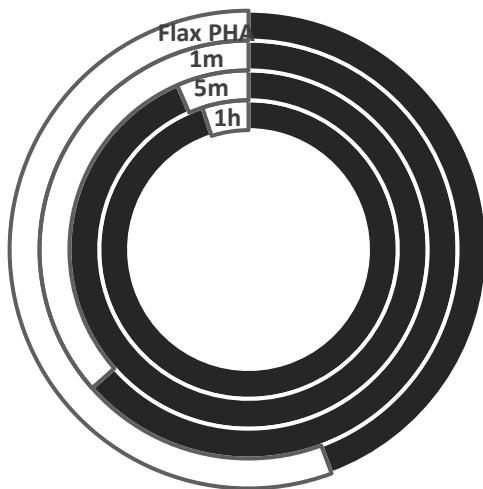


Figure 7.4. Reduction in unsaturated monomers in mcl-PHA cultivated from flax fatty acids after timed ozonolysis. ■, Saturated PHA monomers; □, Unsaturated PHA monomers.

The ozonolysed mcl-PHA from flax fatty acids precipitated during reaction and repeatedly blocked the sparger tip (Figure 7.5A). Analysis of the gas chromatogram indicated almost complete olefin removal and major product peaks have retention times

consistent with the expected aldehyde products. Two significant product peaks were observed downstream of C14 3-HA methyl esters, which could have indicated the formation of dimers. A small aldehyde peak was also observed using $^1\text{H-NMR}$. The ozonated mcl-PHAs (Figure 7.5B) were no longer soluble when refluxed in MeOH, acetone or DCM and a sol/gel analysis resulted in an 85% insoluble fraction. The ozonolysed films were heated to 180 °C without observing a melt. FTIR analysis comparing native, thermally cross-linked and ozonolysed mcl-PHA from flax fatty acids indicate at 1000 cm^{-1} that ozonolysed PHA was similar to crosslinked PHA (Figure 7.6). Only trace levels of aldehydes were observed by FTIR. The presence of possible dimers on GC, the sol-gel analysis and FTIR spectra taken together indicate that polymer crosslinking is occurring during ozonolysis.

Methanol was included as a cosolvent to react with the Criegee intermediate (CI) of ozonolysis to produce a hydroperoxide in an attempt to prevent crosslinking of unsaturated mcl-PHAs. This reaction observed an almost complete removal of unsaturated mcl-PHA monomers in place of newly formed ozonolysis peaks, but the polymer still precipitated out of the solvent (Figure 7.5C). Instead of forming solid pellets, the mcl-PHAs instead presented as a gel or slime, likely due lower crosslinking density. Upon drying, the ozonolysed polymer produced a film that would not dissolve in MeOH or DCM and tore easily.

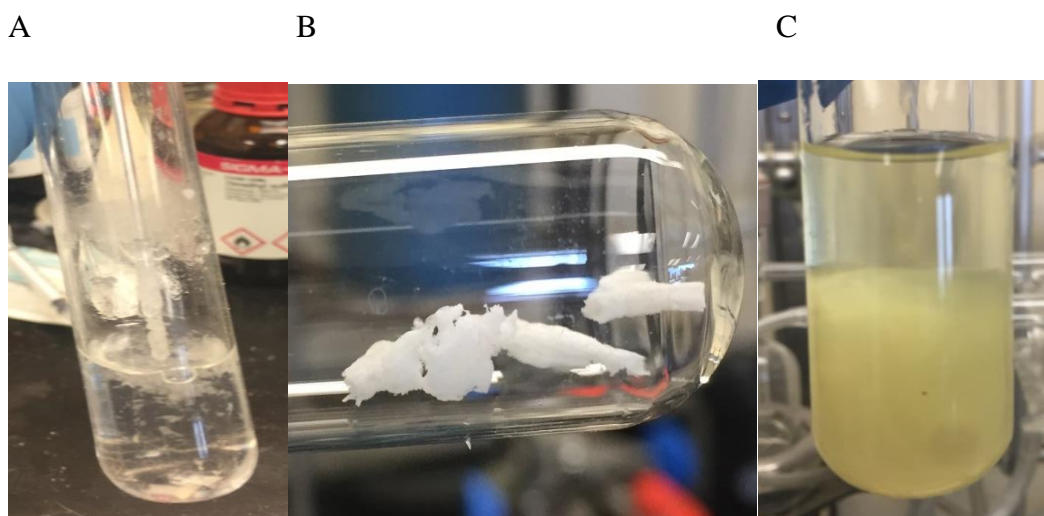


Figure 7.5. A) and B) Ozonolysis product of unsaturated mcl-PHAs from flax LCFAs in DCM; C) Precipitation of PHA polymer from the DCM/MeOH solution.

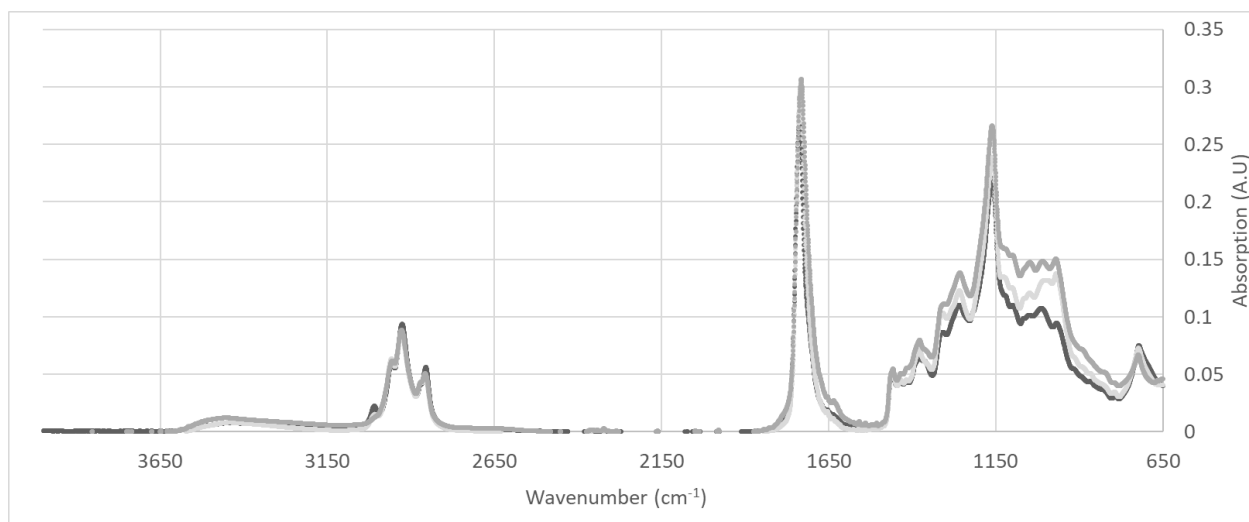


Figure 7.6. FTIR spectrum of modified PHA produced by *P. putida* LS46 from flax fatty acids. ■, Flax PHA; ▨, Thermally cross-linked flax PHA; ▩, Ozonated flax PHA

7.5.2. Osmium Tetroxide Catalysed Olefin Cleavage

A positive control using oleic acid was performed to optimize reaction conditions and confirm expected products using gas chromatography. The oxidative cleavage of oleic acid using OsO_4 and oxone resulted in a 51% conversion into the expected nonanedioic and nonanoic acid products consistent with previous reports (Travis et al., 2002). When the

starting substrate concentration of oleic acid was lowered from 100 mg to 50 mg, the product conversion was improved to 92.1%. The concentration of saturated fatty acid contaminants of technical grade oleic acid, steric and palmitic acid, were unaffected. Table 7.2 outlines the experimental conditions for the OsO₄ catalysed cleavage of fatty acids and mcl-PHAs. The content of unsaturated monomers in the final polymer dropped by 89.8%, 82.3%, 81.8%, and 59.0% for conditions Flax PHA 1, Flax PHA 2, Canola PHA 1, and Canola PHA 2, respectively. Although Flax PHAs are amorphous liquids, the reacted flax PHAs crystallized into a film as the solvent was evaporated. This crystallization occurred more rapidly than PHO (Gagnon et al., 1992). The reacted flax PHAs were now soluble in methanol, consistent with increased hydrophilicity reported of hydroxylated and carboxylated PHOU (Lee et al., 2000a; Kurth et al., 2001; Stigers and Tew, 2003).

Table 7.2. Experimental reaction conditions. The bold conditions did not yield a film but resulted in a fragrant, black liquid.

Substrate	Initial Mass (mg)	Exp. OsO ₄ Eq.	Exp. Oxone Eq.	Temp (°C)/ Time (h)	Exp. NaSO ₃ Eq.	Final Mass (mg)
Oleic Acid 1	102.9	0.0087	4.54	60/22	5.88	81.3
Oleic Acid 2	112.6	0.0074	4.34	60/22	5.61	107.4
Canola Oil 1	108.4	0.0077	4.29	60/22	5.43	102.1
Oleic Acid 3	52.4	0.0145	8.29	60/22	10.44	59.0
Oleic Acid 4	109.7	0.0076	8.18	60/22	10.95	115.0
Oleic Acid 5	110.3	0.0076	4.44	21/22	5.44	107.8
Flax PHA 1	63.0	0.0088	5.23	60/22	6.36	61.7
Flax PHA 2	52.9	0.0110	5.91	21/22	7.56	61.3
Flax PHA 3	60.8	0.0092	5.13	21/22	6.60	50.8
Canola PHA 1	93.9	0.0332	18.42	21/22	23.88	105.6
Canola PHA 2	213.0	0.0145	8.10	21/22	10.50	249.1
Canola PHA 3	213.9	0.0146	8.10	21/22	10.50	165.0
Oleic Acid 6	49.0	0.017	0	21/22	12.24	38.8
Oleic Acid 7	42.1	0	11.02	21/22	14.28	28.6
Canola PHA 4	44.9	0	38.56	21/22	49.98	20.1

Hexanoic acid, nonanoic acid, and azelaic acid were also identified by GC after the cleavage of mcl-PHAs in quantities consistent with expected side-chain products. Several new peaks were observed in the product (Figure 7.7). One of the expected monomer products of oxidative cleavage of mcl-PHAs was 3-hydroxypentadioic acid (3-hydroxyglutarate). Standards of dimethyl 3-hydroxyglutarate and glutaric anhydride were compared against the flax PHA products to assess the possible cyclisation of this product. There was no peak for glutaric anhydride present in flax PHA products. Dimethyl-3-hydroxyglutarate shares a retention time with C10-1 PHA monomers at 10.7 mins, but the product peak obtained appeared consistent with the standard and increased in size when using canola PHAs (Figure 7.8). 3-hydroxyglutarate was the largest of the flax PHA product peaks, consistent with theoretical yields (Table 7.3). Considering the expected retention time shifts and theoretical proportions of 3-hydroxyadipate and 3-hydroxypimelate, they are likely presented at 11.9 and 12.5 minutes.

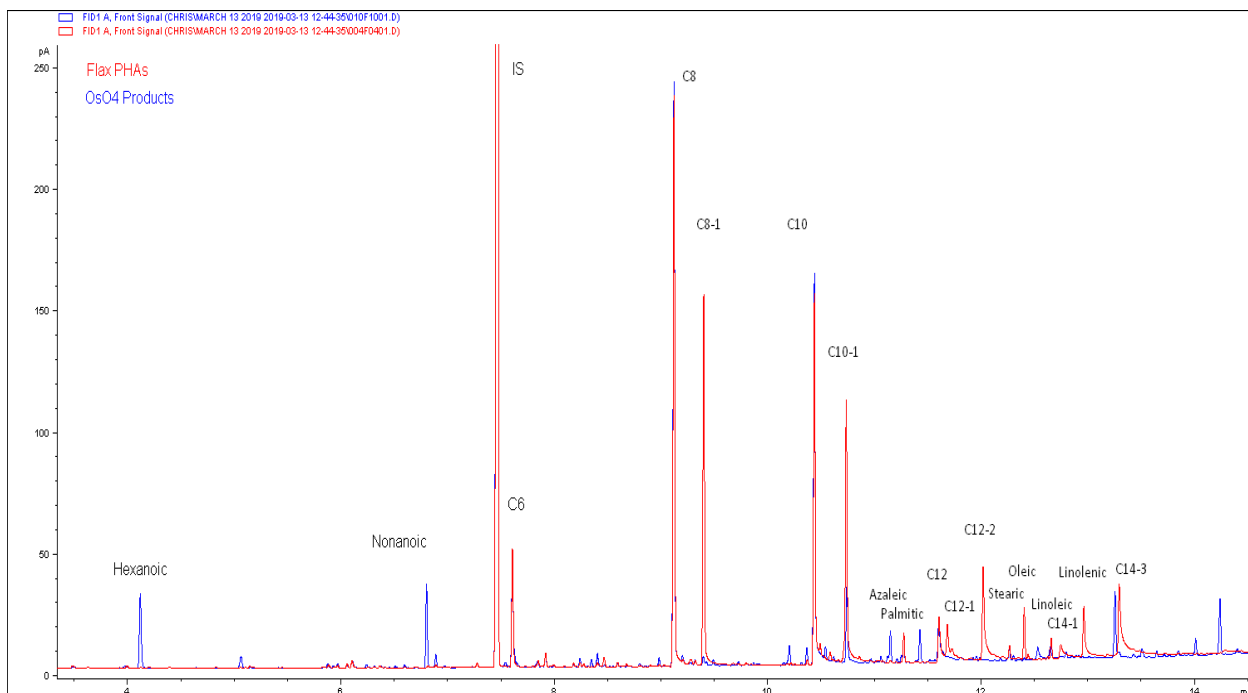


Figure 7.7. Gas chromatogram of flax mcl-PHAs (red) and their OsO₄ cleavage products (blue).

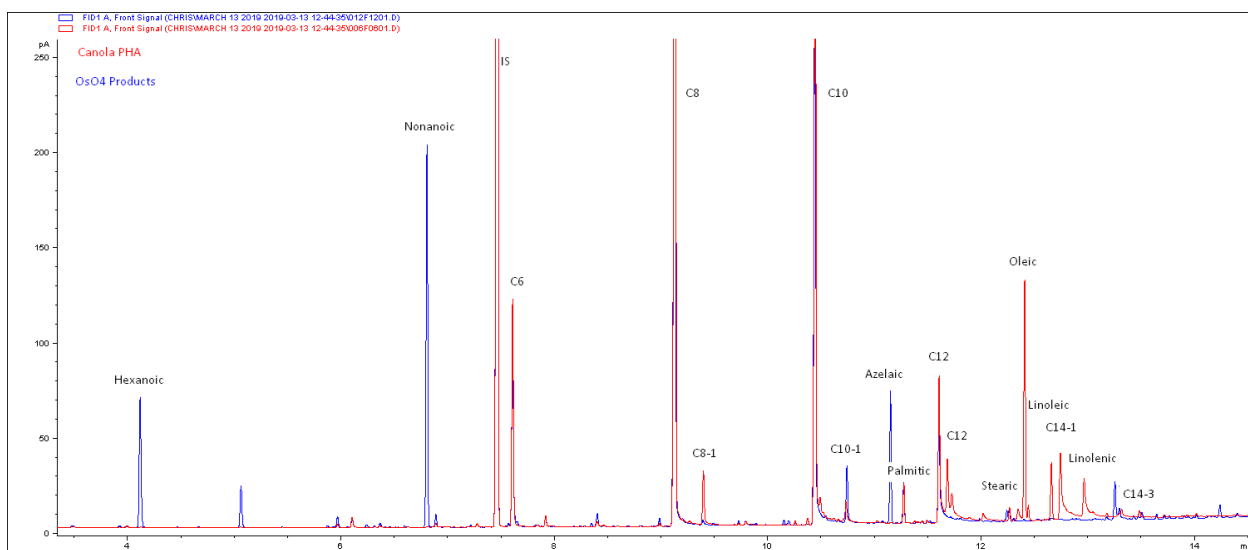
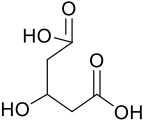
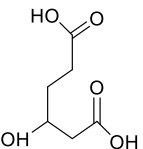
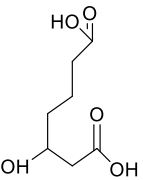


Figure 7.8. Gas chromatogram of canola mcl-PHAs (red) and their OsO₄ cleavage products (blue).

Table 7.3. Expected monomer products from unsaturated mcl-PHAs after OsO₄ cleavage.

Expected Monomer Products	Monomer Substrates	Cumulative Monomer Mol % - Flax PHAs	Cumulative Monomer Mol % - Canola PHAs
3-hydroxyglutarate 	C8-1 C14-1 C14-2 C14-3	25.6 %	8.9 %
3-hydroxyadipate 	C12-1 C12-2	6.5 %	2.7 %
3-hydroxypimelate 	C10-1	13.0 %	1.8 %

The new crystallinity and solubility of the polymer, disappearance of unsaturated monomers, the proportion of hexanoic and nonanoic acids produced, and the three aforementioned product peaks, are all consistent with the expected cleavage of unsaturated mcl-PHAs by OsO₄. However, these three product peaks were not sufficient to account for the removed unsaturated monomers. Significant peaks were observed downstream at 13.2, 14.0, and 14.2 minutes, and a few smaller peaks were also detected in that range. Based on the retention times of these unknown peaks, they could represent: i) oxidized mcl-PHA monomers that were not cleaved (i.e. dihydroxylation); ii) dimeric products; or iii) di- or tri-unsaturated monomers which have been partially cleaved containing residual vinyl

moieties (Figure 7.9). Dimeric products are unlikely since these peaks were not observed during autoxidative crosslinking or after ozonolysis (data not shown).

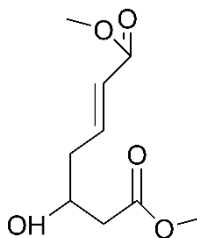


Figure 7.9. Proposed unsaturated OsO₄-catalysed partial cleavage product of polyunsaturated mcl-PHAs detected by gas chromatography.

NMR analyses were consistent with the GC analysis. The peaks associated with vinylic and allylic positions were no longer observed on ¹H-NMR or ¹³C-NMR after OsO₄-catalysed cleavage of oleic acid, canola PHAs or flax PHAs (supplementary material). In addition, peaks at 2.4 and 5.5 ppm were obtained which are consistent with terminal carboxylic acids (Kurth et al., 2001; Stigers and Tew, 2003), but this is also indicative of fatty acid products. The above reaction conditions without oxone would produce diol products, which were observed in trace at 3.8 ppm with oleic acid, since it is a two-step reaction and the low starting equivalence of osmium tetroxide. The reaction was also completed on oleic acid and canola PHAs without OsO₄. In this case, no polymer cross-linking occurred, and small peaks were obtained at 3.8 ppm and 4.9 ppm. The peak at 3.8 ppm was not observed in oleic acid or decanoic acid, but it was present in canola PHA indicating some auto-oxidation may have already begun. The products of canola and flax PHAs also contained small peaks at 3.8 ppm. In the case of tri-substituted vinyl moieties, secondary dihydroxylation products were observed (Travis et al., 2002). Taken together with the GC data, a small amount of secondary oxidation products could present as small

peaks after 13 minutes on the GC but do not account for the larger peaks at 13.2, 14.0, and 14.2 minutes.

GC-MS could identify with high certainty, saturated monomers of C6, C8, and C10 through the NIST library. The certainty decreased as low as 9% for longer and unsaturated mcl-PHA monomers but could still be identified as 3-hydroxyalkanoates and showed some of the characteristic fragments (Figure 7.10). Higher unsaturation has been reported to result in multiple radical cation formation with less predictable fragmentation (Murphy and Axelsen, 2011). Some of the unknown peaks produced after OsO₄-catalyzed cleavage of flax PHA were identified as PHAs but as low as 2% certainty, therefore their fragmentation patterns were analyzed. All the unknown peaks produced small fragments containing the methyl-ester moiety or the hydroxyl moiety. They also all contained an m/e 137 fragment, which presented in all unsaturated monomers and not in saturated monomers or fatty acids. This has been described in ω -3 3-hydroxytetradecenoate as the terminal aliphatic diene radical fragment (Lee and Choi, 1995). In this instance, the fragment of m/e 137 may need other explanation, since it was observed in all monomers containing an unsaturation. Rearrangements and cyclization are common for compounds with unsaturated and ester moieties during fragmentation (Murphy and Axelsen, 2011; Weitzel et al., 2011), and may explain some unknown fragmentation peaks if the monomers were cyclizing prior to further fragmentation (Figure 7.11). Considering that the m/e 137 was observed in various unsaturated positions, potentially with terminal carboxylates, it appears reasonable that an allylic cyclisation could have occurred in which the tails are cleaved.

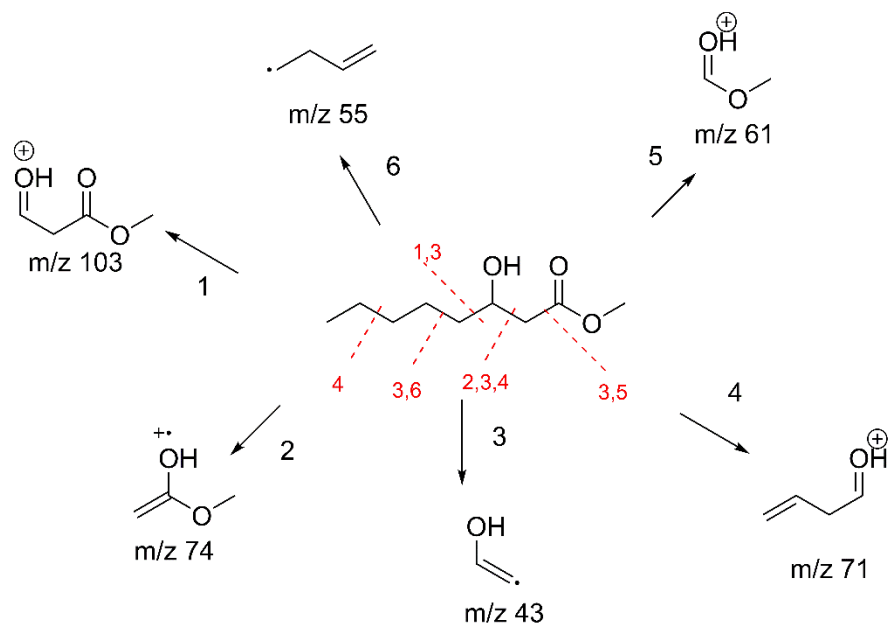


Figure 7.10. GC-MS fragmentation products of methanolysed polyhydroxyoctanoate numbered by relative abundance.

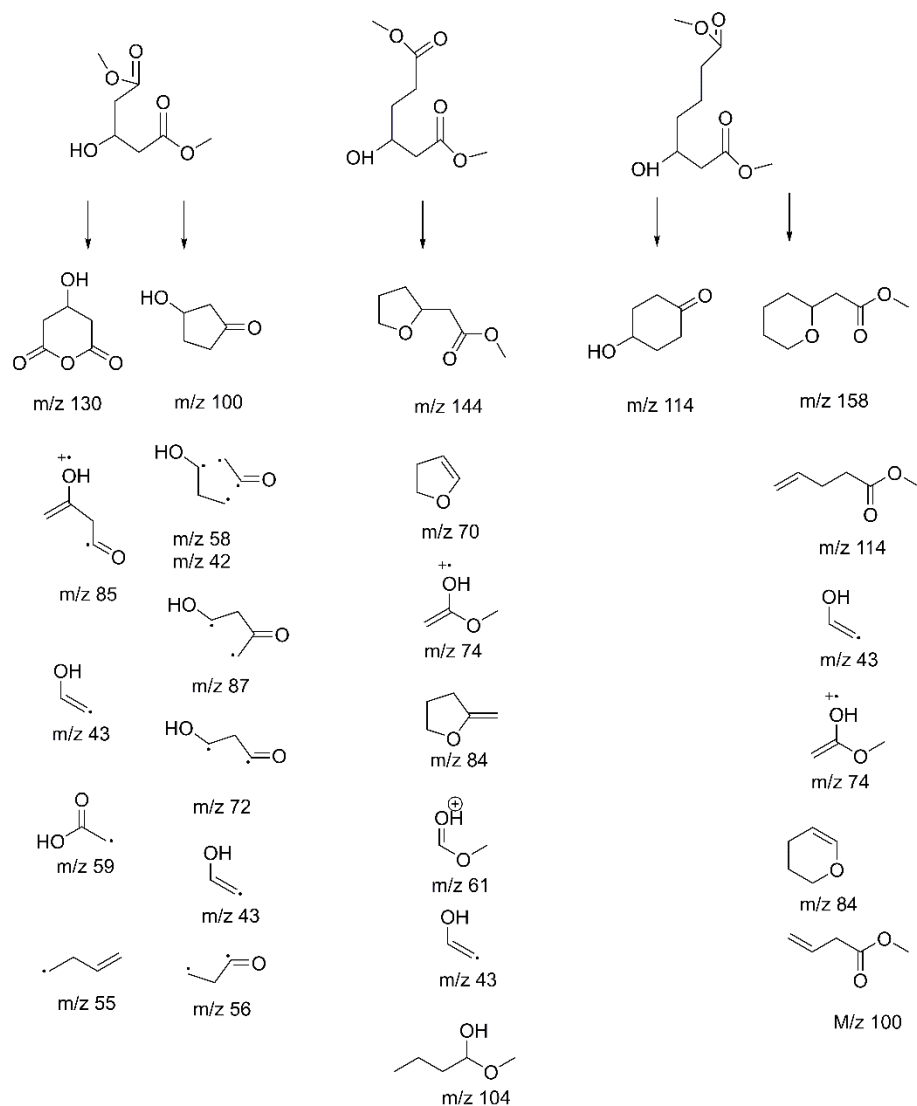


Figure 7.11. Possible eV cyclization of mcl-PHA OsO₄-catalysed cleavage products prior to further fragmentation during GC-MS.

The two largest unknown peaks with retention times of 13.2 and 14.2 minutes exhibited fragments consistent with terminal carboxylate. This included short-chain, unsaturated fatty acid fragments. The former peak contained many fragmentation peaks between m/e 50-60 consistent with 3-4 carbon fragments resulting of two unsaturated moieties. The short carboxylic acid fragments and hydroxyl fragments were consistent

with expected vinyl positions. The latter peak contained a characteristic m/e 157 which might identify the monomer as a C12-2 which has been cleaved at the ω -3 vinyl moiety. This would be consistent with the relative peak sizes between flax PHA and canola PHA products. The abundance of the peak at 13.2 minutes in canola oil is inconsistent with the small proportion of di- or tri-unsaturated monomers from this substrate. This peak was not observed in the OsO_4 -catalysed cleavage of flax fatty acids or canola oil. The fragmentation patterns were not consistent with epoxidation or hydroxylation.

7.6. Discussion

7.6.1. Ozonolysis

The unsaturated mcl-PHAs cross-linked during the ozonolysis reaction, and a hypothesized lower cross-linking density was observed when methanol was used as a co-solvent based on appearance of the reacted polymer. This is consistent with reports of secondary oxidation of olefins from hydroxyl-radicals which resulted in auto-oxidation, in which methanol behaved as a scavenger for radical CIs (Zeng et al., 2020). The CI is known to produce hydroxyl-radicals during deterioration to an aldehyde and those radicals would be sufficient for the hydrogen abstraction, or radical hydroxyl addition at the vinylic moieties, to propagate crosslinking (Hasson et al., 2003). The reaction of CI with the double bonds or ester bonds of mcl-PHAs is not expected to significantly affect the process but the reaction of CI with free carboxylic acids, produced aldehydes, and other CI could be a significant source of secondary ozonides and oligomeric products (Hearn et al., 2005; Vereecken et al., 2014; Gallimore et al., 2017; Vereecken, 2017).

The presence of nonanoic acid after ozonolysis of oleic acid in DCM reduced by DMS could also be resultant of hydroxyl-radicals over oxidizing the cleavage products. To

improve the fidelity of ozonolysis and reduce levels of autooxidation, increased concentrations of methanol or inclusion of carbonate and bicarbonate should be employed (Chiang et al., 2006; Zeng et al., 2020). Although the presence of methanol did appear to lower cross-linking density in this study, some reports indicate that hydroxyl-radicals are still produced in the presence of CI scavengers (Hearn et al., 2005). Secondary oxidation products are regularly identified from ozonolysis, and with this in consideration, the autooxidation and crosslinking of unsaturated mcl-PHAs may be unavoidable.

7.6.2. Osmium Tetroxide Catalysed Olefin Cleavage

The oxidative cleavage of mcl-PHAs resulted in semi-crystalline films with various degrees of increased hydrophilicity. The canola PHA product was still insoluble in methanol, but the flax PHA product was soluble. GC and NMR data indicated complete disappearance of unsaturated monomers. The main monomer product was identified as 3-hydroxyglutaric acid. Based on the fragmentation pattern of the unknown peaks in which 3-hydroxy fragments, fatty acid fragments and characteristic unsaturated fragments were observed, the simplest explanation is that they are PHA monomers which have undergone partial oxidative cleavage. The reason for the partial cleavage could be steric hindrance. The minor unidentified peaks between 13.2 and 14.2 minutes are most likely the result of trace fatty acids present in flax such as linolelaidic, gamma-linolenic, and eicosenoic acids producing PHA monomers with different vinyl positions (Mungure and Birch, 2014).

The NMR data suggests small amounts of secondary oxidation-products might be expected. The formation of epoxides and diols could be expected to form from oxone (Rani and Vankar, 2003). Heating of olefins in acetonitrile:water with oxone resulted in production of diols and upon reflux was sufficient without catalyst to cleave the olefin and

oxidize the resulting aldehyde to a terminal carboxylic acid (Parida and Moorthy, 2014). Dihydroxylation could also be expected from steric effects on the OsO₄ reaction in which oxone is unable to hydrolyse the ester complex (Schroder, 1980; Travis et al., 2002). The GC and GCMS data suggest that secondary oxidation was minimized.

In some instances, a black product was obtained. Osmium tetroxide has been used to prepare electron microscopy specimens by tissue fixation through protein and lipid cross-linking. The reduction of osmium produces osmium black as it ligated protein and lipid. Osmium tetroxide cross-links the protein sidechains at the nitrogen or sulfur functional-groups and the olefin moiety of lipids, but does not react with ester or peptide bonds (Hopwood, 1970; Nielson and Griffith, 1979). The reaction of olefinic lipids with OsO₄ produced black products are proposed to be dimeric monoester and monomeric diester complexes prior to reduction to diol products, with the diester complexes being favoured by sterically large molecules. Notably, steric hindrances also reduced the rate at which a secondary oxidant hydrolysed the osmium esters (Schroder, 1980). The black products obtained during our experimentation with mcl-PHAs from LCFAs could be the result of monomeric diester complexes which are slow to oxidize due to steric hindrances of the polymer sidechains. Based on the substrate loading, the black product was more likely caused by overoxidation.

Although the OsO₄-catalysed cleavage product of flax PHA remained stable stored in methanol, the dried film appeared to cross-link and could not be resolubilized in chloroform or methanol. This is consistent with the behaviour of unsaturated mcl-PHAs and would be consistent with partially oxidized monomers in which some unsaturation persisted.

7.7. Conclusions

The largest associated cost to the production of mcl-PHAs is the substrate requirements. Mcl-PHAs with the highest crystallinity and tensile strength are conventionally produced using high-cost medium chain length fatty acids. Vegetable oils, and their waste streams, provide an inexpensive alternative for high-yield production of mcl-PHAs. The unsaturated fatty acids are incorporated into mcl-PHAs which greatly reduced crystallinity. Oxidative cleavage of unsaturated mcl-PHAs would result in shorter sidechains and potentially increase crystallinity and hydrophilicity. The ozonolysis reactions with unsaturated mcl-PHAs could not be completed without some degree of cross-linking due to secondary oxidation. The OsO₄-catalysed cleavage reaction was successful at improving polymer crystallinity and increasing hydrophilicity of unsaturated mcl-PHAs from LCFAs. Furthermore, the terminal carboxylic acid could be used for grafting or converted into a click-ready polymer. into more functionalized polymers. The propensity for unsaturated mcl-PHAs to crosslink and the steric effects of the polymer require further reaction optimization to drive completion of the reaction toward 3-hydroxyglutarate, 3-hydroxyadipate, and 3-hydroxypimelate while avoiding overoxidation through insufficient substrate loading.

7.8. Acknowledgements

The co-authors John L. Sorensen, Nazim Cicek, and David B. Levin provided guidance on experimental design and manuscript revisions. This study was funded by Genome Canada, through the Genome Applications and Partnership Program (GAPP), and the Natural Sciences and Engineering Research Council (NSERC) of Canada through a Collaborative Research and Development (CRD) grant with Minto BioProducts Ltd. as the

industrial partner (grant number CRDPJ-490630-15). The authors disclose they have no conflict of interest. This article does not contain any studies with human participants or animals performed by any of the authors.

7.9. Supplementary Material

The proton and carbon NMR spectra representing the observed loss of unsaturated moieties in mcl-PHAs due to the described osmium tetroxide cleavage are provided below in Figures 7.12 and 7.13 respectively. The carbon assignments were determined from referenced work (de Waard et al.,1993). For $^1\text{H-NMR}$: $\delta = 0.9$ (terminal CH_3), $\delta = 1.3$ (aliphatic CH_2), $\delta = 1.6$ (C4-CH_2), $\delta = 2.4$ (allylic $=\text{CH-CH}_2$), $\delta = 2.6$ (C2-CH_2), $\delta = 2.8$ (allylic $\text{CH}_2\text{-CH=}$), $\delta = 5.2$ (CHO), $\delta = 5.4$ (olefinic CH). The peak at $\delta = 2.0$ is the C2 of fatty acids. The peaks at $\delta = 2.2$ and 4.2 are contaminant ethyl acetate. The reduction in peak size is observed at $\delta = 2.4$, 2.6 and 5.4 after the assumed cleavage reaction. There is also a modest decrease in the relative peak area of terminal CH_3 , however the presence of fatty acid contaminants and expected products makes it difficult to assign any peaks to sidechain carboxylic acid products and would require a purification procedure. For $^{13}\text{C-NMR}$: $\delta = 169$ is C1, $\delta = 123\text{-}134$ are olefinic carbons, $\delta = 71$ is C3, $\delta = 39$ is C2, $\delta = 18\text{-}36$ are sidechain saturated and allylic carbons and $\delta = 14$ is the terminal side chain carbon. Note that the allylic and olefinic signals disappear after the osmium tetroxide catalysed cleavage reactions.

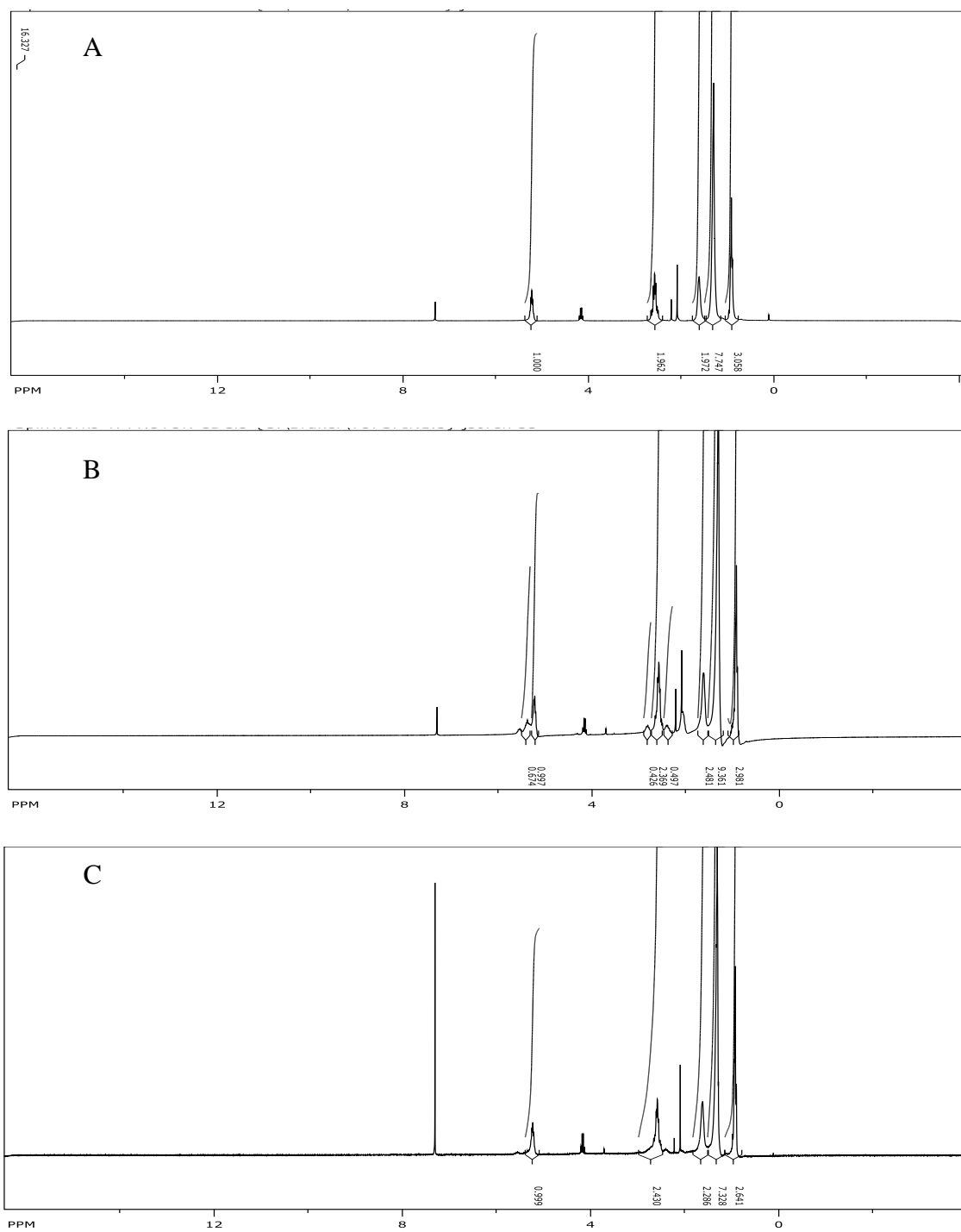


Figure 7.12. The ¹H-NMR (300 MHz, CDCl₃) of mcl-PHA produced by *P. putida* LS46 provided A) decanoic acid, B) Canola LCFAs and C) Canola LCFAs followed by the osmium tetroxide catalyzed cleavage reaction.

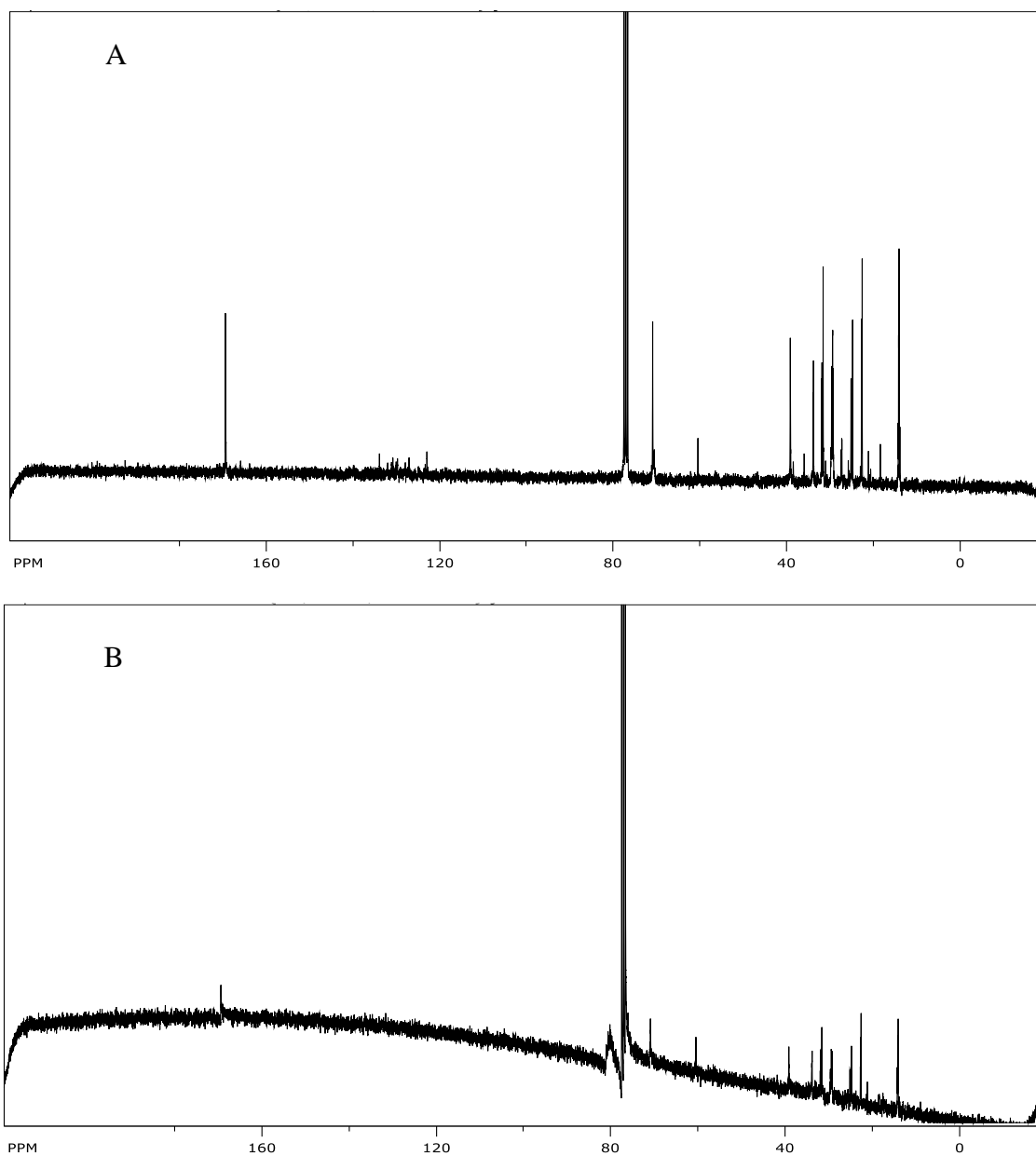


Figure 7.13. The ^{13}C -NMR (75 MHz, CDCl_3) of mcl-PHA produced by *P. putida* LS46 provided A) canola LCFAs and B) Flax LCFAs followed by the osmium tetroxide catalyzed cleavage reaction.

Chapter 8: Engineering Significance and Concluding Remarks

8.1. Engineering Significance

mcl-PHAs are attractive biopolymers due to their sustainability, biodegradability, back-bone consistency, and property variability controllable through cultivation conditions. Their major drawbacks are production costs and processability. This research sought to improve high cell density cultivation of mcl-PHAs from LCFAs utilizing the resulting microaerophilic conditions to promote intracellular polymer accumulation. The data obtained suggests that PHA titers could be maximized for a given k_{La} , which would be advantageous since dissolved oxygen will ultimately be the limiting factor to achieving high cell titers. The challenge with this approach is reduced real-time feedback for maintaining feeding rates, and therefore a better fundamental understanding of the microbial response to microaerophilic conditions that result in mcl-PHA accumulation is required.

Microaerophilic mcl-PHA accumulation in mcl-PHAs was completed at lower cell densities to compare the microbial response to octanoic acid versus LCFAs. Upon onset of oxygen-limiting conditions, *P. putida* LS46 growing on octanoic acid ceased further cell division and diverted substrate utilization to respiration and PHA accumulation. In contrast, biomass production on LCFAs continued at a linear rate after oxygen-limitation, and the slope of the line was correlated to k_{La} . As cultivation continued, NPCM increased, but the rate of cell mass production slowed as cell maintenance required an increased share of the available energy produced by constant respiration rates. Ultimately, PHA production rates continued to increase while NPCM rates declined, resulting in increasing intracellular mcl-PHA content. Co-feeding the substrates under microaerophilic conditions provided further

benefits of higher cell titer. High intracellular PHA content with a high mol% of C8 monomers, and greater volumetric productivity was achieved. Further optimization of this co-feeding strategy could be effective for tailoring monomer composition, improving productivity, and ultimately reducing costs compared to growth solely on commodity MCFAs.

8.2. Concluding Remarks

P. putida LS46 was grown on a variety of substrates suitable for mcl-PHA accumulation. The mcl-PHAs reported were consistent with various literature reports for polymer yield and monomer composition. The primary monomer from unrelated substrates such as glucose was C10. VFAs result in a small proportion of monomers of equal lengths, but still predominantly produced mcl-PHAs through the *de novo* fatty acid synthesis pathway. As the fatty acids increased in length, the proportion of monomer length increased up to decanoic acid (C10). Fatty acids longer than C9 are shortened by the fatty acid degradation pathway, and C8 is the favoured monomer. Longer and more unsaturated monomers are obtained with representative LCFAs. The monomer composition has a drastic effect on polymer crystallinity. PHAs display the highest crystallinity as the co-monomer content drops. The crystal structure of the polymer incompatibly changes with side-chain length and C6 monomers display very little crystallinity. For these reasons, copolymers of mcl-PHAs and scl-PHAs display drastically reduced crystallinity. Unsaturated monomers also disrupt crystallinity. Taken together, careful control of monomer content is required to obtain desirable film properties.

The oxidative cleavage of unsaturated mcl-PHAs can introduce crystallinity to these polymers and they were observed to form a film more rapidly than any mcl-PHAs produced in Chapter 6. Highly unsaturated films became soluble in methanol after

modification indicating increased amphiphilicity due to terminal carboxylic acid groups. During both ozonolysis and osmium tetroxide catalysis, some variables were observed to cross-link. In the case of ozonolysis, cross-linking may be a function of secondary oxidation products, whereas the cross-linking of osmium-tetroxide catalysed cleavage occurred after reaction, likely due to remaining unsaturated monomers. Due to the reduced cost of mcl-PHA production from LCFAs and the low catalyst loading requirement of OsO_4 , this strategy could result in meaningful cost savings, controlled degrees of crystallinity and amphiphilicity, and as pre-cursor polymers for further chemical modification.

References

- Abe, H., Ishii, N., Sato, S., and Tsuge, T. (2012). Thermal properties and crystallization behaviors of medium-chain-length poly(3-hydroxyalkanoate)s. *Polymer (Guildf)*. 53, 3026–3034. doi:10.1016/j.polymer.2012.04.043.
- Anderson, A., and Dawes, E. (1990). Occurrence, Metabolism, Metabolic Role, and Industrial Uses of Bacterial Polyhydroxyalkanoates. *Microbiol. Rev.* 54, 450–472. doi:10.1016/0022-2852(61)90347-2.
- Andin, N., Longieras, A., Veronese, T., Marcato, F., Molina-Jouve, C., and Uribelarrea, J. L. (2017). Improving carbon and energy distribution by coupling growth and medium chain length polyhydroxyalkanoate production from fatty acids by *Pseudomonas putida* KT2440. *Biotechnol. Bioprocess Eng.* 22, 308–318. doi:10.1007/s12257-016-0449-1.
- Anjum, A., Zuber, M., Zia, K. M., Noreen, A., Anjum, M. N., and Tabasum, S. (2016). Microbial production of polyhydroxyalkanoates (PHAs) and its copolymers: A review of recent advancements. *Int. J. Biol. Macromol.* 89, 161–174. doi:10.1016/j.ijbiomac.2016.04.069.
- Antonio, R. V., Steinbüchel, A., and Rehm, B. H. A. (2000). Analysis of in vivo substrate specificity of the PHA synthase from *Ralstonia eutropha*: Formation of novel copolyesters in recombinant *Escherichia coli*. *FEMS Microbiol. Lett.* 182, 111–117. doi:10.1016/S0378-1097(99)00578-9.
- Arcos-Hernandez, M. V., Gurieff, N., Pratt, S., Magnusson, P., Werker, A., Vargas, A., et al. (2010). Rapid quantification of intracellular PHA using infrared spectroscopy: An application in mixed cultures. *J. Biotechnol.* 150, 372–379. doi:10.1016/j.jbiotec.2010.09.939.
- Arkin, A. H., Hazer, B., and Borcakli, M. (2000). Chlorination of poly(3-hydroxyalkanoates) containing unsaturated side chains. *Macromolecules* 33, 3219–3223. doi:10.1021/ma991535j.
- Ashby, R. D., Cromwick, A. M., and Foglia, T. A. (1998a). Radiation crosslinking of a bacterial medium-chain-length poly(hydroxyalkanoate) elastomer from tallow. *Int. J. Biol. Macromol.* 23, 61–72. doi:10.1016/S0141-8130(98)00034-8.
- Ashby, R. D., and Foglia, T. A. (1998). Poly(hydroxyalkanoate) biosynthesis from triglyceride substrates. *Appl. Microbiol. Biotechnol.* 49, 431–437. doi:10.1007/s002530051194.
- Ashby, R. D., Foglia, T. A., Liu, C., and Hampson, J. W. (1998b). Improved film properties of radiation-treated medium-chain-length poly(hydroxyalkanoates). *Biotechnol. Lett.* 20, 1047–1052.
- Ashby, R. D., Foglia, T. A., Solaiman, D. K. Y., and Liu, C. (2000). Viscoelastic properties of linseed oil-based medium chain length poly (hydroxyalkanoate) films: effects of

- epoxidation and curing. *Int. J. Biol. Macromol.* 27, 355–361.
- Awogbemi, O., Onuh, E. I., and Inambao, F. L. (2019). Comparative study of properties and fatty acid composition of some neat vegetable oils and waste cooking oils. *Int. J. Low-Carbon Technol.* 14, 417–425. doi:10.1093/ijlct/ctz038.
- Babinot, J., Guigner, J. M., Renard, E., and Langlois, V. (2012). A micellization study of medium chain length poly(3-hydroxyalkanoate)-based amphiphilic diblock copolymers. *J. Colloid Interface Sci.* 375, 88–93. doi:10.1016/j.jcis.2012.02.042.
- Babinot, J., Renard, E., and Langlois, V. (2010). Preparation of *Clickable* Poly(3-hydroxyalkanoate) (PHA): Application to Poly(ethylene glycol) (PEG) Graft Copolymers Synthesis. *Macromol. Rapid Commun.* 31, 619–624. doi:10.1002/marc.200900803.
- Babinot, J., Renard, E., Le Droumaguet, B., Guigner, J. M., Mura, S., Nicolas, J., et al. (2013). Facile synthesis of multicompartment micelles based on biocompatible poly(3-hydroxyalkanoate). *Macromol. Rapid Commun.* 34, 362–368. doi:10.1002/marc.201200692.
- Bart, J. C. J., Palmeri, N., and Cavallaro, S. (2010). “Feedstocks for biodiesel production,” in *Biodiesel Science and Technology*, 130–225. doi:10.1533/9781845697761.130.
- Bassas, M., Diaz, J., Rodriguez, E., Espuny, M. J., Prieto, M. J., and Manresa, A. (2008). Microscopic examination *in vivo* and *in vitro* of natural and cross-linked polyunsaturated mclPHA. *Appl. Microbiol. Biotechnol.* 78, 587–596. doi:10.1007/s00253-008-1350-4.
- Bear, M. M., Leboucher-Durand, M. A., Langlois, V., Lenz, R. W., Goodwin, S., and Guérin, P. (1997). Bacterial poly-3-hydroxyalkanoates with epoxy groups in the side chains. *React. Funct. Polym.* 34, 65–77. doi:10.1016/S1381-5148(97)00024-2.
- Benessere, V., Cucciolo, M. E., De Santis, A., Di Serio, M., Esposito, R., Ruffo, F., et al. (2015). Sustainable Process for Production of Azelaic Acid Through Oxidative Cleavage of Oleic Acid. *JAOCs, J. Am. Oil Chem. Soc.* 92, 1701–1707. doi:10.1007/s11746-015-2727-z.
- Berg, P., Feber, D., Granskog, A., Nordigarden, D., and Ponkshe, S. (2020). Can system-level approaches, including collaboration along the value chain, make our approach to packaging more sustainable? *McKinsey Co.* Available at: <https://www.mckinsey.com/industries/paper-forest-products-and-packaging/our-insights/the-drive-toward-sustainability-in-packaging-beyond-the-quick-wins>.
- Bioplastics market data (2020). *Eur. Bioplastics*. Available at: <https://www.european-bioplastics.org/market/>.
- Blunt, W., Dartailh, C., Sparling, R., Gapes, D., Levin, D. B., and Cicek, N. (2017). Microaerophilic environments improve the productivity of medium chain length polyhydroxyalkanoate biosynthesis from fatty acids in *Pseudomonas putida* LS46.

- Process Biochem.* 59, 18–25. doi:10.1016/j.procbio.2017.04.028.
- Blunt, W., Dartiailh, C., Sparling, R., Gapes, D., Levin, D. B., and Cicek, N. (2018a). Carbon flux to growth or polyhydroxyalkanoate synthesis under microaerophilic conditions is affected by fatty acid chain-length in *Pseudomonas putida* LS46. *Appl. Microbiol. Biotechnol.* 102, 6437–6449. doi:10.1007/s00253-018-9055-9.
- Blunt, W., Hossain, M. E., Gapes, D., Sparling, R., Levin, D. B., and Cicek, N. (2014). Real-time monitoring of microbial fermentation end-products in biofuel production with titrimetric off-gas analysis (TOGA). *Biol. Eng. Trans.* 6, 203–219. doi:10.13031/bet.6.10496.
- Blunt, W., Lagassé, A., Jin, Z., Dartiailh, C., Sparling, R., Gapes, D. J., et al. (2019). Efficacy of medium chain-length polyhydroxyalkanoate biosynthesis from different biochemical pathways under oxygen-limited conditions using *Pseudomonas putida* LS46. *Process Biochem.* 82, 19–31. doi:10.1016/j.procbio.2019.04.013.
- Blunt, W., Levin, D. B., and Cicek, N. (2018b). Bioreactor operating strategies for improved polyhydroxyalkanoate (PHA) productivity. *Polymers (Basel)*. 10. doi:10.3390/polym10111197.
- Bonartsev, a P., Myshkina, V. L., Nikolaeva, D. a, Furina, E. K., and Makhina, T. a (2007). Biosynthesis , biodegradation , and application of poly(3- hydroxybutyrate) and its copolymers - natural polyesters produced by diazotrophic bacteria. *Appl. Microbiol.*, 295–307. doi:10.1002/btpr.2247.
- Brandl, H., Gross, R. a, Lenz, R. W., and Fuller, R. C. (1988). *Pseudomonas oleovorans* as a Source for novel Poly(β -Hydroxyalkanoates) for Potential Applications as Biodegradable Polyesters. *Appl. Environ. Microbiol.* 54, 1977–1982.
- Bugnicourt, E., Cinelli, P., Lazzeri, A., and Alvarez, V. (2014). Polyhydroxyalkanoate (PHA): Review of synthesis, characteristics, processing and potential applications in packaging. *Express Polym. Lett.* 8, 791–808. doi:10.3144/expresspolymlett.2014.82.
- Cakmakli, B., Hazer, B., and Borcakli, M. (2001). Poly(styrene peroxide) and Poly(methyl methacrylate peroxide) for Grafting on Unsaturated Bacterial Polyesters. *Macromol. Biosci.* 1, 348–354. doi:10.1002/1616-5195(20011101)1:8<348::aid-mabi348>3.3.co;2-9.
- Casini, E., De Rijk, T. C., De Waard, P., and Eggink, G. (1997). Synthesis of poly(hydroxyalkanoate) from hydrolyzed linseed oil. *J. Environ. Polym. Degrad.* 5, 153–158.
- Chanprateep, S. (2010). Current trends in biodegradable polyhydroxyalkanoates. *J. Biosci. Bioeng.* 110, 621–632. doi:10.1016/j.jbiosc.2010.07.014.
- Chen, G.-Q. (2010). Industrial Production of PHA. *Plast. from Bact. Nat. Funct. Appl.* 14, 121–132. doi:10.1007/978-3-642-03287-5_6.
- Chen, Y., Awasthi, A. K., Wei, F., Tan, Q., and Li, J. (2021). Single-use plastics:

- Production, usage, disposal, and adverse impacts. *Sci. Total Environ.* 752, 141772. doi:10.1016/j.scitotenv.2020.141772.
- Chhetri, A. B., Watts, K. C., and Islam, M. R. (2008). Waste Cooking Oil as an Alternate Feedstock for Biodiesel Production. *Energies* 1, 3–18. doi:10.3390/en1010003.
- Chiang, Y. P., Liang, Y. Y., Chang, C. N., and Chao, A. C. (2006). Differentiating ozone direct and indirect reactions on decomposition of humic substances. *Chemosphere* 65, 2395–2400. doi:10.1016/j.chemosphere.2006.04.080.
- Choi, J. Il, and Lee, S. Y. (1997). Process analysis and economic evaluation for poly(3-hydroxybutyrate) production by fermentation. *Bioprocess Eng.* 17, 335–342. doi:10.1007/s004490050394.
- Choi, J. Il, and Lee, S. Y. (1999a). High-level production of poly(3-hydroxybutyrate-co-3-hydroxyvalerate) by fed-batch culture of recombinant *Escherichia coli*. *Appl. Environ. Microbiol.* 65, 4363–4368. doi:10.1128/aem.65.10.4363-4368.1999.
- Choi, J., and Lee, S. Y. (1999b). Factors affecting the economics of polyhydroxyalkanoate production by bacterial fermentation. *Appl. Microbiol. Biotechnol.* 51, 13–21. doi:10.1007/s002530051357.
- Chowdhury, K., Banu, L., Khan, S., and Latif, A. (1970). Studies on the Fatty Acid Composition of Edible Oil. *Bangladesh J. Sci. Ind. Res.* 42, 311–316. doi:10.3329/bjsir.v42i3.669.
- Chuah, J. A., Yamada, M., Taguchi, S., Sudesh, K., Doi, Y., and Numata, K. (2013). Biosynthesis and characterization of polyhydroxyalkanoate containing 5-hydroxyvalerate units: Effects of 5HV units on biodegradability, cytotoxicity, mechanical and thermal properties. *Polym. Degrad. Stab.* 98, 331–338. doi:10.1016/j.polymdegradstab.2012.09.008.
- Chung, C. W., Kim, H. W., Kim, Y. B., and Rhee, Y. H. (2003). Poly(ethylene glycol)-grafted poly(3-hydroxyundecenoate) networks for enhanced blood compatibility. *Int. J. Biol. Macromol.* 32, 17–22. doi:10.1016/S0141-8130(03)00020-5.
- Ciesielski, S., Mozejko, J., and Pisutpaisal, N. (2015). Plant oils as promising substrates for polyhydroxyalkanoates production. *J. Clean. Prod.* 106, 408–421. doi:10.1016/j.jclepro.2014.09.040.
- Conte, E., Catara, V., Greco, S., Russo, M., Alicata, R., Strano, L., et al. (2006). Regulation of polyhydroxyalkanoate synthases (phaC1 and phaC2) gene expression in *Pseudomonas corrugata*. *Appl. Microbiol. Biotechnol.* 72, 1054–1062. doi:10.1007/s00253-006-0373-y.
- Cruz, M. V., Araújo, D., Alves, V. D., Freitas, F., and Reis, M. A. M. (2016). Characterization of medium chain length polyhydroxyalkanoate produced from olive oil deodorizer distillate. *Int. J. Biol. Macromol.* 82, 243–248. doi:10.1016/j.ijbiomac.2015.10.043.

- Cvetković, I., Milić, J., Ionescu, M., and Petrović, Z. S. (2008). Preparation of 9-hydroxynonanoic acid methyl ester by ozonolysis of vegetable oils and its polycondensation. *Hem. Ind.* 62, 319–328. doi:10.2298/HEMIND0806319C.
- Dartailh, C., Blunt, W., Sharma, P. K., Liu, S., Cicek, N., and Levin, D. B. (2021). The Thermal and Mechanical Properties of Medium Chain-Length Polyhydroxyalkanoates Produced by *Pseudomonas putida* LS46 on Various Substrates. *Front. Bioeng. Biotechnol.* 8, 1–9. doi:10.3389/fbioe.2020.617489.
- Davis, R., Chandrashekar, A., and Shamala, T. R. (2008). Role of (R)-specific enoyl coenzyme A hydratases of *Pseudomonas* sp in the production of polyhydroxyalkanoates. *Antonie van Leeuwenhoek, Int. J. Gen. Mol. Microbiol.* 93, 285–296. doi:10.1007/s10482-007-9203-1.
- Davis, R., Duane, G., Kenny, S. T., Cerrone, F., Guzik, M. W., Babu, R. P., et al. (2015). High cell density cultivation of *Pseudomonas putida* KT2440 using glucose without the need for oxygen enriched air supply. *Biotechnol. Bioeng.* 112, 725–733. doi:10.1002/bit.25474.
- de Koning, G. J. M., van Bilsen, H. M. M., Lemstra, P. J., Hazenberg, W., Witholt, B., Preusting, H., et al. (1994). A biodegradable rubber by crosslinking poly(hydroxyalkanoate) from *Pseudomonas oleovorans*. *Polymer (Guildf)*. 35, 2090–2097. doi:10.1016/0032-3861(94)90233-X.
- De Waard, P., Van der Wal, H., Huijberts, G. N. M., and Eggink, G. (1993). Heteronuclear NMR analysis of unsaturated fatty acids in poly(3-hydroxyalkanoates). Study of β -oxidation in *Pseudomonas putida*. *J. Biol. Chem.* 268, 315–319. doi:10.1016/s0021-9258(18)54151-x.
- Desbois, A. P., and Smith, V. J. (2010). Antibacterial free fatty acids: Activities, mechanisms of action and biotechnological potential. *Appl. Microbiol. Biotechnol.* 85, 1629–1642. doi:10.1007/s00253-009-2355-3.
- DiRusso, C. C. (1990). Primary sequence of the *Escherichia coli* *fadBA* operon, encoding the fatty acid-oxidizing multienzyme complex, indicates a high degree of homology to eucaryotic enzymes. *J. Bacteriol.* 172, 6459–6468. doi:10.1128/jb.172.11.6459-6468.1990.
- Dirusso, C. C., and Black, P. N. (2004). Bacterial long chain fatty acid transport: Gateway to a fatty acid-responsive signaling system. *J. Biol. Chem.* 279, 49563–49566. doi:10.1074/jbc.R400026200.
- Doi, Y., Kanesawa, Y., Kunioka, M., and Saito, T. (1990). Biodegradation of Microbial Copolyesters: Poly(3-hydroxybutyrate-co-3-hydroxyvalerate) and Poly(3-hydroxybutyrate-co-4-hydroxybutyrate). *Macromolecules* 23, 26–31. doi:10.1021/ma00203a006.
- Du, C., Sabirova, J., Soetaert, W., and Ki Carol Lin, S. (2012). Polyhydroxyalkanoates Production From Low-cost Sustainable Raw Materials. *Curr. Chem. Biol.* 6, 14–25.

doi:10.2174/187231312799984394.

- Dufresne, A., Reche, L., Marchessault, R. H., and Lacroix, M. (2001). Gamma-ray crosslinking of poly(3-hydroxyoctanoate-co-undecenoate). *Int. J. Biol. Macromol.* 29, 73–82. doi:10.1016/S0141-8130(01)00152-0.
- Durner, R., Witholt, B., and Egli, T. (2000). Accumulation of poly[(R)-3-hydroxyalkanoates] in *Pseudomonas oleovorans* during growth with octanoate in continuous culture at different dilution rates. *Appl. Environ. Microbiol.* 66, 3408–3414. doi:10.1128/AEM.66.8.3408-3414.2000.
- Durner, R., Zinn, M., Witholt, B., and Egli, T. (2001). Accumulation of poly[(R)-3-hydroxyalkanoates] in *Pseudomonas oleovorans* during growth in batch and chemostat culture with different carbon sources. *Biotechnol. Bioeng.* 72, 278–288. doi:10.1002/1097-0290(20010205)72:3<278::AID-BIT4>3.0.CO;2-G.
- Eggink, G., de Waard, P., and Huijberts, G. N. M. (1992). The role of fatty acid biosynthesis and degradation in the supply of substrates for poly(3-hydroxyalkanoate) formation in *Pseudomonas putida*. *FEMS Microbiol. Lett.* 103, 159–163. doi:10.1016/0378-1097(92)90305-8.
- Eggink, G., De waard, P., and Huijberts, G. N. M. (1995). Formation of novel poly(hydroxyalkanoates) from long-chain fatty acids. *Can. J. Microbiol.* 41, 14–21. doi:10.1139/m95-163.
- Elbahloul, Y., and Steinbüchel, A. (2009). Large-scale production of poly(3-hydroxyoctanoic acid) by *Pseudomonas putida* GPo1 and a simplified downstream process. *Appl. Environ. Microbiol.* 75, 643–651. doi:10.1128/AEM.01869-08.
- Enferadi Kerenkan, A., Béland, F., and Do, T. O. (2016). Chemically catalyzed oxidative cleavage of unsaturated fatty acids and their derivatives into valuable products for industrial applications: A review and perspective. *Catal. Sci. Technol.* 6, 971–987. doi:10.1039/c5cy01118c.
- Favaro, L., Basaglia, M., and Casella, S. (2019). Improving polyhydroxyalkanoate production from inexpensive carbon sources by genetic approaches: a review. *Biofuels, Bioprod. Biorefining* 13, 208–227. doi:10.1002/bbb.1944.
- Fernández, D., Rodríguez, E., Bassas, M., Viñas, M., Solanas, A. M., Llorens, J., et al. (2005). Agro-industrial oily wastes as substrates for PHA production by the new strain *Pseudomonas aeruginosa* NCIB 40045: Effect of culture conditions. *Biochem. Eng. J.* 26, 159–167. doi:10.1016/j.bej.2005.04.022.
- Fiedler, S., Steinbüchel, A., and Rehm, B. H. (2002). The role of the fatty acid β -oxidation multienzyme complex from *Pseudomonas oleovorans* in polyhydroxyalkanoate biosynthesis: Molecular characterization of the *fadBA* operon from *P. oleovorans* and of the enoyl-CoA hydratase genes *phaA* and *phaB*. *Arch. Microbiol.* 178, 149–160. doi:10.1007/s00203-002-0444-0.

- Follonier, S., Henes, B., Panke, S., and Zinn, M. (2012). Putting cells under pressure: A simple and efficient way to enhance the productivity of medium-chain-length polyhydroxyalkanoate in processes with *Pseudomonas putida* KT2440. *Biotechnol. Bioeng.* 109, 451–461. doi:10.1002/bit.23312.
- Follonier, S., Riesen, R., and Zinn, M. (2015). Pilot-scale production of functionalized mcl-PHA from grape pomace supplemented with fatty acids. *Chem. Biochem. Eng. Q.* 29, 113–121. doi:10.15255/CABEQ.2014.2251.
- Fonseca, P., de la Peña, F., and Prieto, M. A. (2014). A role for the regulator PsrA in the polyhydroxyalkanoate metabolism of *Pseudomonas putida* KT2440. *Int. J. Biol. Macromol.* 71, 14–20. doi:10.1016/j.ijbiomac.2014.04.014.
- Fontaine, P., Mosrati, R., and Corroler, D. (2017). Medium chain length polyhydroxyalkanoates biosynthesis in *Pseudomonas putida* mt-2 is enhanced by co-metabolism of glycerol/octanoate or fatty acids mixtures. *Int. J. Biol. Macromol.* 98, 430–435. doi:10.1016/j.ijbiomac.2017.01.115.
- Fu, J., Sharma, U., Sparling, R., Cicek, N., and Levin, D. B. (2014). Evaluation of medium-chain-length polyhydroxyalkanoate production by *Pseudomonas putida* LS46 using biodiesel by-product streams. *Can. J. Microbiol.* 60, 461–468. doi:10.1139/cjm-2014-0108.
- Fujita, Y., Matsuoka, H., and Hirooka, K. (2007). Regulation of fatty acid metabolism in bacteria. *Mol. Microbiol.* 66, 829–839. doi:10.1111/j.1365-2958.2007.05947.x.
- Fukui, T., and Doi, Y. (1997). Cloning and analysis of the poly(3-hydroxybutyrate-co-3-hydroxyhexanoate) biosynthesis genes of *Aeromonas caviae*. *J. Bacteriol.* 179, 4821–4830. doi:10.1128/jb.179.15.4821-4830.1997.
- Gagnon, K. D., Lenz, R. W., Farris, R. J., and Fuller, R. C. (1992). Crystallization behavior and its influence on the mechanical properties of a thermoplastic elastomer produced by *Pseudomonas oleovorans*. *Macromolecules* 25, 3723–3728. doi:10.1021/ma00040a018.
- Gallimore, P. J., Griffiths, P. T., Pope, F. D., Reid, J. P., and Kalberer, M. (2017). Comprehensive modeling study of ozonolysis of oleic acid aerosol based on real-time, online measurements of aerosol composition. *J. Geophys. Res.* 122, 4364–4377. doi:10.1002/2016JD026221.
- Garcia-Ochoa, F., Gomez, E., Santos, V. E., and Merchuk, J. C. (2010). Oxygen uptake rate in microbial processes: An overview. *Biochem. Eng. J.* 49, 289–307. doi:10.1016/j.bej.2010.01.011.
- Grousseau, E., Blanchet, E., Délérís, S., Albuquerque, M. G. E., Paul, E., and Uribe Larrea, J. L. (2013). Impact of sustaining a controlled residual growth on polyhydroxybutyrate yield and production kinetics in *Cupriavidus necator*. *Bioresour. Technol.* 148, 30–38. doi:10.1016/j.biortech.2013.08.120.

- Gruzdiene, D., and Anelauskaite, E. (2010). Chemical composition and stability of rapeseed oil produced from various cultivars grown in Lithuania. *Jfae*, 1–4. Available at: <http://www.icef11.org/content/papers/epf/EPF278.pdf>.
- Guedon, E., Payot, S., Desvaux, M., and Petitdemange, H. (1999). Carbon and electron flow in *Clostridium cellulolyticum* grown in chemostat culture on synthetic medium. *J. Bacteriol.* 181, 3262–3269. doi:10.1128/jb.181.10.3262-3269.1999.
- Haba, E., Vidal-Mas, J., Bassas, M., Espuny, M. J., Llorens, J., and Manresa, A. (2007). Poly 3-(hydroxyalkanoates) produced from oily substrates by *Pseudomonas aeruginosa* 47T2 (NCBIM 40044): Effect of nutrients and incubation temperature on polymer composition. *Biochem. Eng. J.* 35, 99–106. doi:10.1016/j.bej.2006.11.021.
- Hartmann, R., Hany, R., Pletscher, E., Ritter, A., Witholt, B., and Zinn, M. (2006). Tailor-made olefinic medium-chain-length poly[(R)-3-hydroxyalkanoates] by *Pseudomonas putida* GPo1: Batch versus chemostat production. *Biotechnol. Bioeng.* 93, 737–746. doi:10.1002/bit.20756.
- Hartmann, R., Hany, R., Witholt, B., and Zinn, M. (2010). Simultaneous biosynthesis of two copolymers in *Pseudomonas putida* GPO1 using a two-stage continuous culture system. *Biomacromolecules* 11, 1488–1493. doi:10.1021/bm100118t.
- Hasson, A. S., Chung, M. Y., Kuwata, K. T., Converse, A. D., Krohn, D., and Paulson, S. E. (2003). Reaction of criegee intermediates with water vapor - An additional source of OH radicals in alkene ozonolysis? *J. Phys. Chem. A* 107, 6176–6182. doi:10.1021/jp0346007.
- Hazenbergh, W., and Witholt, B. (1997). Efficient production of medium-chain-length poly(3-hydroxyalkanoates) from octane by *Pseudomonas oleovorans*: Economic considerations. *Appl. Microbiol. Biotechnol.* 48, 588–596. doi:10.1007/s002530051100.
- Hazer, B. (2015). Simple synthesis of amphiphilic poly(3-hydroxyalkanoate)s with pendant hydroxyl and carboxylic groups via thiol-ene photo click reactions. *Polym. Degrad. Stab.* 119, 159–166. doi:10.1016/j.polymdegradstab.2015.04.024.
- Hazer, B., Demirel, S. I., Borcakli, M., Eroglu, M. S., Cakmak, M., and Erman, B. (2001). Free radical crosslinking of unsaturated bacterial polyesters obtained from soybean oily acids. *Polym. Bull.* 46, 389–394. doi:10.1007/s002890170047.
- Hazer, B., Hazer, D. B., and Çoban, B. (2010). Synthesis of microbial elastomers based on soybean oil. Autoxidation kinetics, thermal and mechanical properties. *J. Polym. Res.* 17, 567–577. doi:10.1007/s10965-009-9345-0.
- Hazer, B., and Steinbüchel, A. (2007). Increased diversification of polyhydroxyalkanoates by modification reactions for industrial and medical applications. *Appl. Microbiol. Biotechnol.* 74, 1–12. doi:10.1007/s00253-006-0732-8.
- Hazer, D. B., Hazer, B., and Kaymaz, F. (2009). Synthesis of microbial elastomers based

- on soybean oily acids. Biocompatibility studies. *Biomed. Mater.* 4, 035011. doi:10.1088/1748-6041/4/3/035011.
- Hearn, J. D., Lovett, A. J., and Smith, G. D. (2005). Ozonolysis of oleic acid particles: Evidence for a surface reaction and secondary reactions involving Criegee intermediates. *Phys. Chem. Chem. Phys.* 7, 501–511. doi:10.1039/b414472d.
- Hong, K., Sun, S., Tian, W., Chen, G. Q., and Huang, W. (1999). A rapid method for detecting bacterial polyhydroxyalkanoates in intact cells by Fourier transform infrared spectroscopy. *Appl. Microbiol. Biotechnol.* 51, 523–526. doi:10.1007/s002530051427.
- Hopwood, D. (1970). The reactions between formaldehyde, glutaraldehyde and osmium tetroxide, and their fixation effects on bovine serum albumin and on tissue blocks. *Histochemie* 24, 50–64. doi:10.1007/BF00310003.
- Hori, K., Soga, K., and Doi, Y. (1994). Effects of culture conditions on molecular weights of poly (3hydroxyalkanoates) produced by *Pseudomonas putida* from octanoate. *Biotechnol. Lett.* 16, 709–714. doi:10.1007/BF00136476.
- Huijberts, G. N. M., and Eggink, G. (1996). Production of poly(3-hydroxyalkanoates) by *Pseudomonas putida* KT2442 in continuous cultures. *Appl. Microbiol. Biotechnol.* 46, 233–239. doi:10.1007/s002530050810.
- Huijberts, G. N. M., Eggink, G., De Waard, P., Huisman, G. W., and Witholt, B. (1992). *Pseudomonas putida* KT2442 cultivated on glucose accumulates poly(3-hydroxyalkanoates) consisting of saturated and unsaturated monomers. *Appl. Environ. Microbiol.* 58, 536–544.
- Huijberts, G. N. M., Eggink, G., De Waard, P., Huisman, G. W., and Witholt, B. (1994). ¹³C Nuclear Magnetic Resonance Studies of *Pseudomonas putida* Fatty Acid Metabolic Routes Involved in Poly(3-Hydroxyalkanoate) Synthesis. *Synthesis (Stuttg.)* 176, 1661–1666.
- Icoz, D. (2008). Understanding molecular and thermodynamic miscibility of carbohydrate biopolymers. *Thesis.* Available at: <http://mss3.libraries.rutgers.edu/dlr/showfed.php?pid=rutgers-lib:24402>.
- Ienczak, J. L., Schmidell, W., and De Aragão, G. M. F. (2013). High-cell-density culture strategies for polyhydroxyalkanoate production: A review. *J. Ind. Microbiol. Biotechnol.* 40, 275–286. doi:10.1007/s10295-013-1236-z.
- Ilter, S., Hazer, B., Borcakli, M., and Atici, O. (2001). Graft copolymerisation of methyl methacrylate onto a bacterial polyester containing unsaturated side chains. *Macromol. Chem. Phys.* 202, 2281–2286. doi:10.1002/1521-3935(20010701)202:11<2281::AID-MACP2281>3.0.CO;2-9.
- Impallomeni, G., Ballistreri, A., Carnemolla, G. M., Guglielmino, S. P. P., Nicolò, M. S., and Cambria, M. G. (2011). Synthesis and characterization of poly(3-

- hydroxyalkanoates) from *Brassica carinata* oil with high content of erucic acid and from very long chain fatty acids. *Int. J. Biol. Macromol.* 48, 137–145. doi:10.1016/j.ijbiomac.2010.10.013.
- Jain-Beuguel, C., LI, X., Houel-Renault, L., Modjinou, T., Simon-Colin, C., Gref, R., et al. (2019). Water-Soluble Poly(3-hydroxyalkanoate) Sulfonate: Versatile Biomaterials Used as Coatings for Highly Porous Nano-Metal Organic Framework. *Biomacromolecules* 20, 3324–3332. doi:10.1021/acs.biomac.9b00870.
- Jarboe, L. R., Royce, L. A., and Liu, P. (2013). Understanding biocatalyst inhibition by carboxylic acids. *Front. Microbiol.* 4, 1–8. doi:10.3389/fmicb.2013.00272.
- Jendrossek, D., and Handrick, R. (2002). Microbial Degradation of Polyhydroxyalkanoates. *Annu. Rev. Microbiol.* 56, 403–432. doi:10.1146/annurev.micro.56.012302.160838.
- Jendrossek, D., Knoke, I., Habibian, R. B., Steinbüchel, A., and Schlegel, H. G. (1993). Degradation of poly(3-hydroxybutyrate), PHB, by bacteria and purification of a novel PHB depolymerase from *Comamonas* sp. *J. Environ. Polym. Degrad.* 1, 53–63. doi:10.1007/BF01457653.
- Jiang, G., Hill, D. J., Kowalczyk, M., Johnston, B., Adamus, G., Irorere, V., et al. (2016). Carbon sources for polyhydroxyalkanoates and an integrated biorefinery. *Int. J. Mol. Sci.* 17. doi:10.3390/ijms17071157.
- Jiang, X. J., Sun, Z., Ramsay, J. A., and Ramsay, B. A. (2013). Fed-batch production of MCL-PHA with elevated 3-hydroxynonanoate content. *AMB Express* 3, 50. doi:10.1186/2191-0855-3-50.
- Jiang, X., Sun, Z., Marchessault, R. H., Ramsay, J. A., and Ramsay, B. A. (2012). Biosynthesis and properties of medium-chain-length polyhydroxyalkanoates with enriched content of the dominant monomer. *Biomacromolecules* 13, 2926–2932. doi:10.1021/bm3009507.
- Jung, K., Hazenberg, W., Prieto, M., and Witholt, B. (2001). Two-stage continuous process development for the production of medium-chain-length poly(3-hydroxyalkanoates). *Biotechnol. Bioeng.* 72, 19–24. doi:10.1002/1097-0290(20010105)72:1<19::AID-BIT3>3.0.CO;2-B.
- Kalpakjian, S., and Schmid, S. (1985). *Manufacturing processes for engineering materials*. Pearson Education doi:10.1016/0020-7357(85)90061-7.
- Kang, D. K., Lee, C. R., Lee, S. H., Bae, J. H., Park, Y. K., Rhee, Y. H., et al. (2017). Production of polyhydroxyalkanoates from sludge palm oil using *Pseudomonas putida* S12. *J. Microbiol. Biotechnol.* 27, 990–994. doi:10.4014/jmb.1612.12031.
- Kang, Y., Nguyen, D. T., Son, M. S., and Hoang, T. T. (2008). The *Pseudomonas aeruginosa* PsrA responds to long-chain fatty acid signals to regulate the fadBA5 β -oxidation operon. *Microbiology* 154, 1584–1598. doi:10.1099/mic.0.2008/018135-0.

- Kaur, G., and Roy, I. (2015). Strategies for Large-scale Production of Polyhydroxyalkanoates. *Chem. Biochem. Eng. Q.* 29, 157–172. doi:10.15255/CABEQ.2014.2255.
- Kellerhals, M. B., Hazenberg, W., and Witholt, B. (1999). High cell density fermentations of *Pseudomonas oleovorans* for the production of mcl-PHAs in two-liquid phase media. *Enzyme Microb. Technol.* 24, 111–116. doi:10.1016/S0141-0229(98)00113-6.
- Kellerhals, M. B., Kessler, B., Witholt, B., Tchouboukov, A., and Brandl, H. (2000). Renewable long-chain fatty acids for production of biodegradable medium-chain-length polyhydroxyalkanoates (mcl-PHAs) at laboratory and pilot plant scales. *Macromolecules* 33, 4690–4698. doi:10.1021/ma000655k.
- Kim, D., Kim, H., Chung, M., and RheeYH (2007). Biosynthesis, modification, and biodegradation of bacterial medium-chain-length polyhydroxyalkanoates. *J. Microbiol.* 45, 87–97.
- Kim, G. J., Lee, I. Y., Yoon, S. C., Shin, Y. C., and Park, Y. H. (1997). Enhanced yield and a high production of medium-chain-length poly(3-hydroxyalkanoates) in a two-step fed-batch cultivation of *Pseudomonas putida* by combined use of glucose and octanoate. *Enzyme Microb. Technol.* 20, 500–505. doi:10.1016/S0141-0229(96)00179-2.
- Knoll, M., Hamm, T. M., Wagner, F., Martinez, V., and Pleiss, J. (2009). The PHA Depolymerase Engineering Database: A systematic analysis tool for the diverse family of polyhydroxyalkanoate (PHA) depolymerases. *BMC Bioinformatics* 10, 1–8. doi:10.1186/1471-2105-10-89.
- Koçer, H., Borcakli, M., Demirel, S., and Hazer, B. (2003). Production of bacterial polyesters from some various new substrates by *Alcaligenes eutrophus* and *Pseudomonas oleovorans*. *Turkish J. Chem.* 27, 365–373.
- Koller, M. (2018). A review on established and emerging fermentation schemes for microbial production of polyhydroxyalkanoate (PHA) biopolyesters. *Fermentation* 4. doi:10.3390/fermentation4020030.
- Koller, M., and Braunegg, G. (2015). Potential and prospects of continuous polyhydroxyalkanoate (PHA) production. *Bioengineering* 2, 94–121. doi:10.3390/bioengineering2020094.
- Koller, M., Maršálek, L., de Sousa Dias, M. M., and Braunegg, G. (2017). Producing microbial polyhydroxyalkanoate (PHA) biopolyesters in a sustainable manner. *N. Biotechnol.* 37, 24–38. doi:10.1016/j.nbt.2016.05.001.
- Kourmentza, C., Plácido, J., Venetsaneas, N., Burniol-Figols, A., Varrone, C., Gavala, H. N., et al. (2017). Recent Advances and Challenges towards Sustainable Polyhydroxyalkanoate (PHA) Production. *Bioengineering* 4, 1–43. doi:10.3390/bioengineering4020055.

- Kraak, M. N., Smits, T. H. M., Kessler, B., and Witholt, B. (1997). Polymerase C1 Levels and Poly (R-3-Hydroxyalkanoate) Synthesis in Wild-Type and Recombinant *Pseudomonas* Strains. *J. Bacteriol.* 179, 4985–4991.
- Kurth, N., Brachet, F., Robic, D., Bourbouze, R., Renard, E., and Guerin, P. (2001). Poly(3-hydroxyoctanoate) containing pendant carboxylic groups for the preparation of nanoparticles aimed at drug transport and release. *Polymer (Guildf)*. 43, 1095–1101. doi:10.1016/S0032-3861(01)00692-9.
- Lageveen, R. G., Huisman, G., Preusting, H., Ketelaar, P., Eggink, G., and Witholt, B. (1989). Formation of Polyesters by *Pseudomonas oleovorans*: Effect of Substrates on Formation and Composition of Poly- (R) -3- Hydroxyalkanoates and Poly- (R) -3- Hydroxyalkenoates. *Appl. Environ. Microbiol.* 54, 2924–2932.
- Lageveen, R. G., Huisman, G. W., Preusting, H., Ketelaar, P., Eggink, G., and Witholt, B. (1988). Formation of Polyesters by *Pseudomonas oleovorans*: Effect of Substrates on Formation and Composition of Poly-(R)-3-Hydroxyalkanoates and Poly-(R)-3-Hydroxyalkenoates. *Appl. Environ. Microbiol.* 54, 2924–2932. doi:10.1128/aem.54.12.2924-2932.1988.
- Lara, A. R., Galindo, E., Ramírez, O. T., and Palomares, L. A. (2006). Living With Heterogeneities in Bioreactors: Understanding the Effects of Environmental Gradients on Cells. *Mol. Biotechnol.* 34, 355–382. doi:10.1385/MB:34:3:355.
- Larrañaga, A., Fernández, J., Vega, A., Etxeberria, A., Ronchel, C., Adrio, J. L., et al. (2014). Crystallization and its effect on the mechanical properties of a medium chain length polyhydroxyalkanoate. *J. Mech. Behav. Biomed. Mater.* 39, 87–94. doi:10.1016/j.jmbbm.2014.07.020.
- Laycock, B., Arcos-Hernandez, M. V., Langford, A., Pratt, S., Werker, A., Halley, P. J., et al. (2014). Crystallisation and fractionation of selected polyhydroxyalkanoates produced from mixed cultures. *N. Biotechnol.* 31, 345–356. doi:10.1016/j.nbt.2013.05.005.
- Le Fer, G., Babinot, J., Versace, D. L., Langlois, V., and Renard, E. (2012). An efficient thiol-ene chemistry for the preparation of amphiphilic PHA-based graft copolymers. *Macromol. Rapid Commun.* 33, 2041–2045. doi:10.1002/marc.201200485.
- Lee, E. Y., and Choi, C. Y. (1995). Gas chromatography-mass spectrometric analysis and its application to a screening procedure for novel bacterial polyhydroxyalkanoic acids containing long chain saturated and unsaturated monomers. *J. Ferment. Bioeng.* 80, 408–414. doi:10.1016/0922-338X(95)94214-C.
- Lee, J. H., Ashby, R. D., Needleman, D. S., Lee, K.-T., and Solaiman, D. K. Y. (2012). Cloning, sequencing, and characterization of lipase genes from polyhydroxyalkanoate (PHA)-synthesizing *Pseudomonas resinovorans*. *Appl. Microbiol. Biotechnol.* 96, 993–1005.
- Lee, M. Y., Park, W. H., and Lenz, R. W. (2000a). Hydrophilic bacterial polyesters

- modified with pendant hydroxyl groups. *Polymer (Guildf)*. 41, 1703–1709. doi:10.1016/S0032-3861(99)00347-X.
- Lee, S. Y. (1996). Bacterial polyhydroxyalkanoates. *Biotechnol. Bioeng.* 49, 1–14. doi:10.1002/(SICI)1097-0290(19960105)49:1<1::AID-BIT1>3.3.CO;2-1.
- Lee, S. Y., Wong, H. H., Choi, J. Il, Lee, S. H., Lee, S. C., and Han, C. S. (2000b). Production of medium-chain-length polyhydroxyalkanoates by high-cell-density cultivation *Pseudomonas putida* under phosphorus limitation. *Biotechnol. Bioeng.* 68, 466–470. doi:10.1002/(SICI)1097-0290(20000520)68:4<466::AID-BIT12>3.0.CO;2-T.
- Levett, I., Birkett, G., Davies, N., Bell, A., Langford, A., Laycock, B., et al. (2016). Techno-economic assessment of poly-3-hydroxybutyrate (PHB) production from methane - The case for thermophilic bioprocessing. *J. Environ. Chem. Eng.* 4, 3724–3733. doi:10.1016/j.jece.2016.07.033.
- Levine, A. C., Heberlig, G. W., and Nomura, C. T. (2016). Use of thiol-ene click chemistry to modify mechanical and thermal properties of polyhydroxyalkanoates (PHAs). *Int. J. Biol. Macromol.* 83, 358–365. doi:10.1016/j.ijbiomac.2015.11.048.
- Levine, A. C., Sparano, A., Twigg, F. F., Numata, K., and Nomura, C. T. (2015). Influence of Cross-Linking on the Physical Properties and Cytotoxicity of Polyhydroxyalkanoate (PHA) Scaffolds for Tissue Engineering. *ACS Biomater. Sci. Eng.* 1, 567–576. doi:10.1021/acsbiomaterials.5b00052.
- Liu, Q., Luo, G., Zhou, X. R., and Chen, G. Q. (2011). Biosynthesis of poly(3-hydroxydecanoate) and 3-hydroxydodecanoate dominating polyhydroxyalkanoates by β -oxidation pathway inhibited *Pseudomonas putida*. *Metab. Eng.* 13, 11–17. doi:10.1016/j.ymben.2010.10.004.
- Liu, W., and Chen, G. Q. (2007). Production and characterization of medium-chain-length polyhydroxyalkanoate with high 3-hydroxytetradecanoate monomer content by *fadB* and *fadA* knockout mutant of *Pseudomonas putida* KT2442. *Appl. Microbiol. Biotechnol.* 76, 1153–1159. doi:10.1007/s00253-007-1092-8.
- López, N. I., Pettinari, M. J., Nikel, P. I., and Méndez, B. S. (2015). Polyhydroxyalkanoates: Much More than Biodegradable Plastics. *Adv. Appl. Microbiol.* 93, 73–106. doi:10.1016/bs.aambs.2015.06.001.
- Maclean, H., Sun, Z., Ramsay, J., and Ramsay, B. (2008). Decaying exponential feeding of nonanoic acid for the production of medium-chain-length poly (3-hydroxyalkanoates) by *Pseudomonas putida*. *Can. J. Chem.* 86, 564–569. doi:10.1139/V08-062.
- Madison, L. L., and Huisman, G. W. (1999). Metabolic engineering of poly(3-hydroxyalkanoates): from DNA to plastic. *Microbiol. Mol. Biol. Rev.* 63, 21–53.
- Mallegol, J., Gardette, J.-L., and Lemaire, J. (2000). Long-term behaviour of oil-based

- varnishes and paints. Fate of hydroperoxides in drying oils. *Jaocs* 77, 249–255.
- Marchessault, R. H., Monasterios, C. J., Morin, F. G., and Sundararajan, P. R. (1990). Chiral poly(β -hydroxyalkanoates): an adaptable helix influenced by the alkane side-chain. *Int. J. Biol. Macromol.* 12, 158–165. doi:10.1016/0141-8130(90)90068-L.
- Marchessault, R., and Yu, G. (2005). Crystallization and material properties of polyhydroxyalkanoates. *Biopolym. Online* 79, 157–166. doi:10.1002/3527600035.bpol3b07.
- Modjinou, T., Lemechko, P., Babinot, J., Versace, D. L., Langlois, V., and Renard, E. (2015). Poly(3-hydroxyalkanoate) sulfonate: From nanoparticles toward water soluble polyesters. *Eur. Polym. J.* 68, 471–479. doi:10.1016/j.eurpolymj.2015.05.018.
- Możejko-Ciesielska, J., and Kiewisz, R. (2016). Bacterial polyhydroxyalkanoates: Still fabulous? *Microbiol. Res.* 192, 271–282. doi:10.1016/j.micres.2016.07.010.
- Mozejko, J., and Ciesielski, S. (2014). Pulsed feeding strategy is more favorable to medium-chain-length polyhydroxyalkanoates production from waste rapeseed oil. *Biotechnol. Prog.* 30, 1243–1246. doi:10.1002/btpr.1914.
- Muizebelt, W. J., Hubert, J. C., and Venderbosch, R. A. M. (1994). Mechanistic study of drying of alkyd resins using ethyl linoleate as a model substance. *Prog. Org. Coatings* 24, 263–279. doi:10.1016/0033-0655(94)85019-4.
- Mungure, T., and Birch, E. (2014). Analysis of intact triacylglycerols in cold pressed canola, flax and hemp seed oils by HPLC and ESI-MS. *SOP Trans. Anal. Chem.* 1, 48–61. doi:10.15764/ache.2014.01005.
- Murphy, R. C., and Axelsen, P. H. (2011). Mass spectrometric analysis of long-chain lipids. *Mass Spectrom. Rev.* 30, 579–599. doi:10.1002/mas.20284.
- Nicholson, L. M., Whitley, K. S., Gates, T. S., and Hinkley, J. a (1999). How molecular structure affects mechanical properties of an advanced polymer. *Int. Sampe Symp. Exhib.*, 794–808.
- Nielson, A., and Griffith, W. (1979). Tissue Fixation by Osmium Tetroxide. *Inorg. Chem.* 18, 997–999.
- Nikel, P. I., and de Lorenzo, V. (2013). Engineering an anaerobic metabolic regime in *Pseudomonas putida* KT2440 for the anoxic biodegradation of 1,3-dichloroprop-1-ene. *Metab. Eng.* 15, 98–112. doi:10.1016/j.ymben.2012.09.006.
- Nikodinovic-Runic, J., Guzik, M., Kenny, S. T., Babu, R., Werker, A., and O'Connor, K. E. (2013). Carbon-rich wastes as feedstocks for biodegradable polymer (polyhydroxyalkanoate) production using bacteria. *Adv. Appl. Microbiol.* 84, 139–200. doi:10.1016/B978-0-12-407673-0.00004-7.
- Nkrumah-Agyeefi, S., and Scholz, C. (2017). Chemical modification of functionalized polyhydroxyalkanoates via “Click” chemistry: A proof of concept. *Int. J. Biol.*

- Macromol.* 95, 796–808. doi:10.1016/j.ijbiomac.2016.11.118.
- Omonov, T. S., Kharraz, E., Foley, P., and Curtis, J. M. (2014). The production of biobased nonanal by ozonolysis of fatty acids. *Rsc Adv.* 4, 53617–53627. doi:10.1039/c4ra07917e.
- Parida, K. N., and Moorthy, J. N. (2014). Oxidation cascade with oxone: Cleavage of olefins to carboxylic acids. *Tetrahedron* 70, 2280–2285. doi:10.1016/j.tet.2014.01.042.
- Park, W. H. O., Lenz, R. W., and Goodwin, S. (1998). Epoxidation of bacterial polyesters with unsaturated side chains. II. Rate of epoxidation and polymer properties. *J. Polym. Sci. Part A Polym. Chem.* 36, 2381–2387. doi:10.1002/(SICI)1099-0518(19980930)36:13<2381::AID-POLA25>3.0.CO;2-5.
- Pinto, A., Ciesla, J. H., Palucci, A., Sutliff, B. P., and Nomura, C. T. (2016). Chemically Intractable No More: In Vivo Incorporation of “click”-Ready Fatty Acids into Poly-[(R)-3-hydroxyalkanoates] in *Escherichia coli*. *ACS Macro Lett.* 5, 215–219. doi:10.1021/acsmacrolett.5b00823.
- Povolo, S., Romanelli, M. G., Fontana, F., Basaglia, M., and Casella, S. (2012). Production of Polyhydroxyalkanoates from Fatty Wastes. *J. Polym. Environ.* 20, 944–949. doi:10.1007/s10924-012-0485-7.
- Preusting, H., Hazenberg, W., and Witholt, B. (1993). Continuous production of poly(3-hydroxyalkanoates) by *Pseudomonas oleovorans* in a high-cell-density, two-liquid-phase chemostat. *Enzyme Microb. Technol.* 15, 311–316. doi:10.1016/0141-0229(93)90156-V.
- Pryor, W. A., Das, B., and Church, D. F. (1991). The Ozonation of Unsaturated Fatty Acids: Aldehydes and Hydrogen Peroxide as Products and Possible Mediators of Ozone Toxicity. *Chem. Res. Toxicol.* 4, 341–348. doi:10.1021/tx00021a014.
- Qi, Q., Rehm, B. H. A., and Steinbüchel, A. (1997). Synthesis of poly(3-hydroxyalkanoates) in *Escherichia coli* expressing the PHA synthase gene *phaC2* from *Pseudomonas aeruginosa*: Comparison of PhaC1 and PhaC2. *FEMS Microbiol. Lett.* 157, 155–162. doi:10.1016/S0378-1097(97)00469-2.
- Qi, Q., Steinbüchel, A., and Rehm, B. H. a. (1998). Metabolic routing towards polyhydroxyalkanoic acid synthesis in recombinant *Escherichia coli* (*fadR*): Inhibition of fatty acid β -oxidation by acrylic acid. *FEMS Microbiol. Lett.* 167, 89–94. doi:10.1016/S0378-1097(98)00368-1.
- Ramos, M. J., Fernández, C. M., Casas, A., Rodríguez, L., and Pérez, Á. (2009). Influence of fatty acid composition of raw materials on biodiesel properties. *Bioresour. Technol.* 100, 261–268. doi:10.1016/j.biortech.2008.06.039.
- Ramsay, B. A., Lomaliza, K., Chavarie, C., Dube, B., Bataille, P., and Ramsay, J. A. (1990). Production of Poly-(β -Hydroxybutyric-Co- β -Hydroxyvaleric) Acids. *Appl.*

Environ. Microbiol. 56, 2093–2098.

- Ramsay, B. A., Saracovan, I., Ramsay, J. A., and Marchessault, R. H. (1991). Continuous Production of Long-Side-Chain Poly-3-Hydroxyalkanoates by *Pseudomonas oleovorans*. *Appl. Environ. Microbiol.* 57, 625–629.
- Rani, S., and Vankar, Y. D. (2003). An efficient one step dihydroxylation of 1,2-glycols with oxone in acetone. *Tetrahedron Lett.* 44, 907–909. doi:10.1016/S0040-4039(02)02774-0.
- Ravindran, R., and Jaiswal, A. K. (2016). Exploitation of Food Industry Waste for High-Value Products. *Trends Biotechnol.* 34, 58–69. doi:10.1016/j.tibtech.2015.10.008.
- Ren, Q., De Roo, G., Ruth, K., Witholt, B., Zinn, M., and Thöny-Meyer, L. (2009). Simultaneous accumulation and degradation of polyhydroxyalkanoates: Futile cycle or clever regulation? *Biomacromolecules* 10, 916–922. doi:10.1021/bm801431c.
- Ren, Q., Sierro, N., Witholt, B., and Kessler, B. (2000). FabG, an NADPH-dependent 3-ketoacyl reductase of *Pseudomonas aeruginosa*, provides precursors for medium-chain-length poly-3-hydroxyalkanoate biosynthesis in *Escherichia coli*. *J. Bacteriol.* 182, 2978–2981. doi:10.1128/JB.182.10.2978-2981.2000.
- Ruiz, C., Kenny, S. T., Ramesh Babu, P., Walsh, M., Narancic, T., and O'Connor, K. E. (2019). High cell density conversion of hydrolysed waste cooking oil fatty acids into medium chain length polyhydroxyalkanoate using *Pseudomonas putida* KT2440. *Catalysts* 9. doi:10.3390/catal9050468.
- Schmid, M., Ritter, A., Grubelnik, A., and Zinn, M. (2007). Autoxidation of medium chain length polyhydroxyalkanoate. *Biomacromolecules* 8, 579–584. doi:10.1021/bm060785m.
- Schroder, M. (1980). Osmium Tetraoxide Cis Hydroxylation of Unsaturated Substrates. *Chem. Rev.* 80, 187–213.
- Shang, L., Jiang, M., Yun, Z., Yan, H. Q., and Chang, H. N. (2008). Mass production of medium-chain-length poly(3-hydroxyalkanoates) from hydrolyzed corn oil by fed-batch culture of *Pseudomonas putida*. *World J. Microbiol. Biotechnol.* 24, 2783–2787. doi:10.1007/s11274-008-9808-1.
- Sharma, P. K., Fu, J., Cicek, N., Sparling, R., and Levin, D. B. (2012). Kinetics of medium-chain-length polyhydroxyalkanoate production by a novel isolate of *Pseudomonas putida* LS46. *Can. J. Microbiol.* 58, 982–9. doi:10.1139/w2012-074.
- Sharma, P. K., Munir, R. I., de Kievit, T., and Levin, D. B. (2017a). Synthesis of polyhydroxyalkanoates (PHAs) from vegetable oils and free fatty acids by wild-type and mutant strains of *pseudomonas chlororaphis*. *Can. J. Microbiol.* 63, 1009–1024. doi:10.1139/cjm-2017-0412.
- Sharma, P., Munir, R., Blunt, W., Dartailh, C., Cheng, J., Charles, T., et al. (2017b). Synthesis and Physical Properties of Polyhydroxyalkanoate Polymers with Different

- Monomer Compositions by Recombinant *Pseudomonas putida* LS46 Expressing a Novel PHA SYNTHASE (PhaC116) Enzyme. *Appl. Sci.* 7, 242. doi:10.3390/app7030242.
- Simic, M. G. (1981). Free radical mechanisms in autoxidation processes. *J. Chem. Educ.* 58, 125. doi:10.1021/ed058p125.
- Sohn, S. B., Kim, T. Y., Park, J. M., and Lee, S. Y. (2010). In silico genome-scale metabolic analysis of *Pseudomonas putida* KT2440 for polyhydroxyalkanoate synthesis, degradation of aromatics and anaerobic survival. *Biotechnol. J.* 5, 739–750. doi:10.1002/biot.201000124.
- Solaiman, D. K. Y., Ashby, R. D., and Foglia, T. A. (2001). Production of polyhydroxyalkanoates from intact triacylglycerols by genetically engineered *Pseudomonas*. *Appl. Microbiol. Biotechnol.* 56, 664–669. doi:10.1007/s002530100692.
- Solaiman, D. K. Y., Ashby, R. D., and Foglia, T. A. (2002). Physiological characterization and genetic engineering of *Pseudomonas corrugata* for medium-chain-length polyhydroxyalkanoates synthesis from triacylglycerols. *Curr. Microbiol.* 44, 189–195. doi:10.1007/s00284-001-0086-5.
- Song, J. H., Jeon, C. O., Choi, M. H., Yoon, S. C., and Park, W. (2008). Polyhydroxyalkanoate (PHA) production using waste vegetable oil by *Pseudomonas* sp. strain DR2. *J. Microbiol. Biotechnol.* 18, 1408–1415.
- Spannring, P., Bruijninx, P. C. A., Weckhuysen, B. M., and Gebbink, R. J. M. K. (2014). Transition metal-catalyzed oxidative double bond cleavage of simple and bio-derived alkenes and unsaturated fatty acids. *Catal. Sci. Technol.* 4, 2182–2209. doi:10.1039/c3cy01095c.
- Sparks, J., and Scholz, C. (2008). Synthesis and characterization of a cationic Poly(β -hydroxyalkanoate). *Biomacromolecules* 9, 2091–2096. doi:10.1021/bm8005616.
- Steinbüchel, A. (2001). Perspectives for Biotechnological Production and Utilization of Biopolymers: Metabolic Engineering of Polyhydroxyalkanoate Biosynthesis Pathways as a Successful Example. *Macromol. Biosci.* 1, 1–24. doi:10.1002/1616-5195(200101)1:1<1::AID-MABI1>3.0.CO;2-B.
- Steinbüchel, A., and Lütke-eversloh, T. (2003). Metabolic engineering and pathway construction for biotechnological production of relevant polyhydroxyalkanoates in microorganisms. 16, 81–96. doi:10.1016/S1369-703X(03)00036-6.
- Steinbüchel, A., and Valentin, H. E. (1995). Diversity of bacterial polyhydroxyalkanoic acids. *FEMS Microbiol. Lett.* 128, 219–228. doi:10.1016/0378-1097(95)00125-O.
- Stigers, D. J., and Tew, G. N. (2003). Poly(3-hydroxyalkanoate)s functionalized with carboxylic acid groups in the side chain. *Biomacromolecules* 4, 193–195. doi:10.1021/bm025728h.

- Sudesh, K., Abe, H., and Doi, Y. (2000). Synthesis, structure and properties of polyhydroxyalkanoates: Biological polyesters. *Prog. Polym. Sci.* 25, 1503–1555. doi:10.1016/S0079-6700(00)00035-6.
- Sun, Z., Ramsay, J. A., Guay, M., and Ramsay, B. A. (2006). Automated feeding strategies for high-cell-density fed-batch cultivation of *Pseudomonas putida* KT2440. *Appl. Microbiol. Biotechnol.* 71, 423–431. doi:10.1007/s00253-005-0191-7.
- Sun, Z., Ramsay, J. A., Guay, M., and Ramsay, B. A. (2007). Fermentation process development for the production of medium-chain-length poly-3-hydroxyalkanoates. *Appl. Microbiol. Biotechnol.* 75, 475–485. doi:10.1007/s00253-007-0857-4.
- Sun, Z., Ramsay, J. A., Guay, M., and Ramsay, B. A. (2009). Carbon-limited fed-batch production of medium-chain-length polyhydroxyalkanoates from nonanoic acid by *Pseudomonas putida* KT2440. *Appl. Microbiol. Biotechnol.* 82, 657–662. doi:10.1007/s00253-008-1785-7.
- Taguchi, K., Aoyagi, Y., Matsusaki, H., Fukui, T., and Doi, Y. (1999). Co-expression of 3-ketoacyl-ACP reductase and polyhydroxyalkanoate synthase genes induces PHA production in *Escherichia coli* HB101 strain. *FEMS Microbiol. Lett.* 176, 183–190. doi:10.1016/S0378-1097(99)00215-3.
- Tappel, R. C., Pan, W., Bergey, N. S., Wang, Q., Patterson, I. L., Ozumba, O. A., et al. (2014). Engineering *Escherichia coli* for improved production of short-chain-length-co-medium-chain-length poly[(R)-3-hydroxyalkanoate] (SCL-co-MCL PHA) copolymers from renewable nonfatty acid feedstocks. *ACS Sustain. Chem. Eng.* 2, 1879–1887. doi:10.1021/sc500217p.
- Tavassoli-Kafrani, M. H., Foley, P., Kharraz, E., and Curtis, J. M. (2016). Quantification of Nonanal and Oleic Acid Formed during the Ozonolysis of Vegetable Oil Free Fatty Acids or Fatty Acid Methyl Esters. *JAOCS, J. Am. Oil Chem. Soc.* 93, 303–310. doi:10.1007/s11746-015-2780-7.
- Thakor, N., Trivedi, U., and Patel, K. C. (2005). Biosynthesis of medium chain length poly(3-hydroxyalkanoates) (mcl-PHAs) by *Comamonas testosteroni* during cultivation on vegetable oils. *Bioresour. Technol.* 96, 1843–1850. doi:10.1016/j.biortech.2005.01.030.
- Tokiwa, Y., Calabria, B. P., Ugwu, C. U., and Aiba, S. (2009). Biodegradability of plastics. *Int. J. Mol. Sci.* 10, 3722–3742. doi:10.3390/ijms10093722.
- Toraman, T., and Hazer, B. (2014). Synthesis and Characterization of the Novel Thermoresponsive Conjugates Based on Poly(3-hydroxy alkanoates). *J. Polym. Environ.* 22, 159–166. doi:10.1007/s10924-014-0646-y.
- Tortajada, M., da Silva, L. F., and Prieto, M. A. (2013). Second-generation functionalized mediumchain- length polyhydroxyalkanoates: The gateway to high-value bioplastic applications. *Int. Microbiol.* 16, 1–15. doi:10.2436/20.1501.01.175.

- Travis, B. R., Narayan, R. S., and Borhan, B. (2002). Osmium tetroxide-promoted catalytic oxidative cleavage of olefins: An organometallic ozonolysis. *J. Am. Chem. Soc.* 124, 3824–3825. doi:10.1021/ja017295g.
- Tsuge, T. (2016). Fundamental factors determining the molecular weight of polyhydroxyalkanoate during biosynthesis. *Polym. J.* 48, 1051–1057. doi:10.1038/pj.2016.78.
- Tsuge, T., Taguchi, K., Taguchi, S., and Doi, Y. (2003). Molecular characterization and properties of (R)-specific enoyl-CoA hydratases from *Pseudomonas aeruginosa*: Metabolic tools for synthesis of polyhydroxyalkanoates via fatty acid β -oxidation. *Int. J. Biol. Macromol.* 31, 195–205. doi:10.1016/S0141-8130(02)00082-X.
- Vendruscolo, F., Rossi, M. J., Schmidell, W., and Ninow, J. L. (2012). Determination of Oxygen Solubility in Liquid Media. *ISRN Chem. Eng.* 2012, 1–5. doi:10.5402/2012/601458.
- Vereecken, L. (2017). The reaction of Criegee intermediates with acids and enols. *Phys. Chem. Chem. Phys.* 19, 28630–28640. doi:10.1039/c7cp05132h.
- Vereecken, L., Harder, H., and Novelli, A. (2014). The reactions of Criegee intermediates with alkenes, ozone, and carbonyl oxides. *Phys. Chem. Chem. Phys.* 16, 4039–4049. doi:10.1039/c3cp54514h.
- Wallace, T., Gibbons, D., O'Dwyer, M., and Curran, T. P. (2017). International evolution of fat, oil and grease (FOG) waste management – A review. *J. Environ. Manage.* 187, 424–435. doi:10.1016/j.jenvman.2016.11.003.
- Wang, F., and Lee, S. Y. (1997). Poly(3-Hydroxybutyrate) Production with High Productivity and High Polymer Content by a Fed-Batch Culture of *Alcaligenes latus* under Nitrogen Limitation. *Appl. Environ. Microbiol.* 63, 3703–3706. doi:10.1023/a:1012222625201.
- Wang, H. H., Zhou, X. R., Liu, Q., and Chen, G. Q. (2011). Biosynthesis of polyhydroxyalkanoate homopolymers by *Pseudomonas putida*. *Appl. Microbiol. Biotechnol.* 89, 1497–1507. doi:10.1007/s00253-010-2964-x.
- Wang, Y., Yin, J., and Chen, G. Q. (2014). Polyhydroxyalkanoates, challenges and opportunities. *Curr. Opin. Biotechnol.* 30, 59–65. doi:10.1016/j.copbio.2014.06.001.
- Weitzel, K., Chemie, F., Rev, M. S., Introduction, I., and Reference, C. (2011). Bond-Dissociation Energies of Cations — Pushing the. *WHO Libr. Cat. Data*, 221–235. doi:10.1002/mas.
- Zeng, M., Heine, N., and Wilson, K. R. (2020). Evidence that criegee intermediates drive autoxidation in unsaturated lipids. *Proc. Natl. Acad. Sci. U. S. A.* 117, 4486–4490. doi:10.1073/pnas.1920765117.